HYWIND Acoustic Measurement Report

Ambient Levels and HYWIND Signature

Submitted to:
Statoil / Fugro
Contract: (Fugro) C10882

Authors:
Bruce Martin
Jeff MacDonnell
Jonathan Vallarta
Eric Lumsden
Robin Burns

JASCO Applied Sciences(UK) Ltd
The Roundel
St Clair's Farm
Wickham Road, Droxford
Hampshire, SO32 3PW
UK
+44(0) 1489 878439

www.jasco.com

14 December 2011
JASCO Project: P001135-001
Report No. 00229
Report Version 1.3

Document Version Control

Version	Date	Name	Change
0.1	20 Oct 2011	B Martin	Initial draft
0.2	27 Oct 2011	R Burns	Review
1.0	27 Oct 2011	R Burns	Copy released to client for review.
1.1	16 Nov 2011	B Martin	Addition of client review points
1.2	25 Nov 2011	B Martin	Additional client comments reviewed.
1.3	14 Dec 2011	B Martin	Corrected above / below 100 hz

Suggested citation:

Martin, B, MacDonnell, J, Vallarta, J, Lumsden, E and Burns, R. 2011. *HYWIND Acoustic Measurement Report: Ambient Levels and HYWIND Signature.* Technical report for Statoil by JASCO Applied Sciences.

Contents

Tables

Figures

1. Introduction

1.1. Background

Jasco Applied Sciences was contracted by Statoil to conduct a continuous underwater acoustic recording programme in order to attempt to identify any discernible underwater acoustic signature from the HYWIND floating wind turbine and structure at the HYWIND test site to the West of Stavanger. In addition to recording at the HYWIND site, Statoil also requested that an identical recording configuration be conducted at a control site with comparable natural environmental conditions, 10km from the HYWIND test site (Figure 1). Both sites are relatively close (within several kilometres) to two local shipping fairways which pass closer to the HYWIND site than the control site.

Jasco completed the 150 day recording programme with 100% data capture in August 2011 and this report provides an initial analysis of elements of the acoustic data recovered from the recording programme.

The HYWIND structure and turbine, photographed during the deployment of the initial phase of recording are shown at Figure 2.

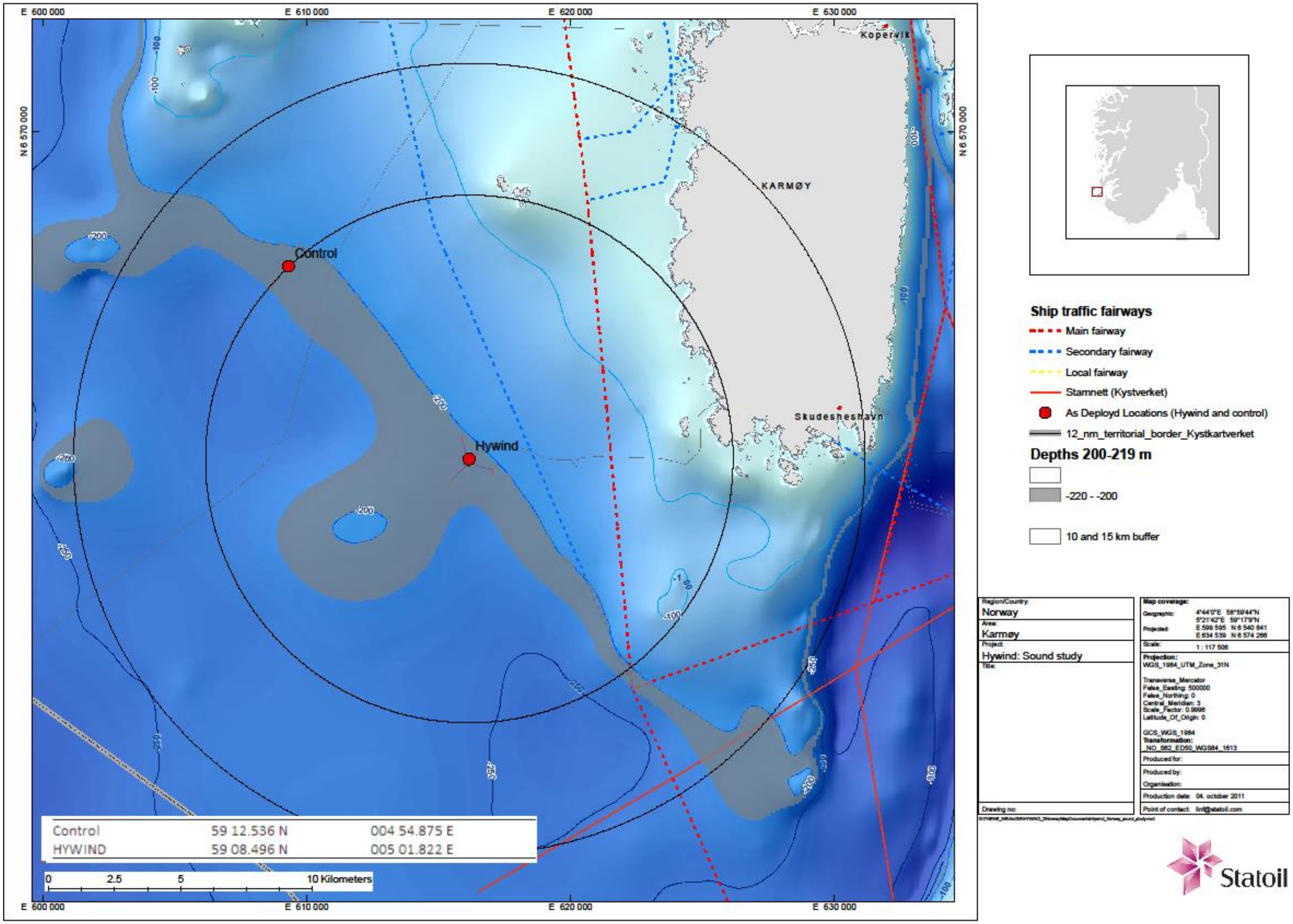

Figure 1: Location of the Statoil HYWIND turbine, the HYWIND recorder, control recorder, and the local shipping fairways.

Figure 2: HYWIND floating wind turbine, 28 March 2011.

The recording programme was structured to provide two, 75 day continuous recording periods using a bespoke mooring system and JASCO's Autonomous, Multi-channel, Acoustic Recorders (AMARs) to provide wideband recording and to achieve a client-specified mid-water column recording geometry relative to the HYWIND structure.

Both recording periods for each of the recording sites returned 100% continuous acoustic data which was extracted from the recorders and combined with third-party AIS and METOCEAN data and delivered to Statoil on two external hard disk drives for archiving and analysis.

1.2. Report Overview

This report provides ambient data analysis for the HYWIND data set, as well as an initial review of three events that JASCO believes are associated with the HYWIND structure. The ambient analysis includes for each deployment and each mooring:

- Plots of the hourly peak amplitude

- Plots of the hourly peak sound energy
- Two-month summary spectrograms, band-level plots and percentile plots.
- Two-week detailed spectrograms, band-level plots and percentile plots.

JASCO has also provided processed data files providing minute-by-minute data for:

- 1/3rd octave levels
- Decade band levels
- Total broadband level
- RMS and peak sound levels
- Number of shipping-like tonals present
- Number of seismic pulses detected, and max seismic pulse SPL.

1.3. Data Collection Overview

A technical description of the recording methodology and equipment as well as the quality control and quality assurance documentation associated with JASCO's deployment, recording and data processing methodologies was provided in JASCO document 00228, dated 21 September 2011. This section provides a brief overview of the recorders used and their data collection properties.

Recordings were made with JASCO's AMAR acoustic recorders. The recorders were set to record continuously at a sampling rate of 40 000 samples per second (40 ksps). The recording electronics have an integral anti-aliasing filter with a 3 dB cut-off of 0.49 * sampling rate, or 19.6 kHz. The filter is down 20 dB at 0.51 * sampling rate, and 120 dB down at .53 * sampling rate. The AMAR has a 24-bit analog-to-digital converter, with a dynamic range of 104 dB. GeoSpectrum M8E hydrophones were used with the AMAR. At a sampling rate of 40 ksps, the spectral noise floor of the AMAR and hydrophone is approximately 25 dB re 1 $\mu Pa^2/Hz$. The maximum input signal level is ~171 dB re 1 μPa.

2. Analysis Methods

2.1. AMBIENT SOUND LEVELS

The aim of ambient sound analysis is to document the range of sound levels encountered and their rate of occurrence. Sound level as a function of time and frequency is known as the spectral density over time, and can be plotted as a spectrogram (see e.g. Figure 12). The spectral density is calculated using the Fourier transform (Oppenheim and Shafer, 1999) and is the sound pressure level in 1 Hz-wide frequency bands. The sound levels within decade bands are also presented as a function of time using band-level plots (e.g. Figure 11). The range and occurrence of sound levels can be found by calculating quartile spectral levels. Quartile spectral levels are histograms of the spectral density values for the 5th, 25th, 50th, 75th, and 95th percentiles, where the 50th percentile is equal to the median of the spectral distribution and the 95th percentile is the level exceeded by 95% of the data (see e.g. Figure 10). The 95th percentile represents the quietest noise state that is expected to occur. The 5th percentile, the loudest state expected to occur, typically represents sound levels associated with occasional events such as nearby shipping or extreme weather.

As a measure of relative overall sound levels and as an indication of possible sources of sound, the percentile level plots can be compared with the so-called Wenz curves (Wenz, 1962) that represent the contributions of various sound sources to ambient sound levels in the oceans (Figure 3). These curves were developed using long-term acoustic recordings from the West Coast of the United States. Recent studies in the same area (Andrew 2011) has shown that ambient noise levels in the frequency range of 10 – 60 Hz have increased by 6-12 dB due to increased levels of shipping.   Levels from 60 – 100 Hz are increased by 2 – 6 dB. The proximity of the shipping fairways (Figure 1) to the project sites suggests that the received levels may exceed the Wenz levels.

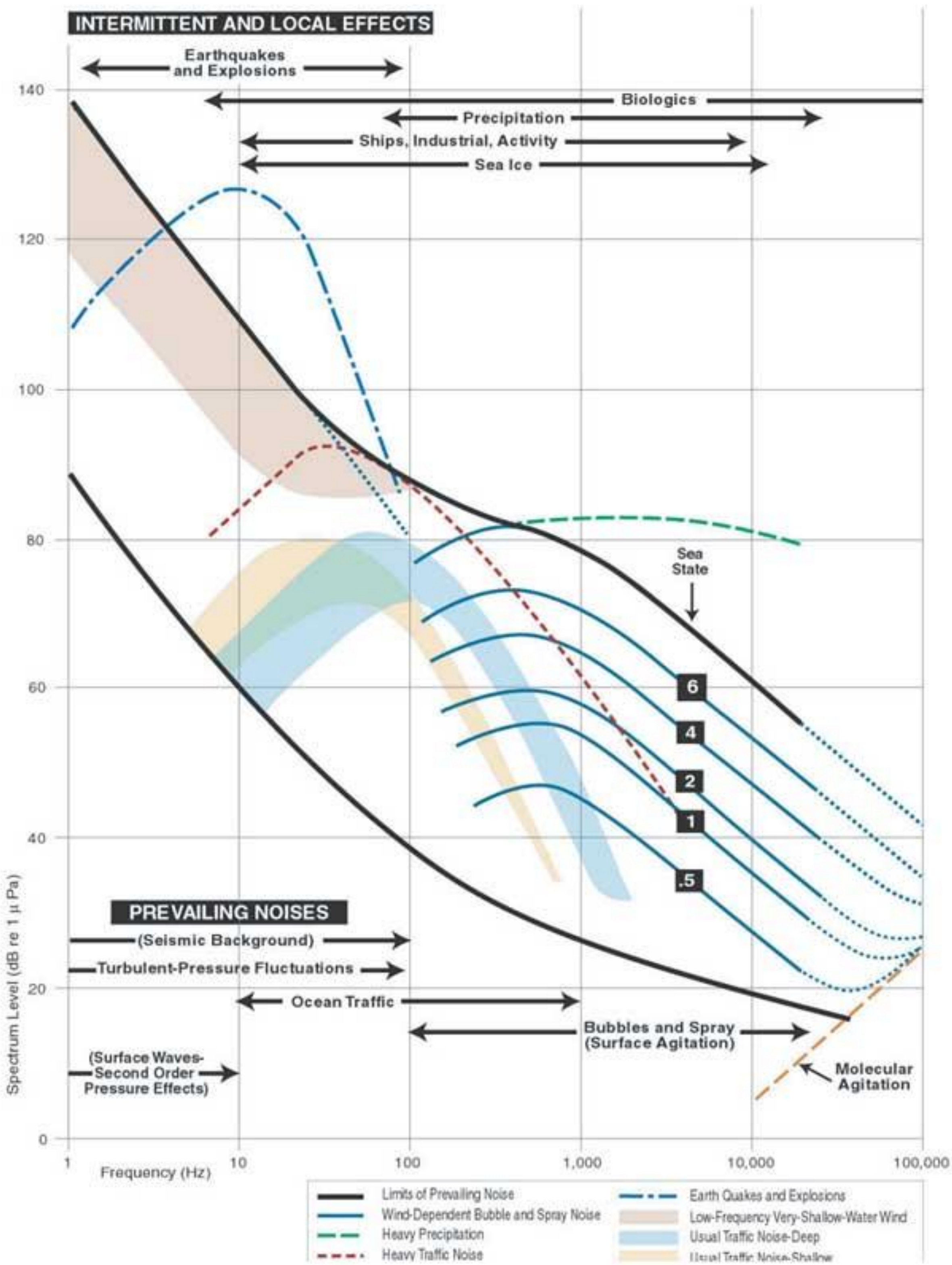

Figure 3: Wenz curves of ambient noise in the ocean (National Research Council, 2003, as adapted from Wenz, 1962).

2.2. TIME SERIES VALUES

The first step in computing the time series peak amplitude and peak sound energy is to perform a spectral calibration on the raw time series. This calibration adjusts the time series to account for the frequency dependent response of our hydrophones. To calibrate the time series it is converted to the frequency domain using an FFT, then divided by the frequency response of the hydrophone, and converted back to the time domain using an inverse FFT. The resulting time series in then stored in units of μPa.

The peak amplitude for each minute of data is found as the absolute value of the calibrated time series (units of dB re 1 μPa). The hourly maximum value is provided as a separate plot. The sound energy density is found using a sliding window one minute long and computing the sum of the square of the calibrated time series. The sum is divided by the number of samples and the square root is taken, which is the one-minute RMS (root-mean-square) sound pressure level (SPL) value. The product of the squared RMS SPL and time is proportional to energy density. The RMS values were multiplied by 60, squared, and summed over each hour of the deployment. The hourly sum of this value was divided by the density of the water as well as the sound speed to give the energy density (unit of J/m^2).

2.3. AUTOMATED SHIPPING DETECTOR

Large shipping vessels generally travel at constant speed. Their acoustic signature consists of a number of narrow, frequency-band peaks (tonals) generated by the vessel's motors, propellers, pumps, and gearing (Arveson and Vendittis 2000) . An automated shipping detector was implemented to detect tonals in the recorded acoustic data.

To detect tonals, the acoustic data were divided into two-second intervals and their spectra calculated using the fast Fourier transform (FFT) with a Hamming window and 50% overlap. Sixty, two-second samples were then averaged to obtain spectrograms representing one minute intervals of recorded data. The spectra were normalized in the frequency band between 1 and 1000 Hz using the split-window normalizing method (Crocker 1999) and searched for narrowband peaks. A positive detection was counted when a tonal was present in three of four adjacent one-minute intervals. Detection confidence was indicated by the number of peaks detected. While this approach works well for heavy shipping traffic, it is not appropriate for detecting fishing vessels or pleasure craft that regularly change speed.

Note that if the HYWIND turbine produces sounds with stable tonal content, then the shipping detector is likely to detect HYWIND as well as shipping.

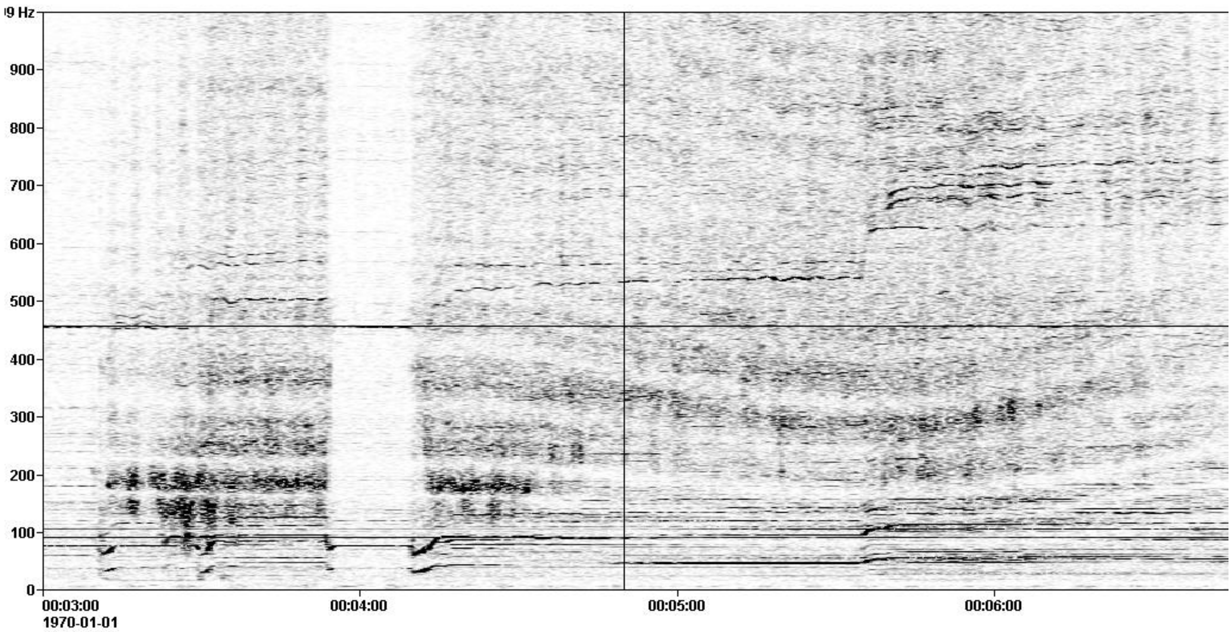

Figure 4: Spectrogram showing tonals from heavy shipping activity. FFT size = 131072 samples, 80000 real data samples, 60000 sample advance, Hamming window. This curved pattern in the center of the image is a typical 'bathtub' pattern that occurs as a vessel approaches and then leaves a sensor (closest point of approach is at the inflection point). Note how many of the tonals from the shipping show rapid changes in frequency as the vessel speed or gearing is changed. This is a generic sample not taken from the HYWIND program.

2.4. SEISMIC EVENT DETECTION

As part of the automated acoustic analysis suite, JASCO has implemented a procedure designed to provide a high probability of detecting and quantifying seismic events in the acoustic recordings. As with the ambient noise analysis, the first step in seismic event detection is to determine the spectral density (sound level as a function of time and frequency). Seismic signals are of short duration (~1 sec), so the spectral density is calculated using a short-time implementation of the fast Fourier transform (STFT) (Oppenheim and Schafer, 1999). There are several STFT parameters (sampling rate, window length, zero padding, and analysis window overlap) and the choice of values affects the overall performance of the detector / classifier. Experience gained through many projects has helped JASCO optimize the parameters for best detection and classification. For seismic events the best results occur with a 16384 sample FFT, using 10000 samples of real data and a 7500 sample overlap.

A detection data space is then defined from the spectral density. This is done by normalizing the levels in each frequency bin at each time step by the median amplitude of the frequency bin for a processing block (i.e. STFT window length). The normalized values are then compared to an empirically chosen detection threshold (typically four times the median value). The bins above the threshold are set to one and the bins below the threshold are set to zero. For each time slice, the total number of frequency cells in the range of 30 – 500 Hz that are ‘1’ are summed to create a detection time series.

Seismic events are detected based on the periodicity of airgun events. The detection time series is then auto-correlated to amplify periodic events. A brute-force search of the possible pulse spacing's (3.5–20 s) is performed. The base time and spacing with the most peaks is further processed to determine the actual peak repetition rate, and to identify all peaks in the series. The sequence is rejected if it has fewer than 10 peaks in 5 minutes, or the peaks are irregular (more than one peak in three are missing). This approach has proven extremely powerful, allowing detection of weak seismic pulses, in the presence of mammal calls, with a high degree of certainty.

Once a period is extracted from the correlation function, it is used to locate the time of each seismic event in the raw time series. The root-mean-square (rms) sound pressure levels (SPLs) are then computed as follows:

1. Compute cumulative energy (square pressure) for the duration of each pulse from 1 s before to 1 s after the detection. The detection time generally falls near the peak of the pulse.
2. Determine the interval over which the cumulative energy for each received pulse increases from 5 to 95% of the total.
3. For each pulse, compute the standard 90% rms SPL by dividing the cumulative square pressure over the 5–95% interval by the number of samples in this period, and taking the square root.
4. For each pulse, compute the sound exposure level (SEL) by time integrating the square pressure over the pulse window in the time domain.

The time and SPL of each seismic event are stored in the XML output file. Sample detections a distant weak seismic sequence is shown in Figure 5.

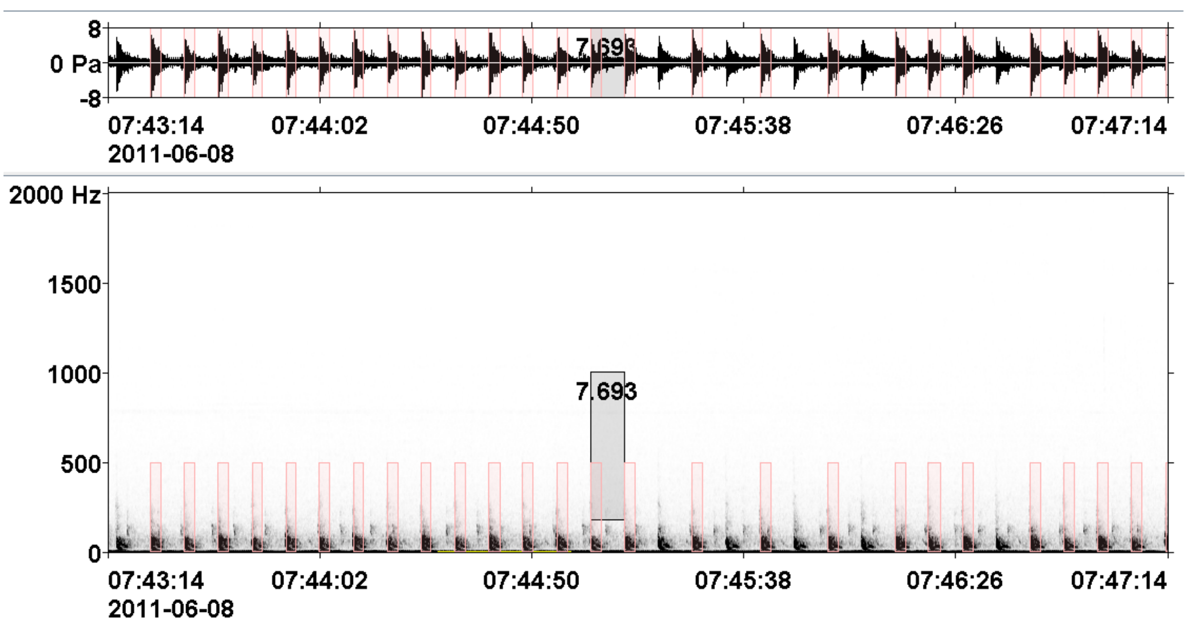

Figure 5: Time series (top, units Pascals) and Spectrogram (bottom) of distant seismic detections from HYWIND Control Station, 8 June 2011. Pink boxes are the auto-detected seismic events. The annotation indicates a pulse spacing of 7.7 seconds. FFT size = 16384 samples, 10000 samples of real data, 2500 second advance, Reisz window. The top window

3. Results

3.1. Deployment 1, 28 March – 31 May 2011

3.1.1. Peak Amplitude

The hourly peak sound pressure levels (SPL) for the spring 2011 deployment for both HYWIND Control Station and HYWIND Monitoring Station are shown in Figure 6 and Figure 7, respectively. The HYWIND station show a much larger occurrence of high level events than the control station.

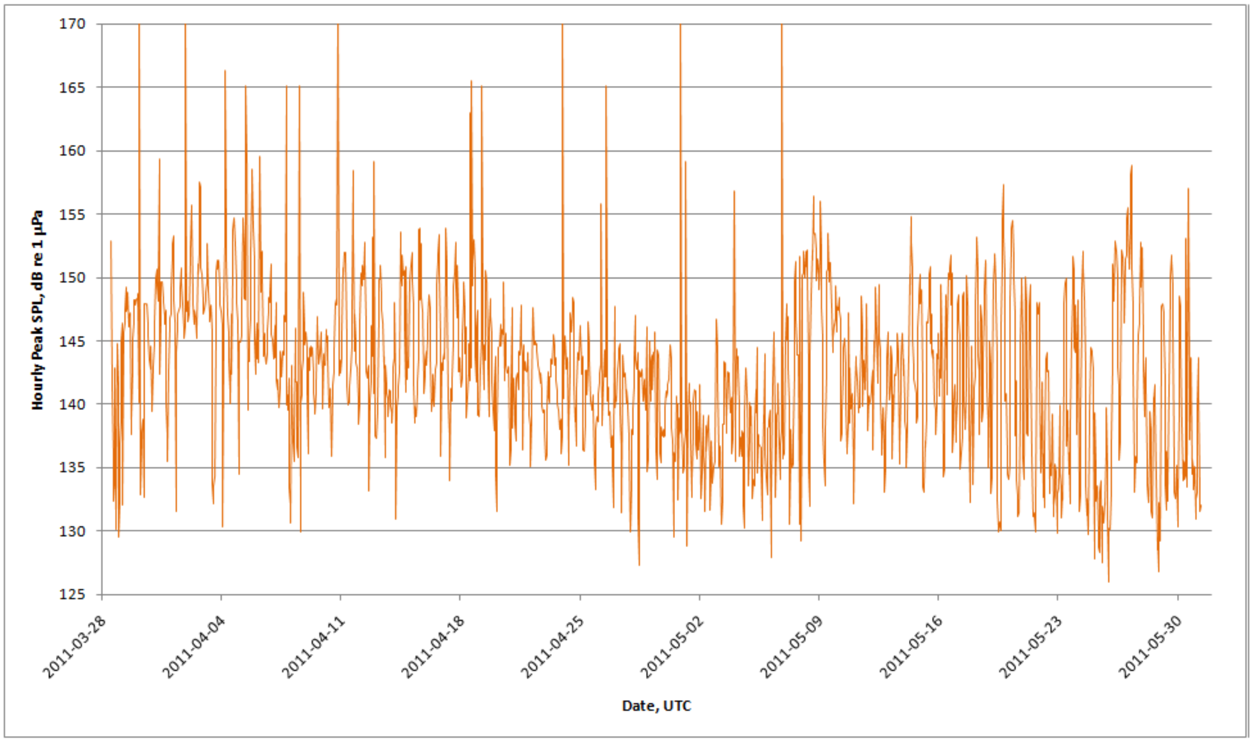

Figure 6: Hourly Peak SPL (dB re 1 µPa) for the spring 2011 deployment at HYWIND Control Station. 171 dB re 1 µPa is the maximum sound pressure level recorded by the AMAR for the HYWIND configuration.

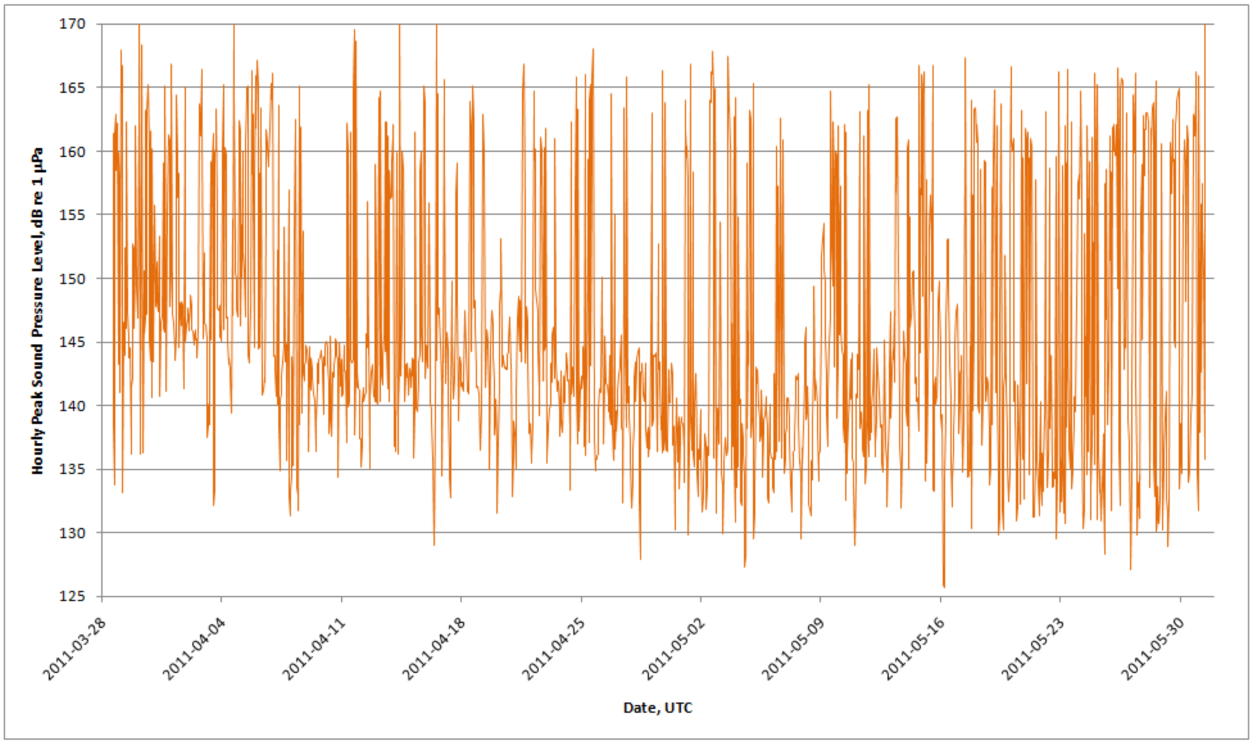

Figure 7: Hourly Peak SPL (dB re 1 µPa) for the spring 2011 deployment at HYWIND Monitoring Station. 171 dB re 1 µPa is the maximum sound pressure level recorded by the AMAR for the HYWIND configuration.

3.1.2. Peak Sound Energy

The hourly sound energy density for the spring 2011 deployment for both HYWIND Control Station and HYWIND Monitoring Station are shown in Figure 8 and Figure 9, respectively.

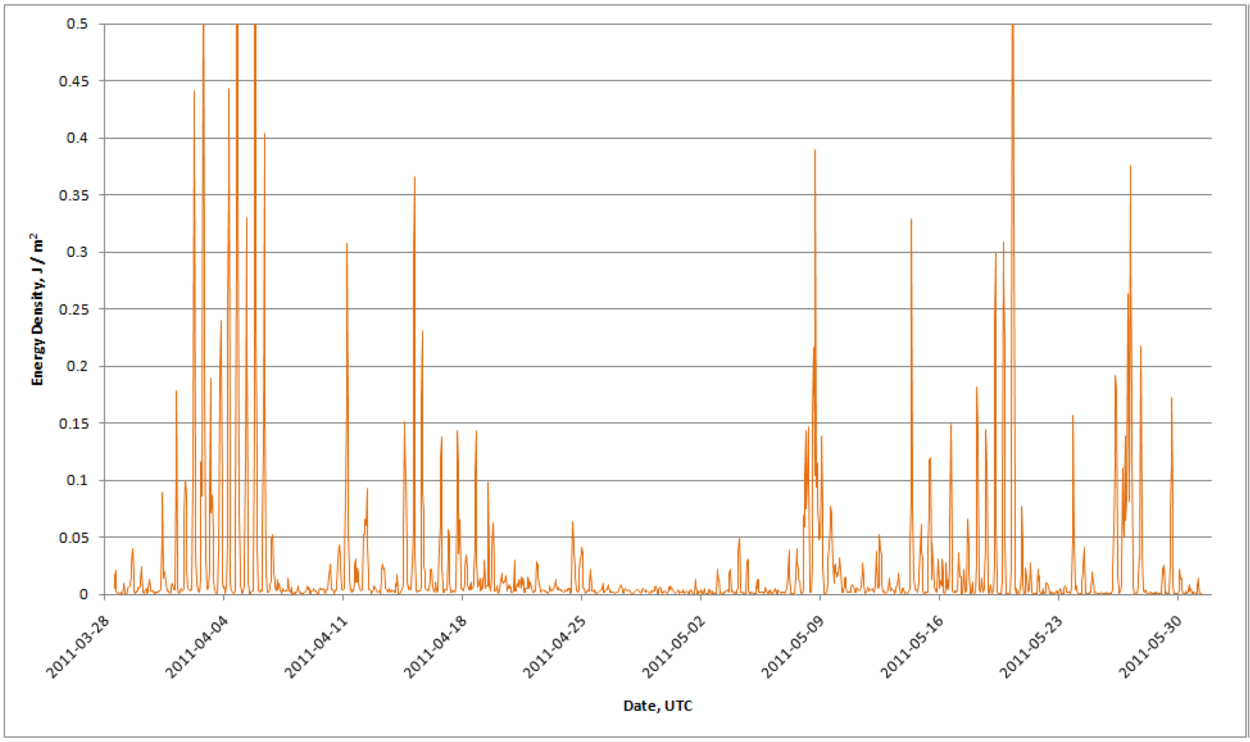

Figure 8: Energy Density (J/m²) for the spring 2011 deployment at HYWIND Control Station

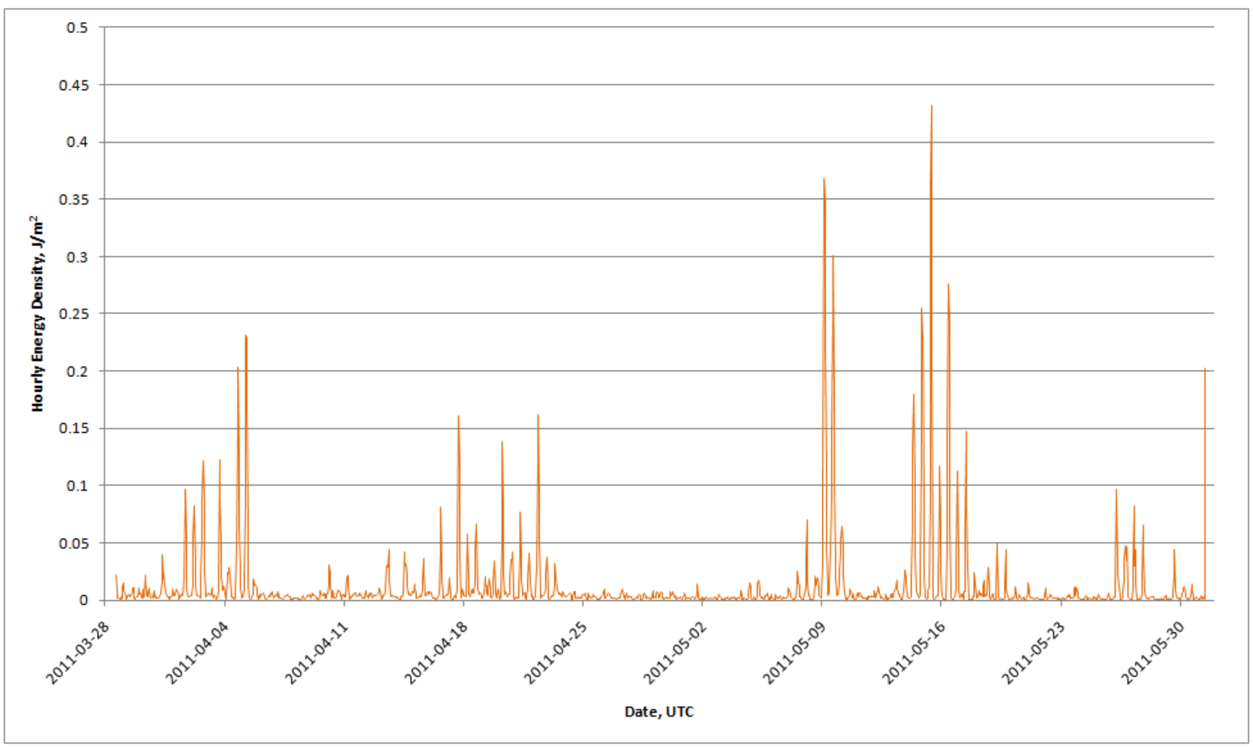

Figure 9: Energy Density (J/m²) for the spring 2011 deployment at HYWIND Monitoring Station

3.1.3. Ambient Plots

The percentile spectral levels for the spring 2011 deployment for both HYWIND Control Station and HYWIND Monitoring Station are shown in Figure 10 and Figure 13, respectively. The levels at both stations decreased essentially linearly from 50 Hz to 20 kHz, but the HYWIND Monitoring Station clearly shows a peak at 25 Hz with a harmonic at 50 Hz, a weak harmonic at 100 Hz and a more pronounced harmonic at 150 Hz. It is proposed that these tones are due to the some sort of electrical device in the mooring. Possible sources include:

1. Mechanical coupling of the rotation of the cooling fan for the power conversion electronics, which runs at 1500 rpm (Peter Marcus Kolderup Greve, 14 Oct 2011)
2. Mechanical coupling of vibrations from the transformers in the AC-DC-AC 22 kVA power conversion electronics.

These tones are unlikely to be induced electro-magnetic fields detected by the AMARs. The AMAR uses shielded hydrophones and shielded electrical cabling to eliminate induced electro-magnetic field pick-up.

The broadband and decade band sound pressure levels (SPL) for the spring 2011 deployment for both HYWIND Control Station and HYWIND Monitoring Station are shown in Figure 11 and Figure 14, respectively.

The spectrograms for the spring 2011 deployment for both HYWIND Control Station and HYWIND Monitoring Station are shown in Figure 12 and Figure 15, respectively.

The band level and spectrogram plots are further broken down into 2-week plots contained in Appendix A.

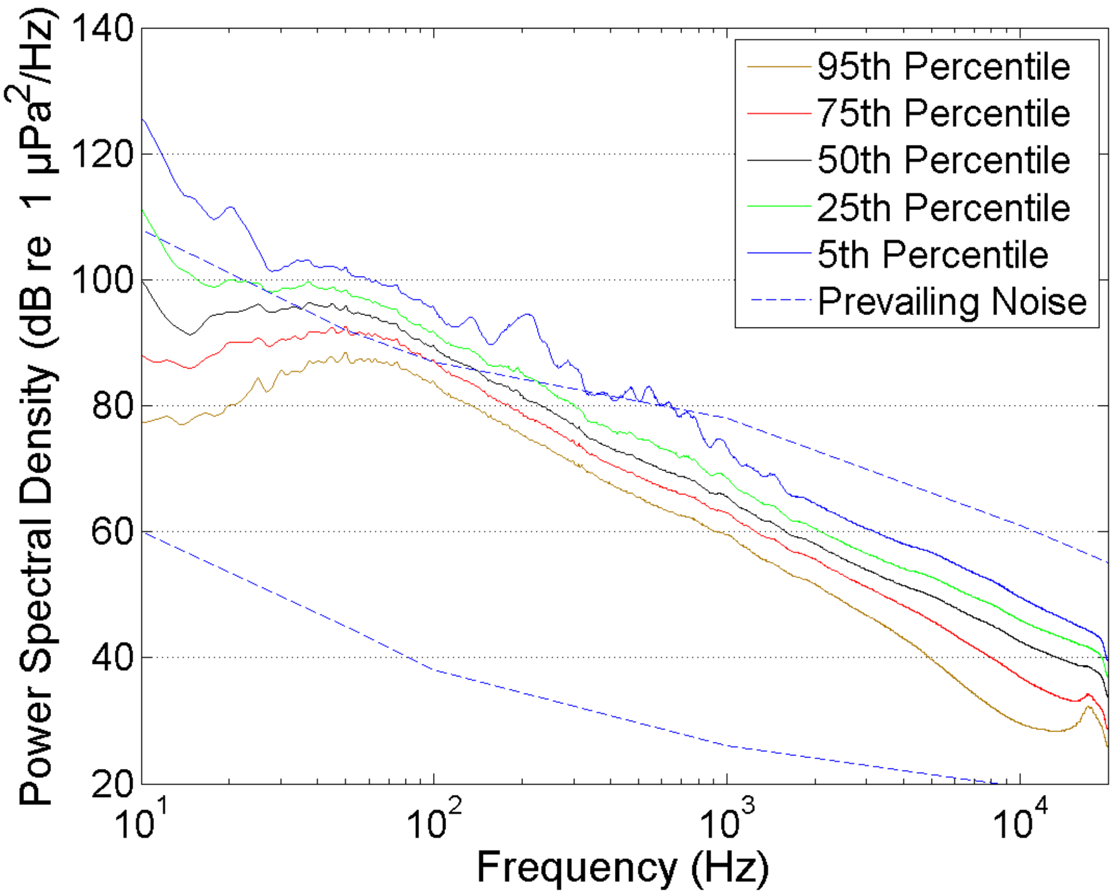

Figure 10: Percentile 1-min power spectral density levels (dB re 1 µPa²/Hz) for the spring 2011 deployment at HYWIND Control Station. The dashed lines are the 'Limits of Prevailing Noise' from the Wenz curves, Figure 3.

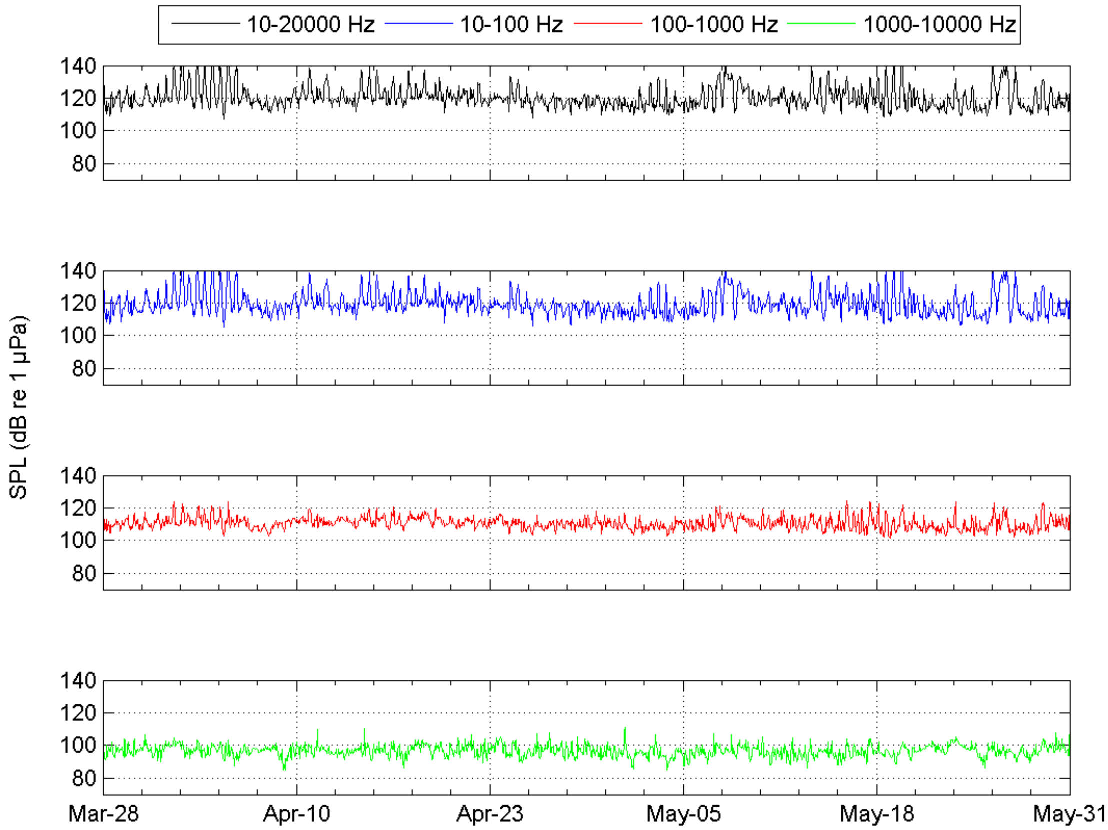

Figure 11: Broadband and decade band sound pressure levels (SPL) for the spring 2011 deployment at HYWIND Control Station.

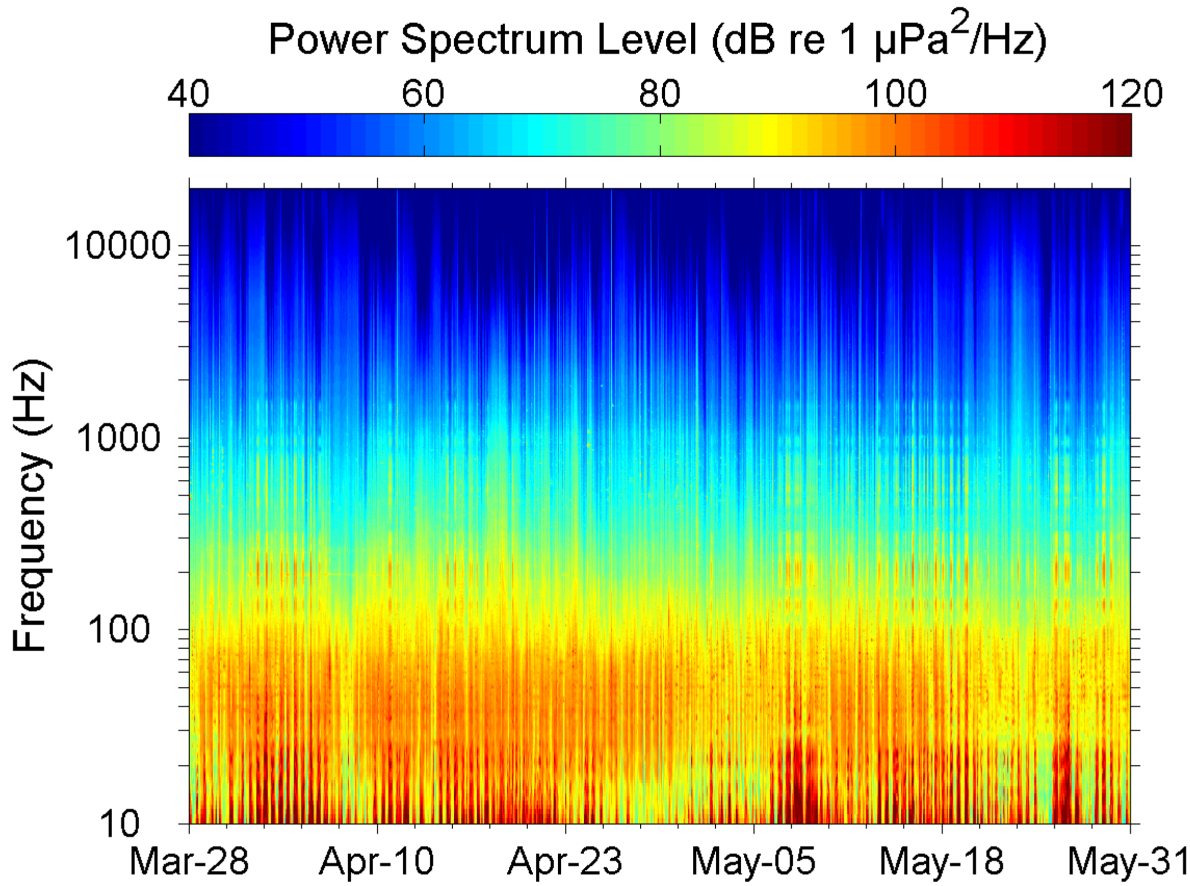

Figure 12: Spectrogram of underwater sound for the spring 2011 deployment at HYWIND Control Station.

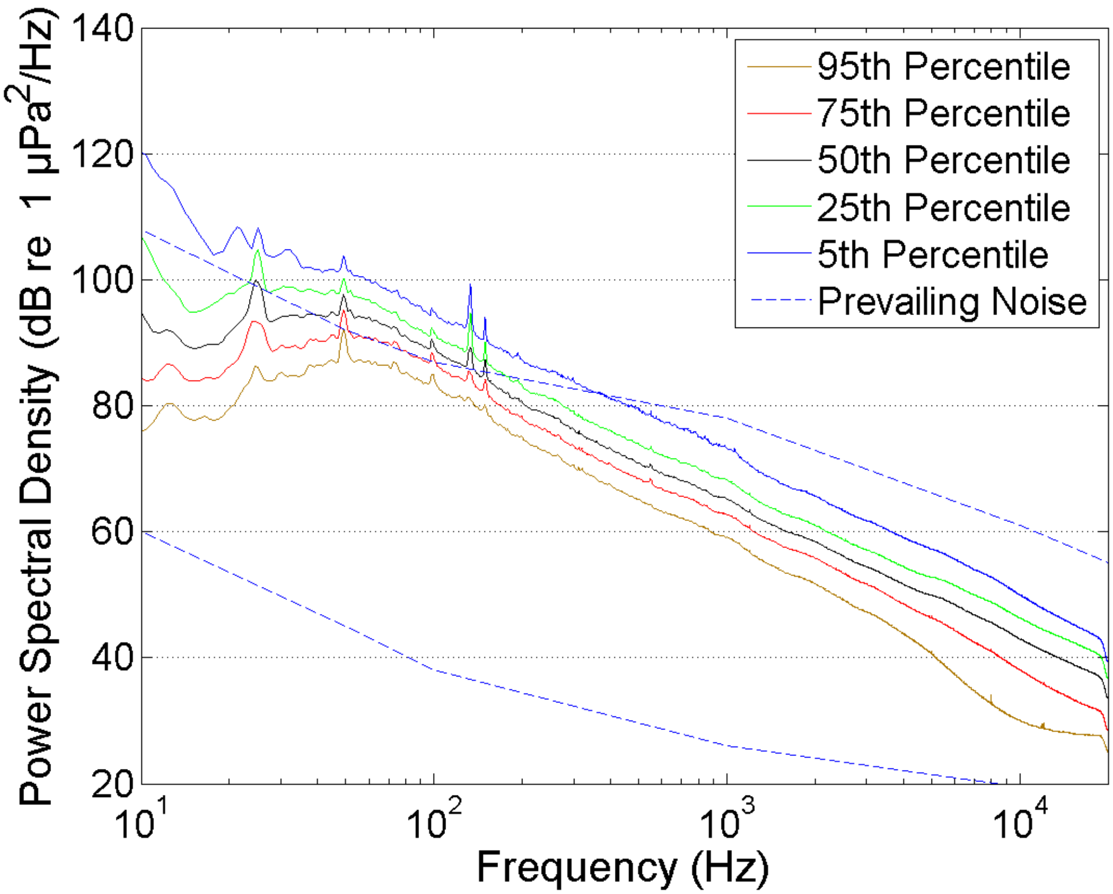

Figure 13: Percentile 1-min power spectral density levels (dB re 1 µPa²/Hz) for the spring 2011 deployment at HYWIND Monitoring Station. The dashed lines are the 'Limits of Prevailing Noise' from the Wenz curves, Figure 3.

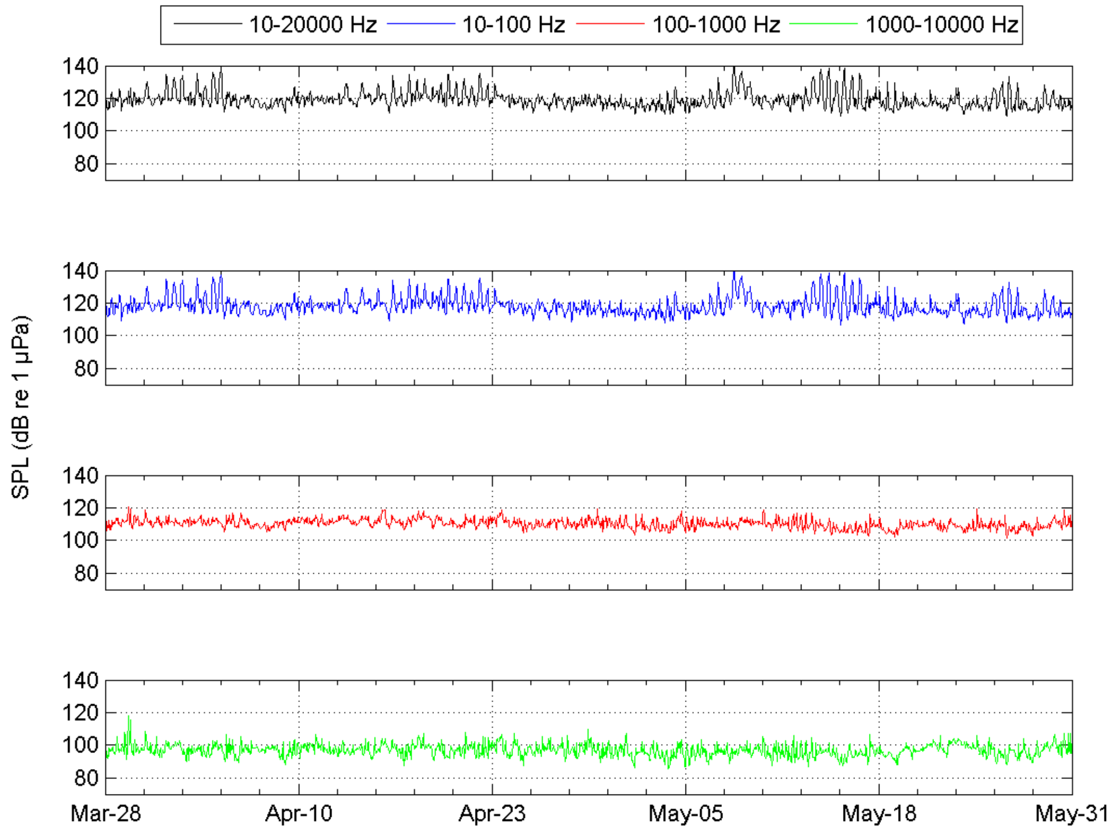

Figure 14: Broadband and decade band sound pressure levels (SPL) for the spring 2011 deployment at HYWIND Monitoring Station.

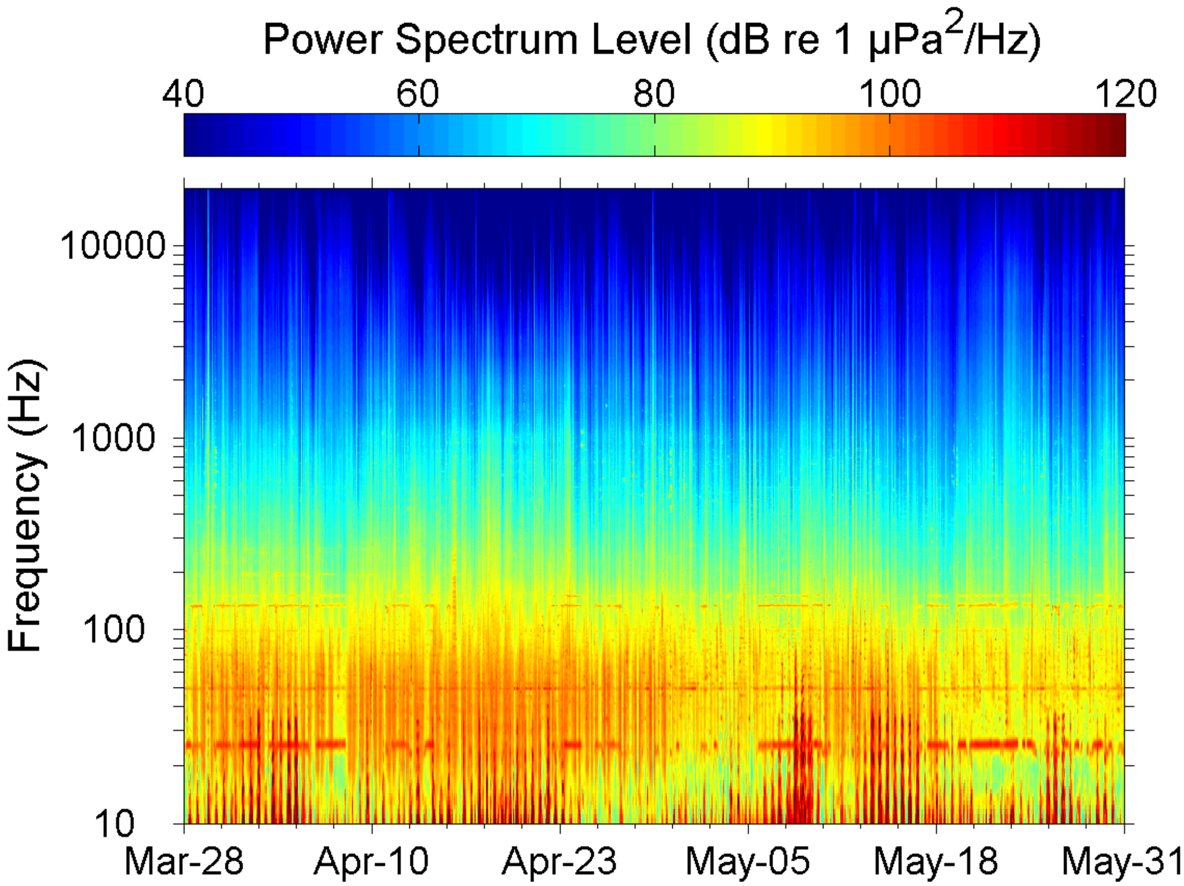

Figure 15: Spectrogram of underwater sound for the spring 2011 deployment at the HYWIND Monitoring Station.

3.1.4. Automatic Shipping Detections

JASCO ran the HYWIND data through its automatic shipping detector. The results are presented in Figure 16 for the spring deployment. It was anticipated that the HYWIND recorder could have a higher detection rate than the Control station since tones generated by the power conversion equipment would trigger the shipping detector.

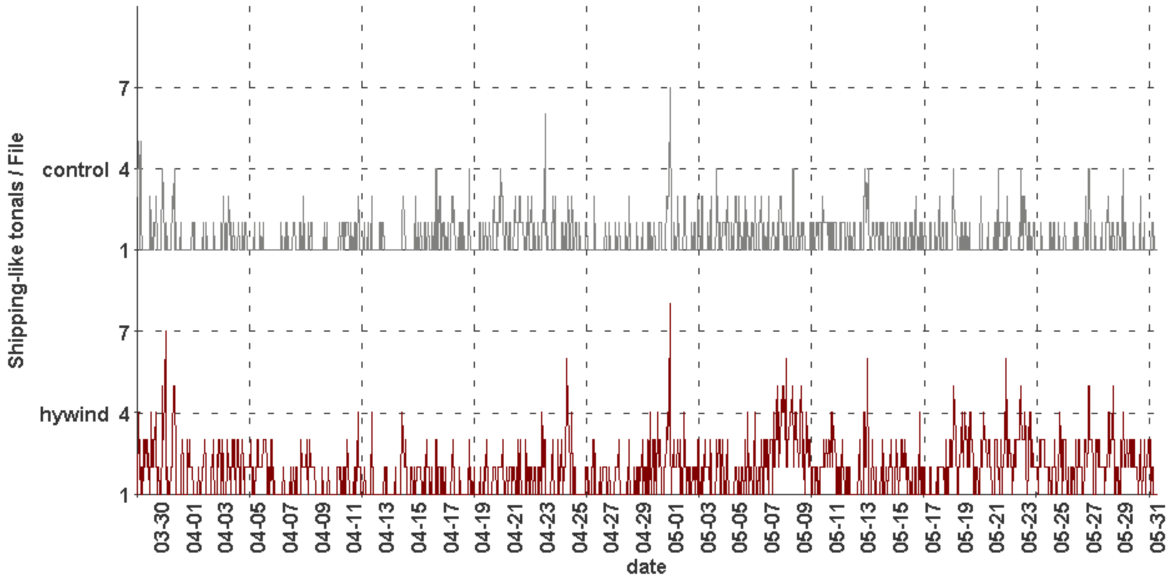

Figure 16: Automatic Shipping Detections, Spring Deployment.

3.1.5. Automatic Seismic Detections

JASCO ran its automatic seismic event detector on the HYWIND data. The results for the spring deployment are shown in Figure 17. The measured per-pulse SPLs appear to be slightly higher for the Control recorder, suggesting that the surveys were conducted north of the study area.

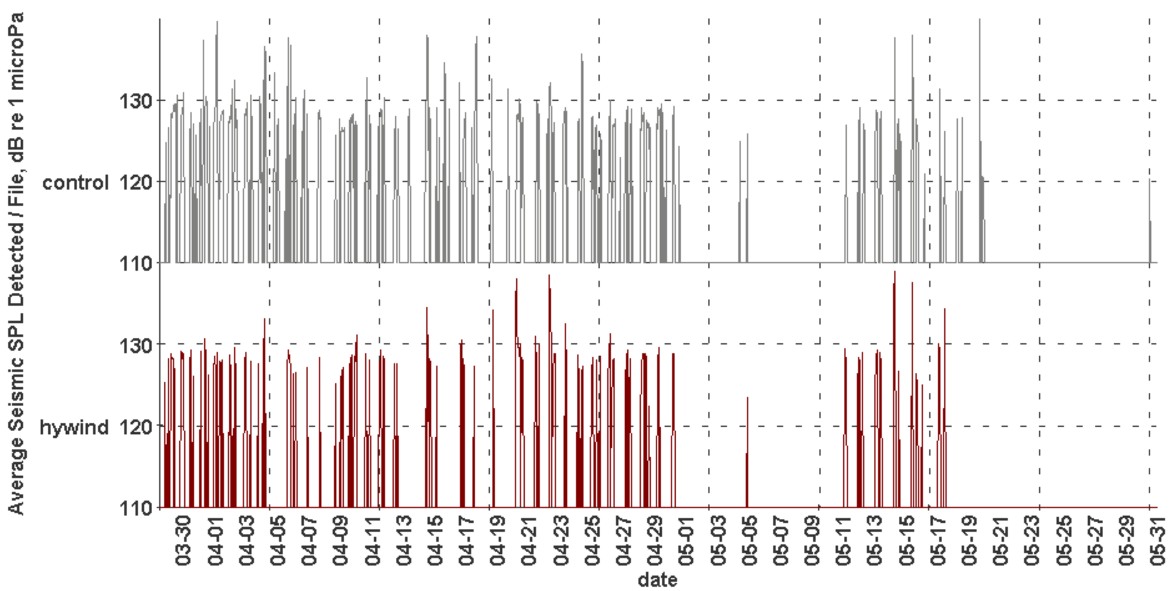

Figure 17: Automatic seismic sequence detections, shown the average pulse SPL per 1/2 hour file, Spring deployment.

3.2. Deployment 2, 31 May – 15 Aug 2011

3.2.1. Peak Amplitude

The hourly peak sound pressure levels (SPL) for the summer 2011 deployment for both HYWIND Control Station and HYWIND Monitoring Station are shown in Figure 18 and Figure 19, respectively. Similar to the spring deployment, there are higher peak level events on the HYWIND recorder than the Control recorder. The large number of peaks during the period of 31 May – 13 Jun are due to the data errors in that time period (see Section 4.4.2).

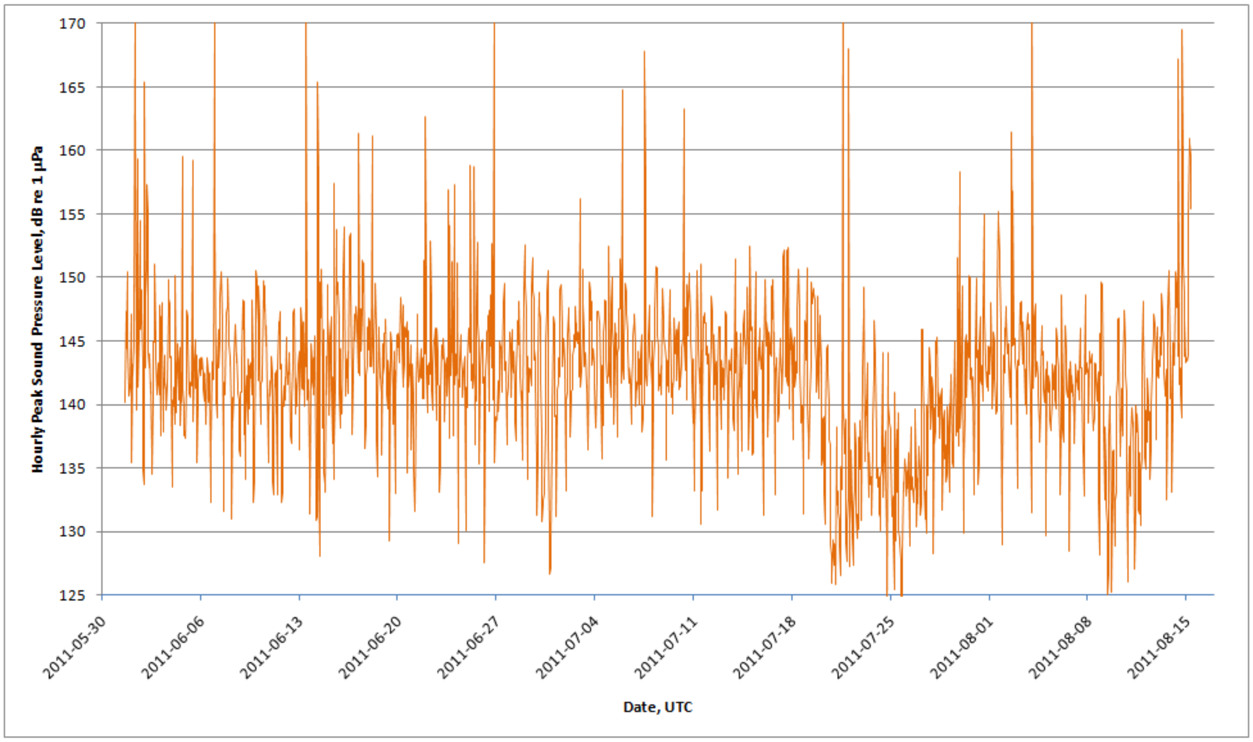

Figure 18: Hourly Peak SPL (dB re 1 µPa) for the summer 2011 deployment at HYWIND Control Station. 171 dB re 1 µPa is the maximum sound pressure level recorded by the AMAR for the HYWIND configuration.

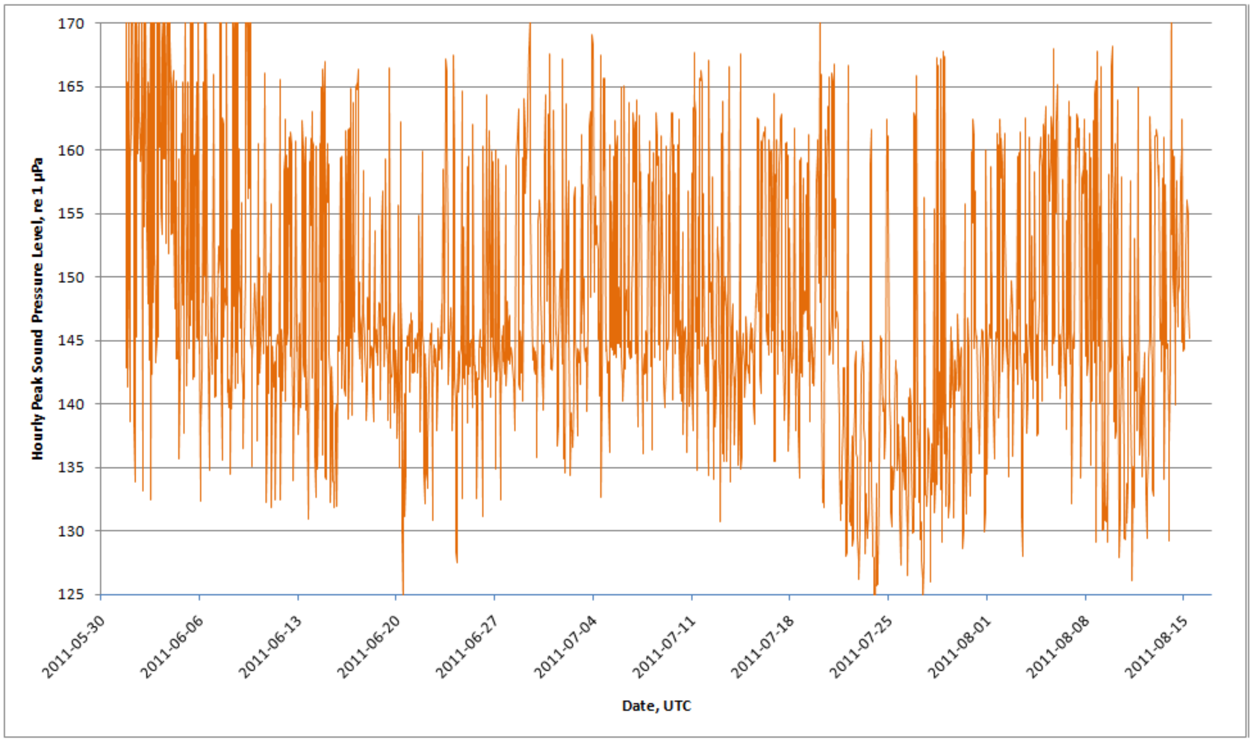

Figure 19: Hourly Peak SPL (dB re 1 µPa) for the summer 2011 deployment at HYWIND Monitoring Station. 171 dB re 1 µPa is the maximum sound pressure level recorded by the AMAR for the HYWIND configuration.

3.2.2. Peak Sound Energy

The hourly sound energy density for the summer 2011 deployment for both HYWIND Control Station and HYWIND Monitoring Station are shown in Figure 20 and Figure 21, respectively.

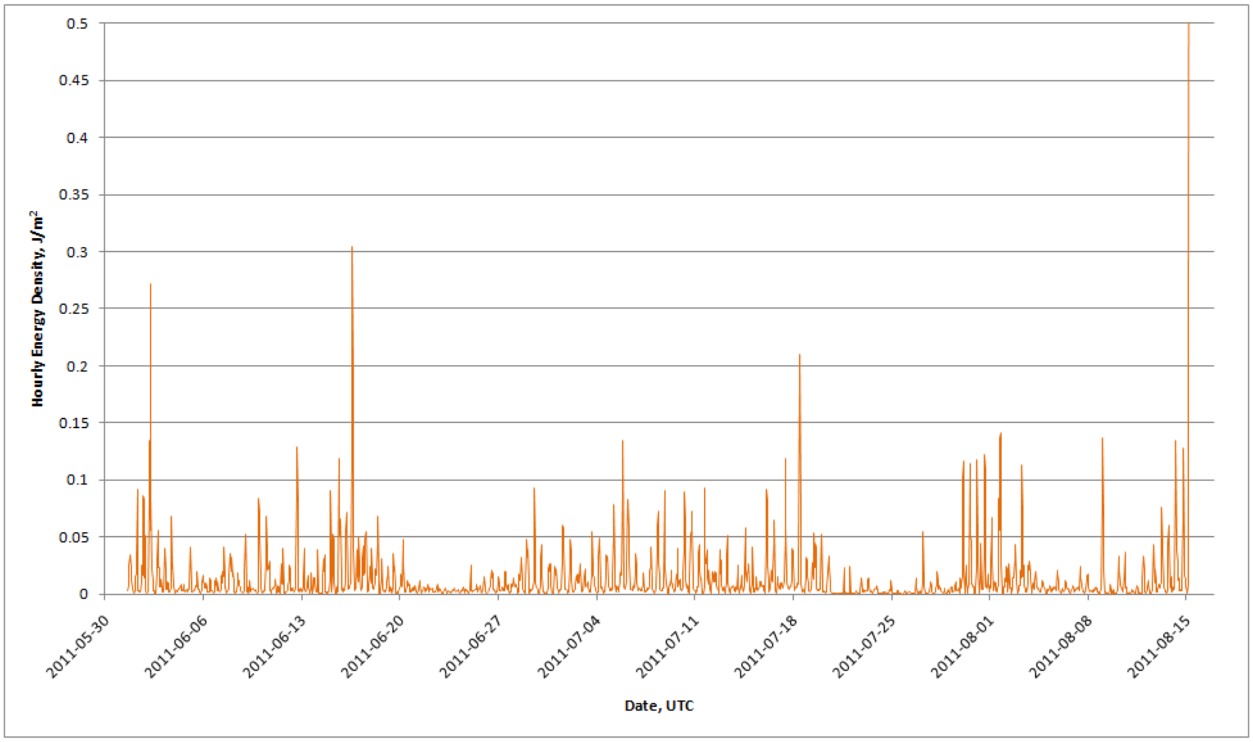

Figure 20: Energy Density (J/m2) for the summer 2011 deployment at HYWIND Control Station.

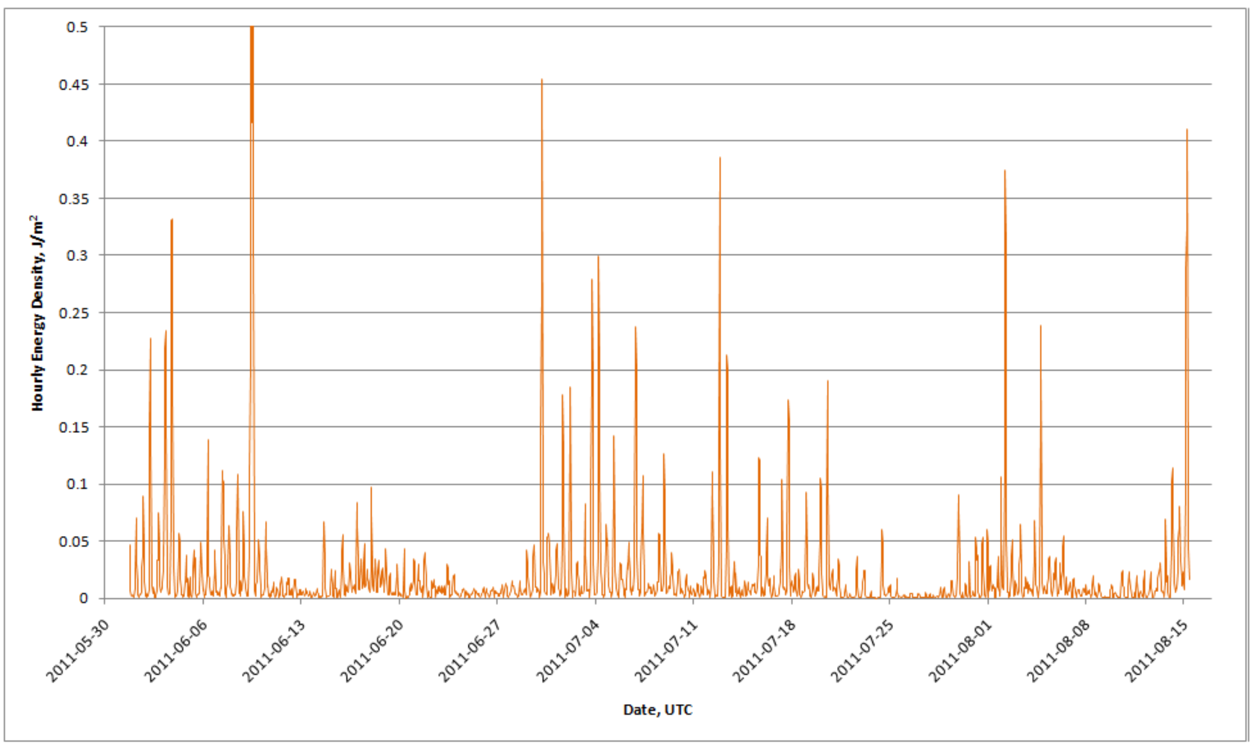

Figure 21: Energy Density (J/m2) for the summer 2011 deployment at HYWIND Monitoring Station.

3.2.3. Ambient Plots

The percentile spectral levels for the summer 2011 deployment for both HYWIND Control Station and HYWIND Monitoring Station are shown in Figure 22 and Figure 25, respectively., The levels at both stations decreased essentially linearly from 50 Hz to 20 kHz, but the HYWIND Monitoring Station clearly shows a peak at 25 Hz with a harmonic at 50 Hz, a weak harmonic at 100 Hz and a more pronounced harmonic at 150 Hz. It is proposed that these tones are due to the some sort of electrical device in the mooring. Possible sources include:

1. Mechanical coupling of the rotation of the cooling fan for the power conversion electronics, which runs at 1500 rpm (25 Hz) (Peter Marcus Kolderup Greve, 14 Oct 2011)
2. Mechanical coupling of vibrations from the transformers in the AC-DC-AC 22 kVA power conversion electronics.

These tones are unlikely to be induced electro-magnetic fields detected by the AMARs. The AMAR uses shielded hydrophones and shielded electrical cabling to eliminate induced electro-magnetic field pick-up.

The broadband and decade band sound pressure levels (SPL) for the summer 2011 deployment for both HYWIND Control Station and HYWIND Monitoring Station are shown in Figure 23 and Figure 26, respectively.

The spectrograms for the summer 2011 deployment for both HYWIND Control Station and HYWIND Monitoring Station are shown in Figure 24 and Figure 27, respectively.

The band level and spectrogram plots are further broken down into 2-week plots are presented in Appendix A.

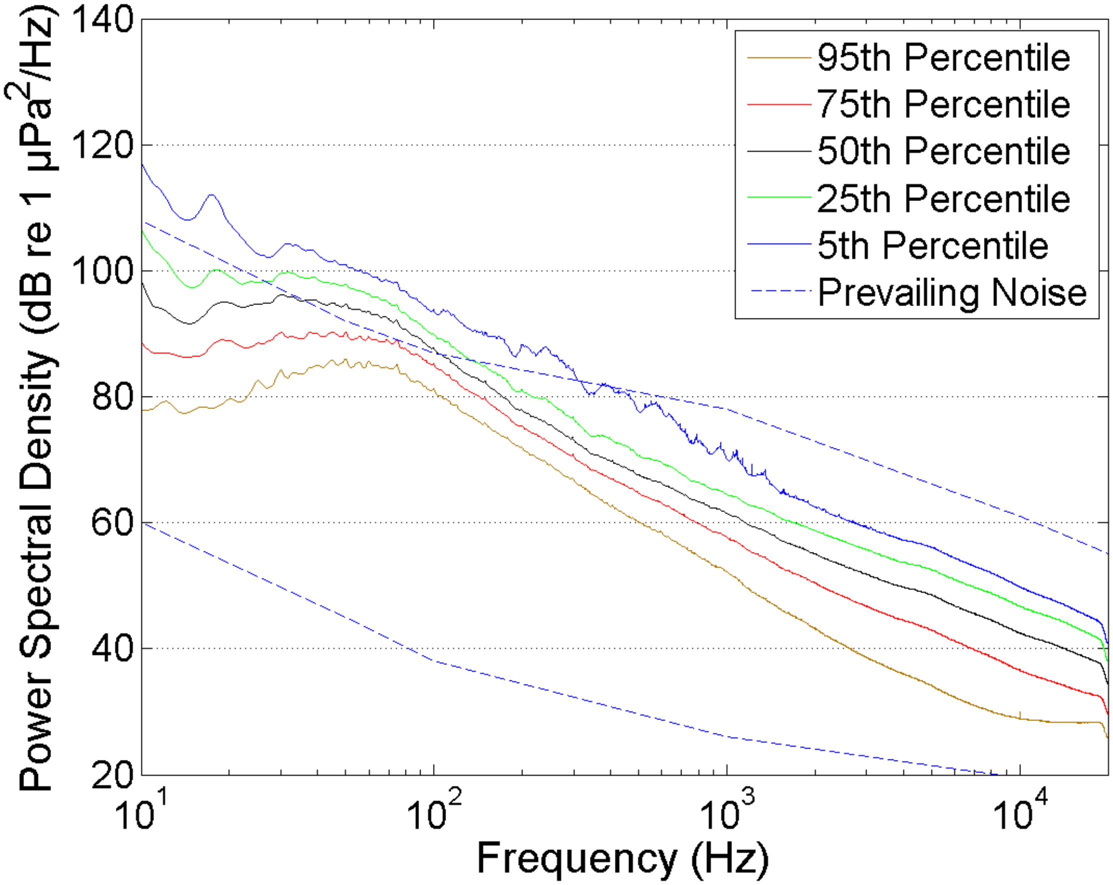

Figure 22: Percentile 1-min power spectral density levels (dB re 1 μPa^2/Hz) for the summer 2011 deployment at HYWIND Control Station. The dashed lines are the 'Limits of Prevailing Noise' from the Wenz curves, Figure 3.

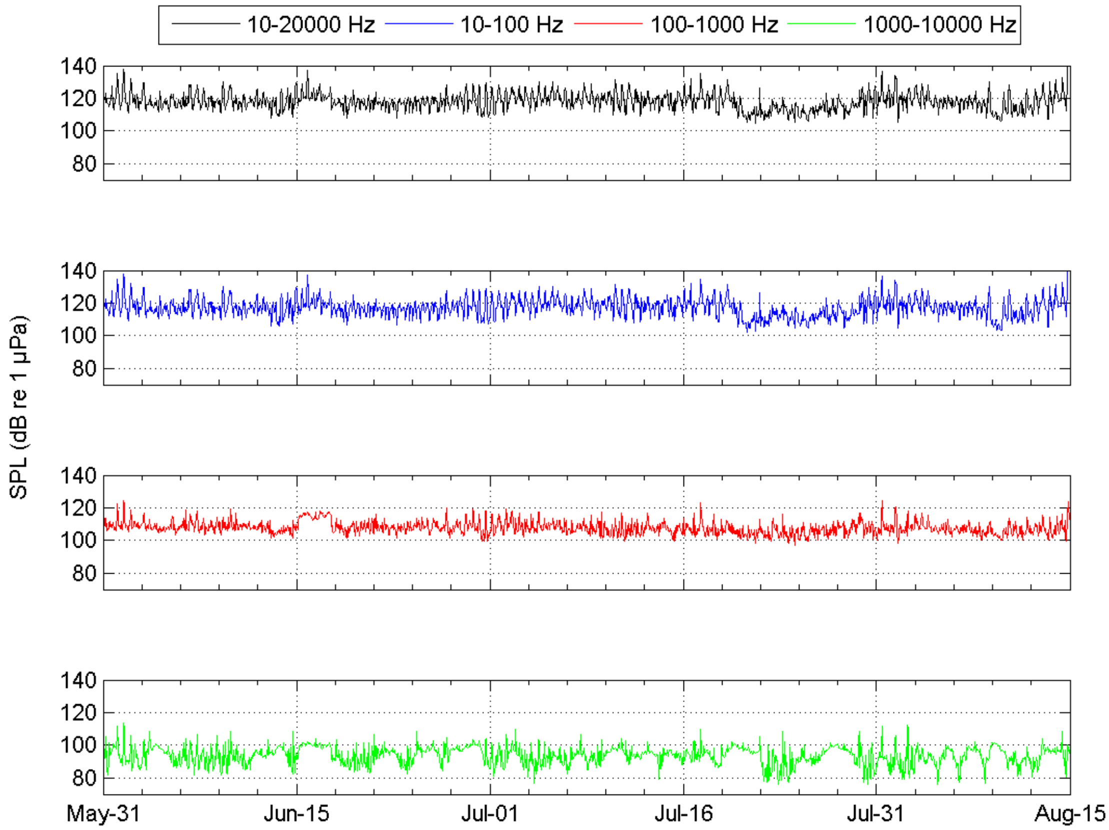

Figure 23: Broadband and decade band sound pressure levels (SPL) for the summer 2011 deployment at HYWIND Control Station.

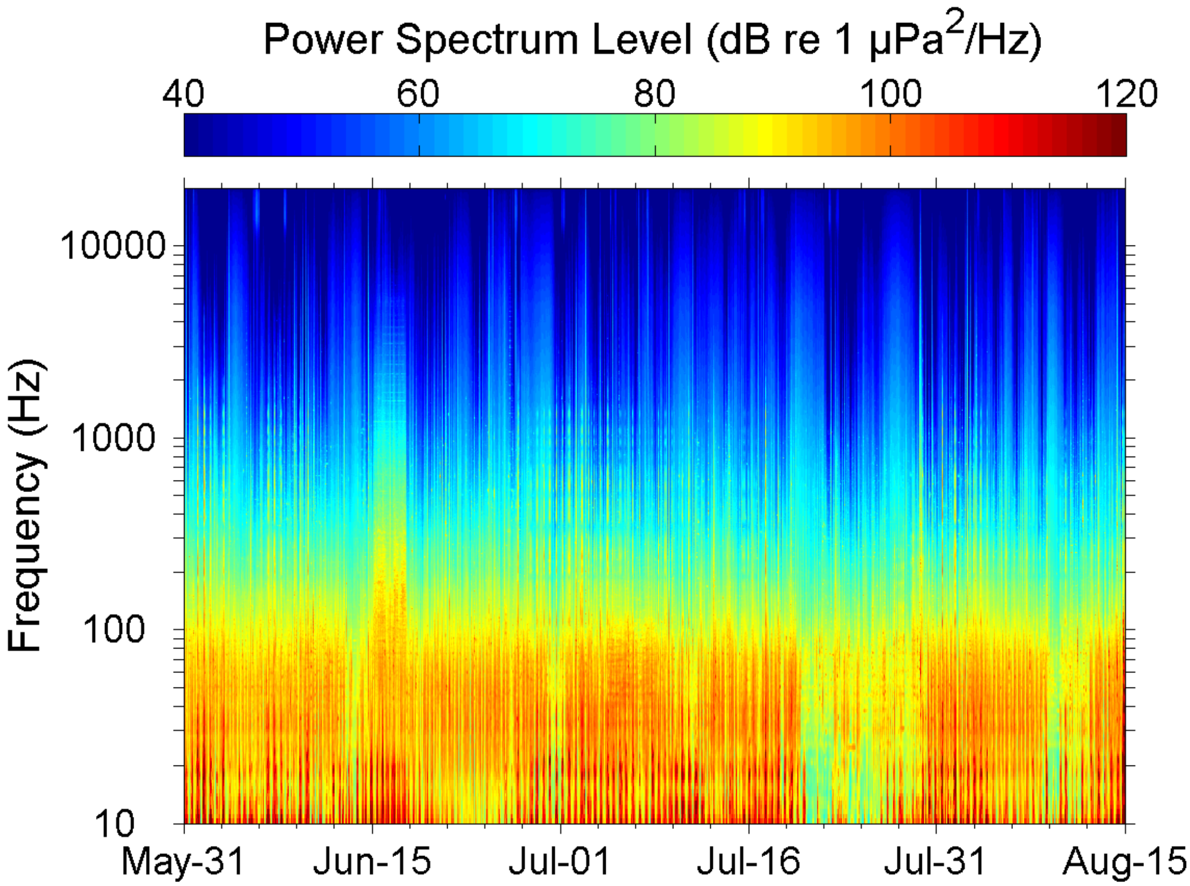

Figure 24: Spectrogram of underwater sound for the summer 2011 deployment at the HYWIND Control Station. There is a high intensity event on15 June that was caused by a vessel that appears to have been stationary near HYWIND for 2 – 3 days.

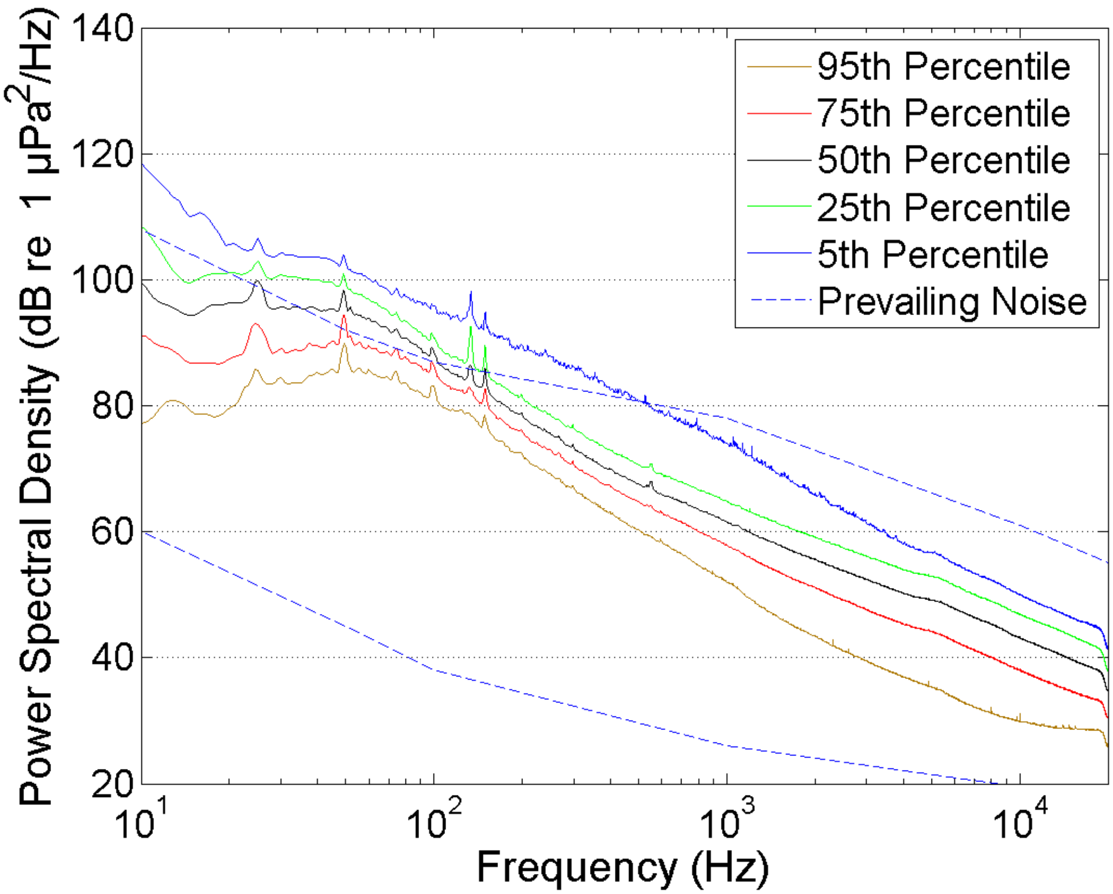

Figure 25: Percentile 1-min power spectral density levels (dB re 1 μPa²/Hz) for the summer 2011 deployment at HYWIND Monitoring Station. The dashed lines are the 'Limits of Prevailing Noise' from the Wenz curves, Figure 3.

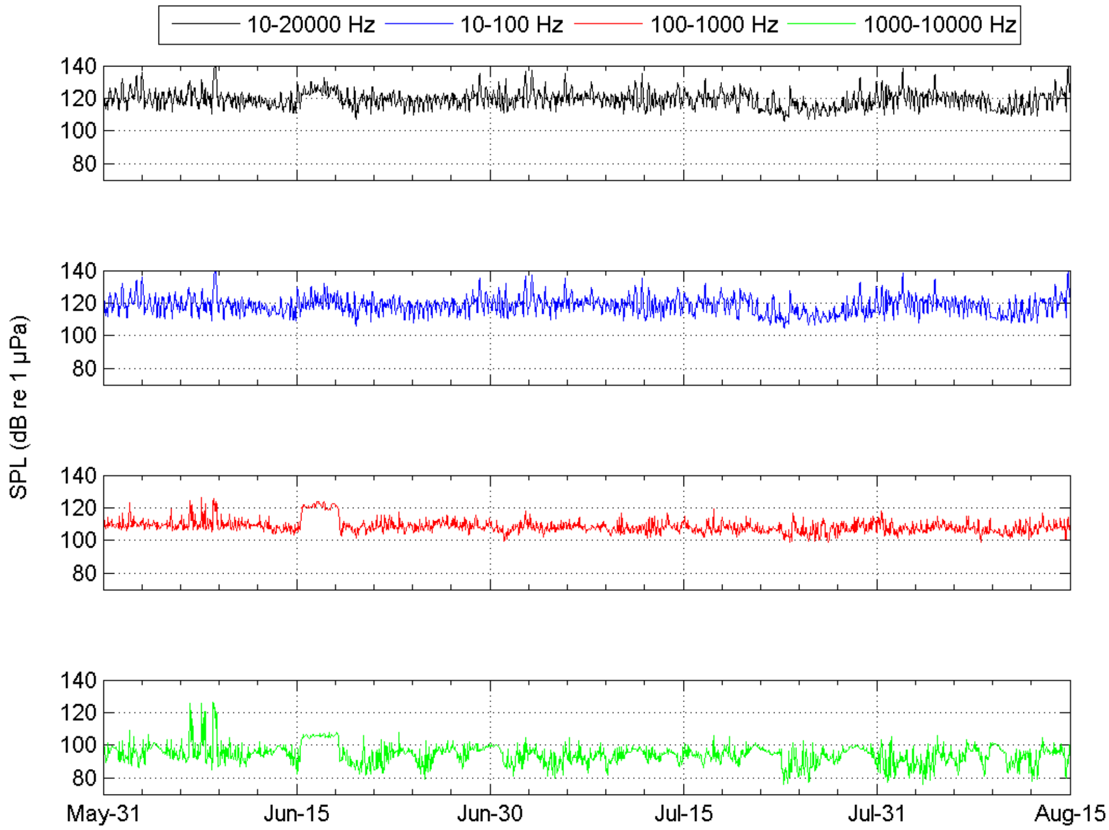

Figure 26: Broadband and decade band sound pressure levels (SPL) for the summer 2011 deployment at HYWIND Monitoring Station. The extended event from June 15 – 18th is from a vessel that appears to have moored near HYWIND for that period. There are three events with band levels above 120 dB in the 1000 – 10000 Hz band between 6 – 9 June 2011. These are associated with another vessel passing close to the HYWIND station.

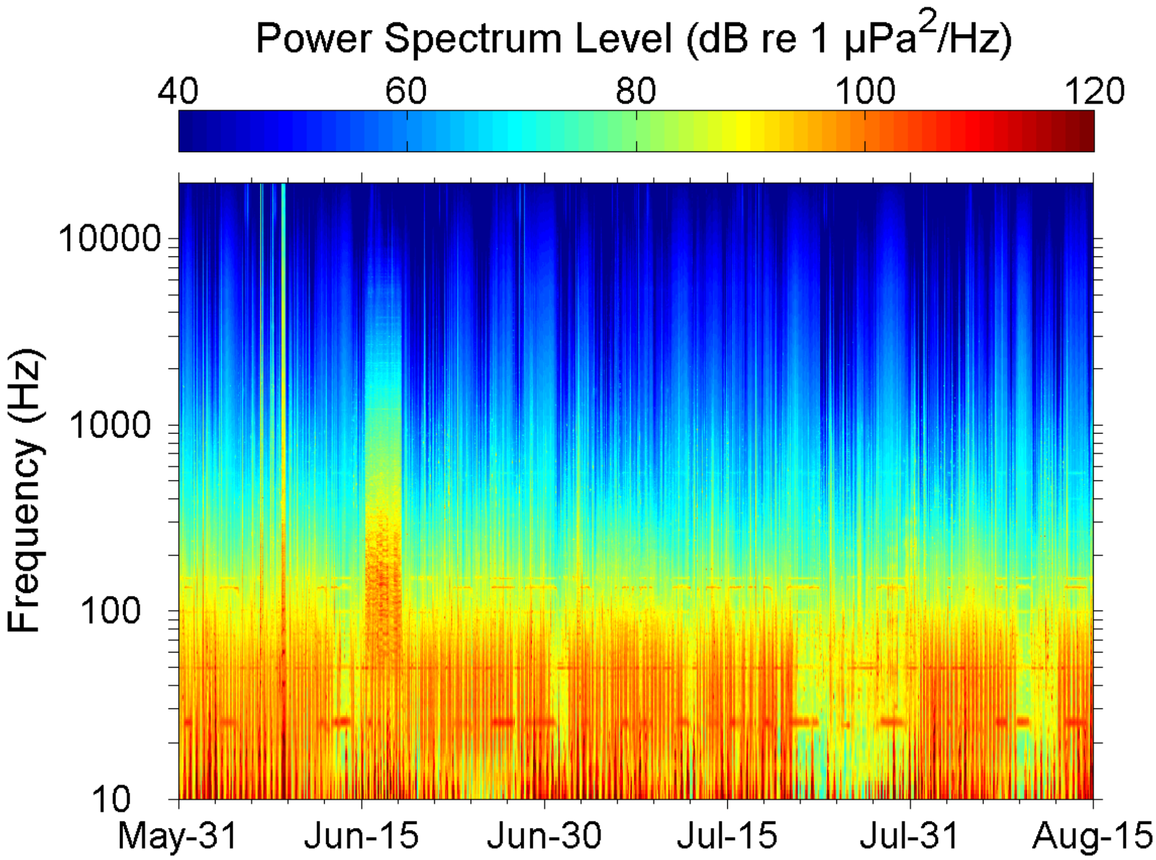

Figure 27: Spectrogram of underwater sound for the summer 2011 deployment at the HYWIND Monitoring Station. There is a high intensity event on15 June that was caused by a vessel that appears to have been stationary near HYWIND for 2 – 3 days.

3.2.4. Automatic Shipping Detections

JASCO ran the HYWIND data through its automatic shipping detector. The results are presented in Figure 28 for the summer deployment. It was anticipated that the HYWIND recorder could have a higher detection rate than the Control station since tones generated by the power conversion equipment would trigger the shipping detector.

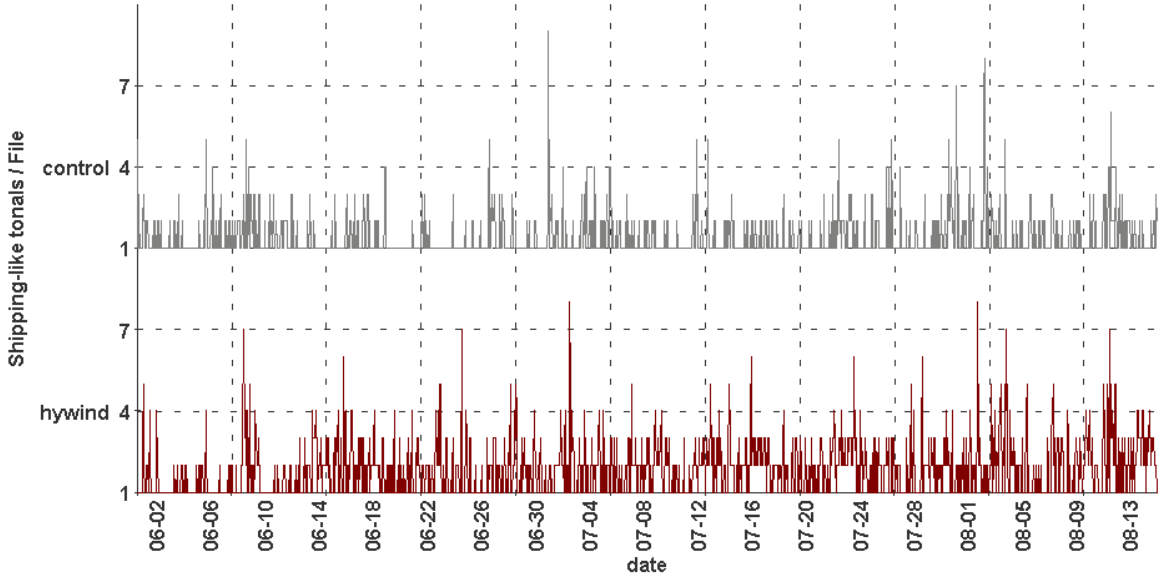

Figure 28: Automatic Shipping detections, summer deployment.

3.2.5. Automatic Seismic Detections

JASCO ran its automatic seismic event detector on the HYWIND data. The results for the summer deployment are shown in Figure 29. The measured per-pulse SPLs appear to be slightly higher for the Control recorder, suggesting that the surveys were conducted north of the study area. Note that the absence of seismic surveys in late July and early August correlates with lower sound levels shown in Figure 27. The vessel positioned near HYWIND 15-18 June increased the background noise such that seismic surveys were difficult to detect in that period.

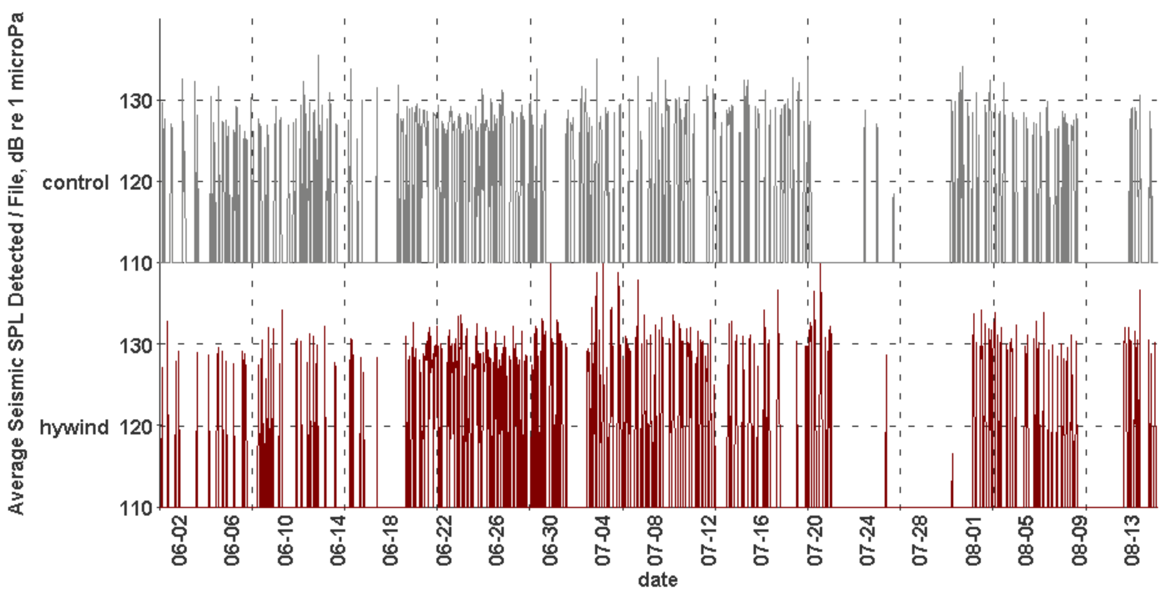

Figure 29: Automatic seismic sequence detections, shown the average pulse SPL per 1/2 hour file, Summer deployment.

3.3. Possible Sounds from HYWIND

This section discusses three sound events that JASCO proposes originate from the HYWIND structure. Comparing the control station spectrograms to the HYWIND station spectrograms (Figure 12 to Figure 15 and Figure 24 to Figure 27) there is a tonal structure regularly present at HYWIND. Comparing the peak sound level plots (Figure 6 to Figure 7 and Figure 18 to Figure 19) there appears to be a transient event occurring at HYWIND that is not present at the control station. Two examples of the tonal or harmonic structure at HYWIND are discussed, as well as one example of the transient event.

3.3.1. Harmonic Sounds

3.3.1.1. 21 May 2011

Figure 30 shows an example of a spectrogram from a period with minimal background noise where the harmonic structure can be seen . The low background levels allow the the multiple harmonics produced by HYWIND to be audible. The maximum received level was 115 dB re 1 $\mu Pa^2/Hz$ with a peak at 24.4 Hz.

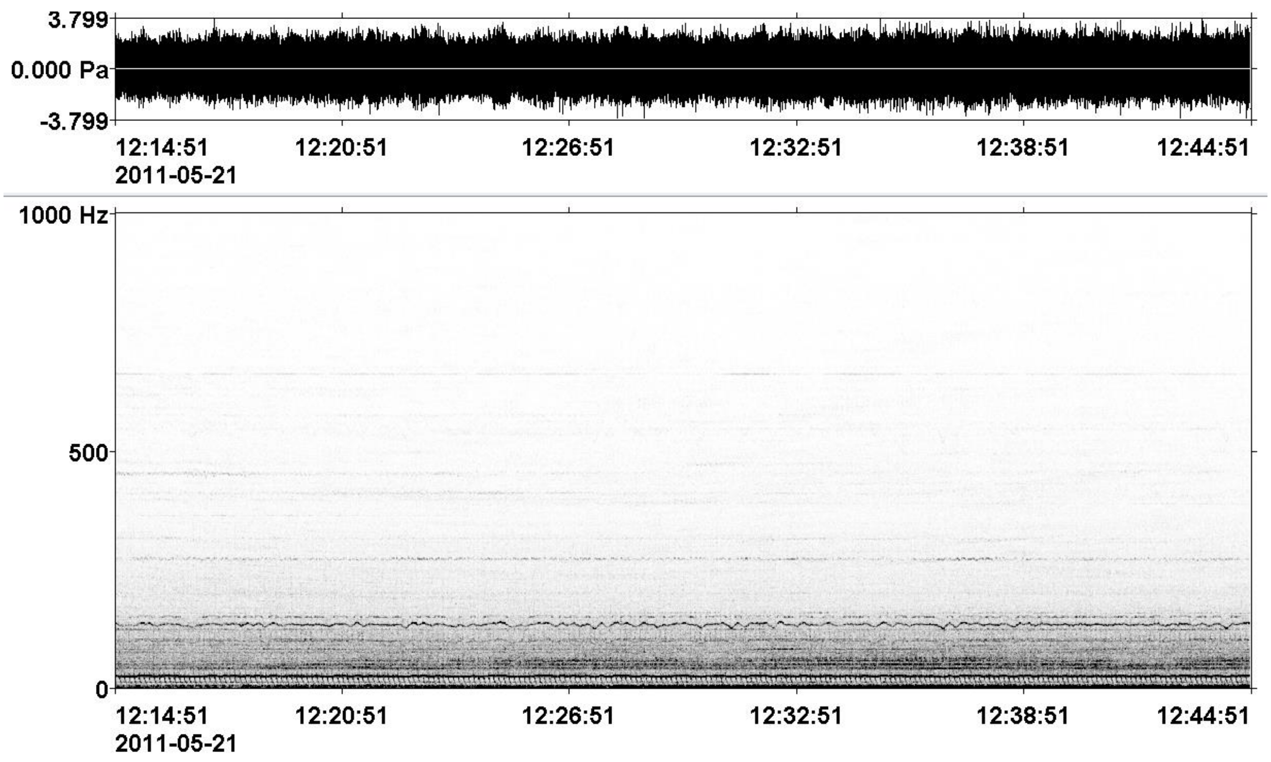

Figure 30: Time series (top, units are Pascals) and spectrogram (bottom) of 30 minutes of data from the HYWIND Monitoring Station, 12:14 21 May 2011, UTC. The peak tonal is at 24.4 Hz, with a spectral density level of 115 dB re 1 $\mu Pa^2/Hz$. FFT size = 65536 samples, 40000 real data samples, 20000 sample overlap, Reisz window.

3.3.1.2. 21 July 2011

Another example of the harmonic structure was evident on 22:20 on the 21st of July. The data from this file can be processed with different FFT parameters to demonstrate the stability of the very low frequencies in the signature, the variability of the medium frequency components as well as an impulsive signal that may be related to the blade passage rate

Figure 31 shows the data processed with a frequency resolution of approximately 0.15 Hz. There are multiple tonal signals present. Most of the tonals have a frequency oscillation. Clearly many of the oscillations occur in phase, indicating a harmonic relationship between the tones. This type of signature is characteristic of gear mesh noise. There are also a number of more stable tones which may be associated with electrical conversion equipment..

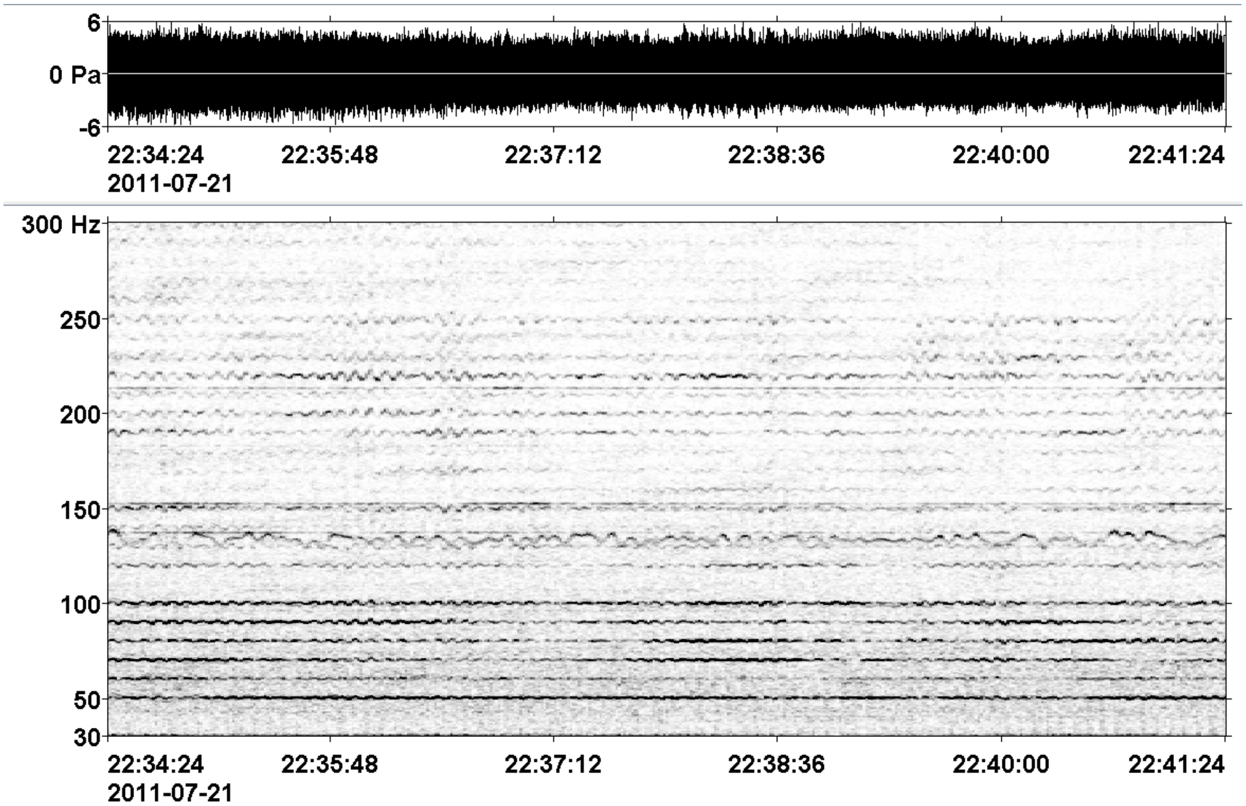

Figure 31: Time series (top) and spectrogram (bottom) of HYWIND Monitoring Station, 22:34, 21 July 2011. FFT size = 262144 samples, 80000 real data samples, 40000 sample overlap, Reisz window. This figure shows a number of different harmonically related sources typical of gear mesh noise and electrical generation noise.

Figure 32 was processed with an extremely long FFT (>100 seconds) for a frequency resolution of 0.01 Hz. It shows an extremely stable set of frequency components at very low frequency, likely associated with a fundamental property of the turbine. There appears to be a gear change or other effect that causes the frequencies to change around 22:20. Note that while the frequency response of the AMAR at 2 Hz is approximately 20 dB below the nominal response of -165 dBV / μPa. Therefore, the AMAR can still measure strong tones at these frequencies and provide calibrated signal levels.

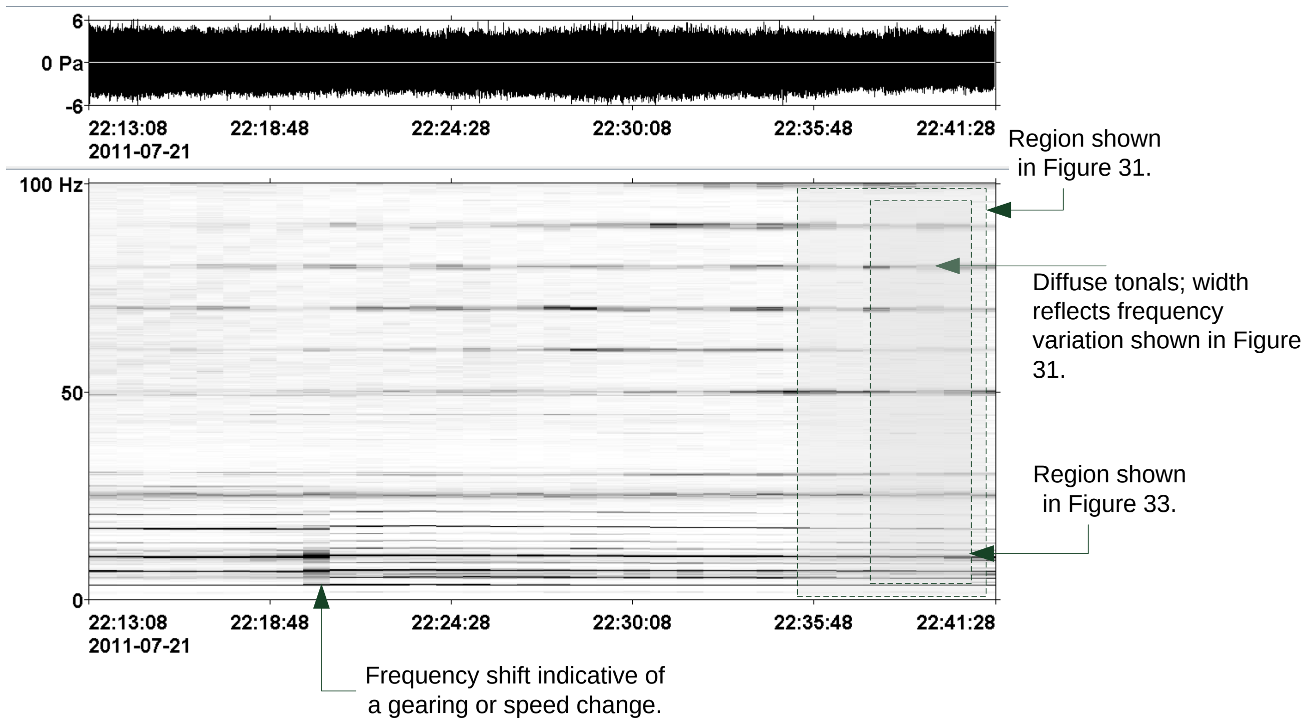

Figure 32: Time series (top) and spectrogram (bottom) of HYWIND Monitoring Station, 22:12 21 July 2011. FFT size = 4194304 samples, 4000000 real data samples, 2000000 sample overlap, Hamming window. This figure shows an extremely stable set of frequency components at low frequency, likely associated with a fundamental property of the turbine. There appears to be a gear change or other effect that causes the frequencies to change around 22:20. The time windows shown in Figure 31 and Figure 33 are highlighted. Note that the frequency variations shown in Figure 33 result in diffuse tonals at the frequency resolution used here.

Figure 33 show a section of the same data file processed with a 10 Hz resolution. It shows an impulsive noise with a period of around 6.164 seconds. This may be the blade passage rate.

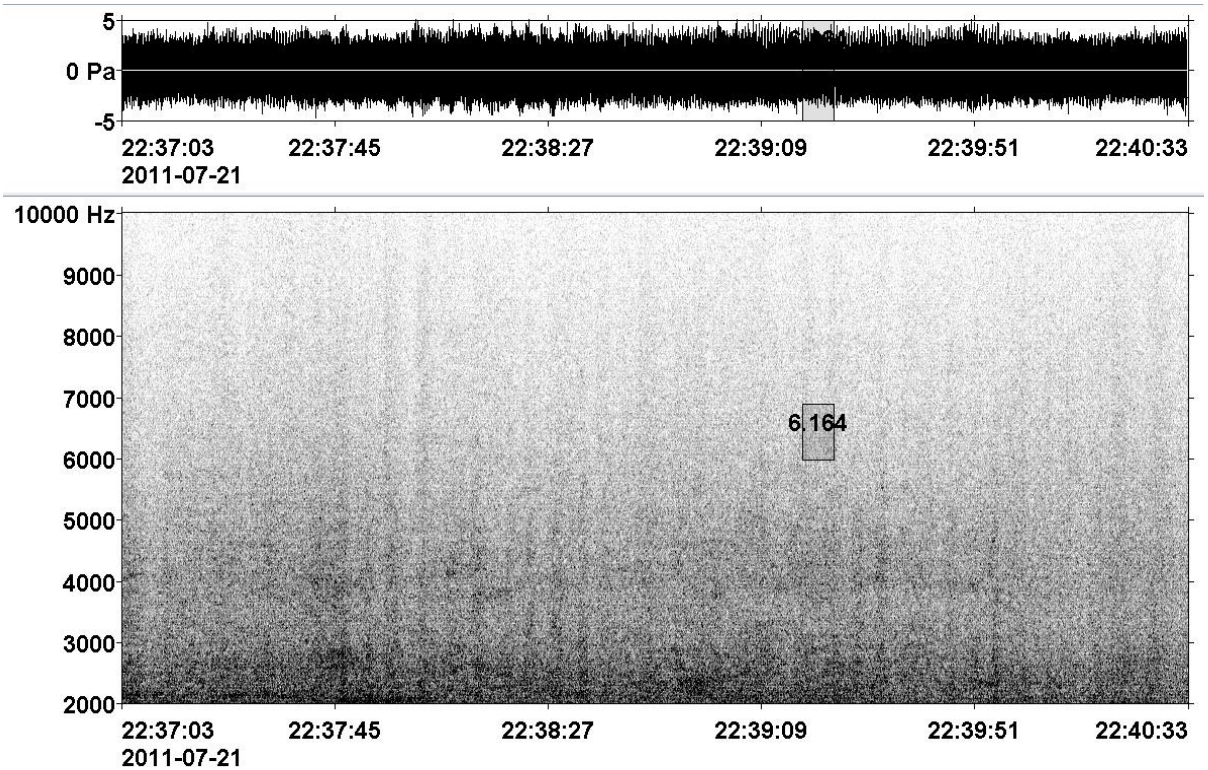

Figure 33: Spectrogram of HYWIND Monitoring Station, 22:37 21 July 2011. FFT size = 4096 samples, 2500 samples of real data, 1250 sample advance. This figure shows a periodic impulsive noise, which may be associated with the blade passage rate.

3.3.2. Transient Sounds

Figure 34 shows an example of a transient impulsive sound recorded at the HYWIND recording station. The very loud impulse has broadband frequency signature and clear reverberation and echoes. There are also a fundamental frequency generated, with a harmonics, at 260 Hz, 520 Hz, and 740 Hz. A plot of the peak sound levels for every minute of the day during the 6^{th} April is shown in Figure 35. Manual analysis of five of the ‘outlier’ events with SPLs above 165 dB, selected at random, showed that the peaks are caused by the same type of event.

Aural analysis of the sounds reveals that they are possibly originating from a steel wire rope under tension ‘snapping’ as it settles into a different position, or if tension changes due to wave actions or wind motion of the turbine. Since the HYWIND mooring lines are a combination of steel wire rope (465 meters) and studded chain (330 meters), they are the likely source of these events. The daily occurrence of the snaps for the spring deployment is shown in Figure 36.

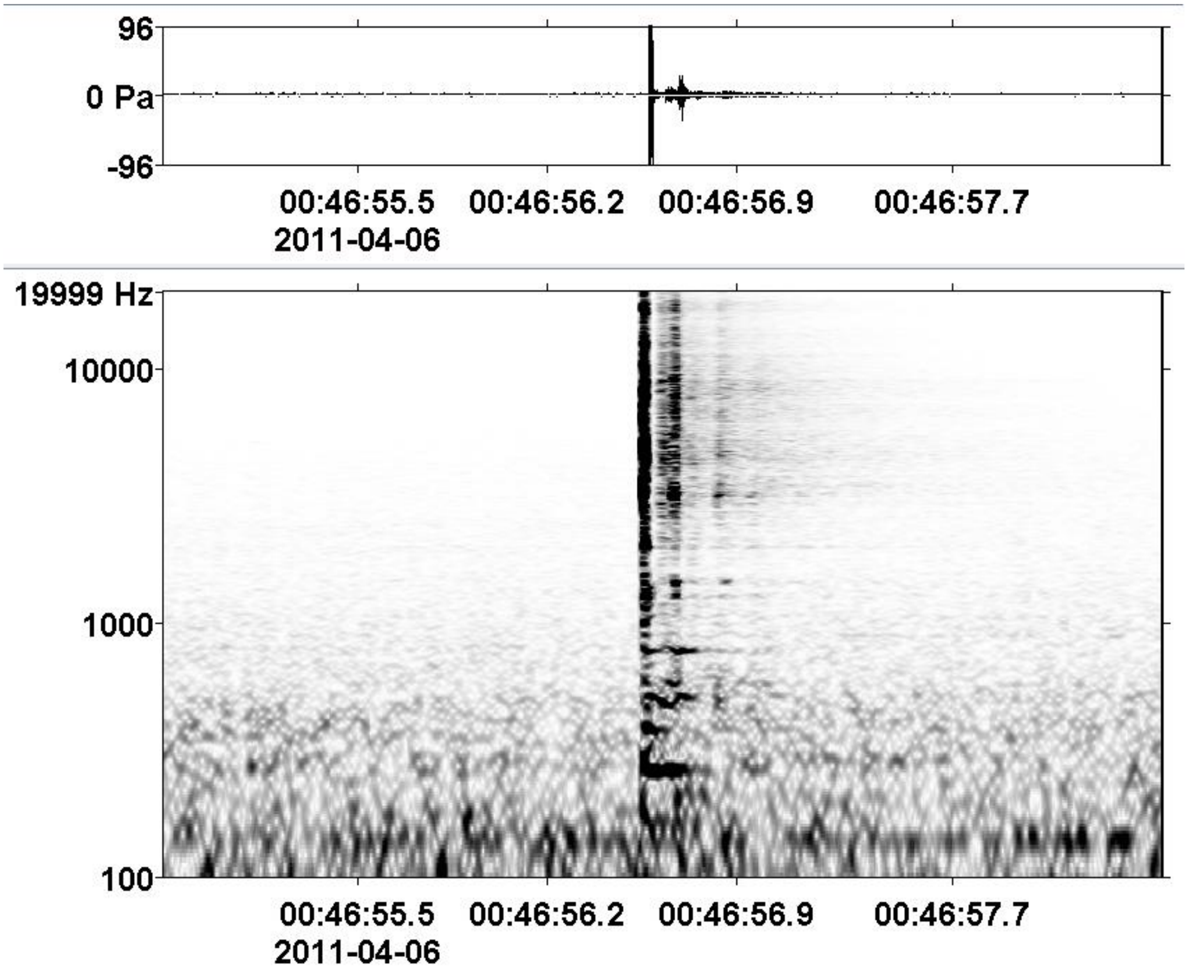

Figure 34: Time series (top) and spectrogram (bottom) of a mooring 'snap' at 00:46, 6 April 2011, HYWIND Monitoring Station. FFT size = 4096 samples, 2000 real data samples, 200 sample advance, Reisz window. Note that this figure uses a logarithmic frequency scale for the spectrogram. The auto-scalling feature of the time-series display clipped the maximum value of the data, which is 150 Pa (163 dB re 1 μPa), 30 dB louder than the peak levels of the sounds shown in this section. The horizontal ‘tones’ at 260, 520, and 740 Hz are consistent with a ‘ringing’ rope under tension.

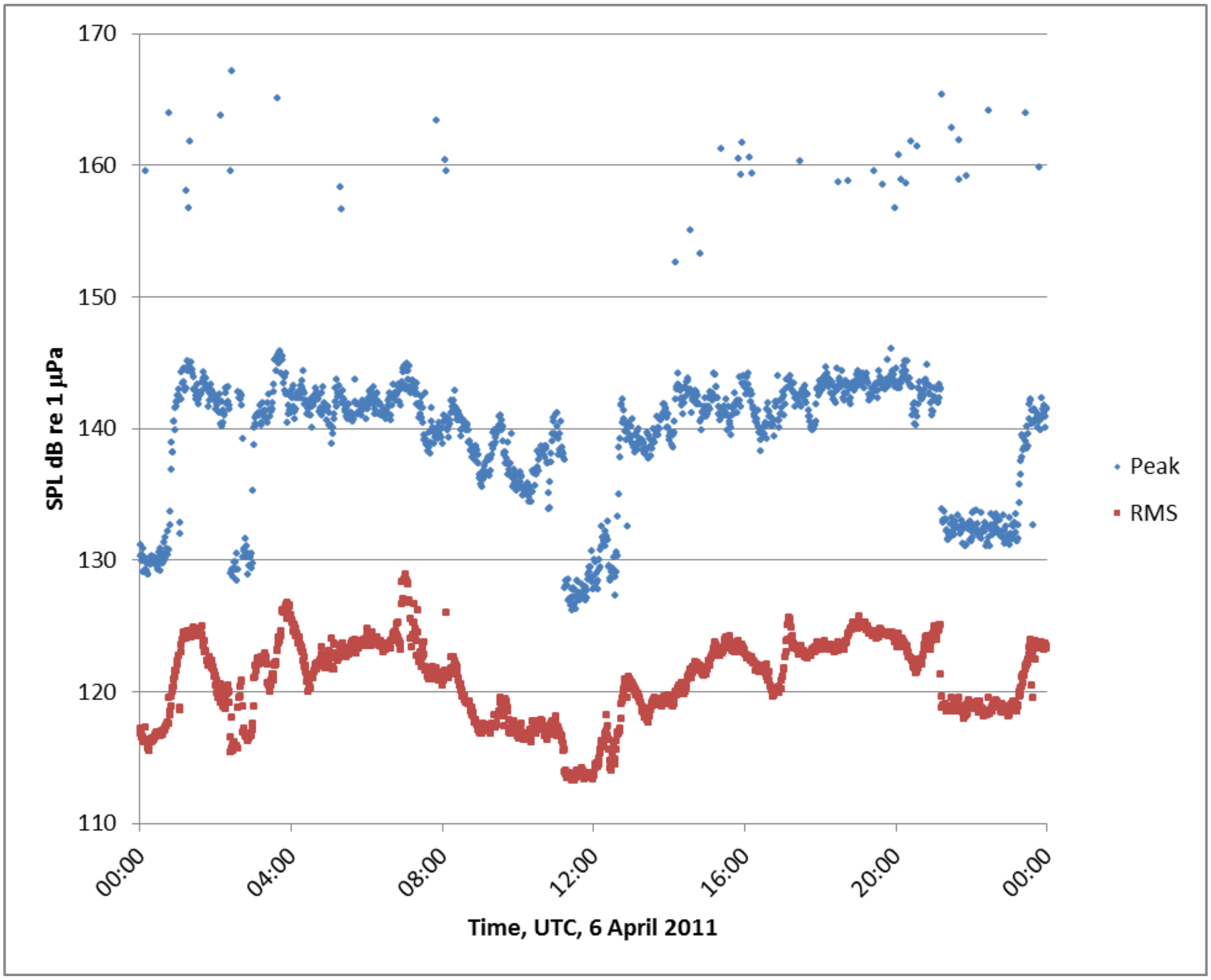

Figure 35: One-minute RMS and Peak SPLs, 6 April 2011, HYWIND Monitoring Station. Outliers in the Peak level are associated with ‘snapping’ sounds, presumably from the HYWIND mooring system.

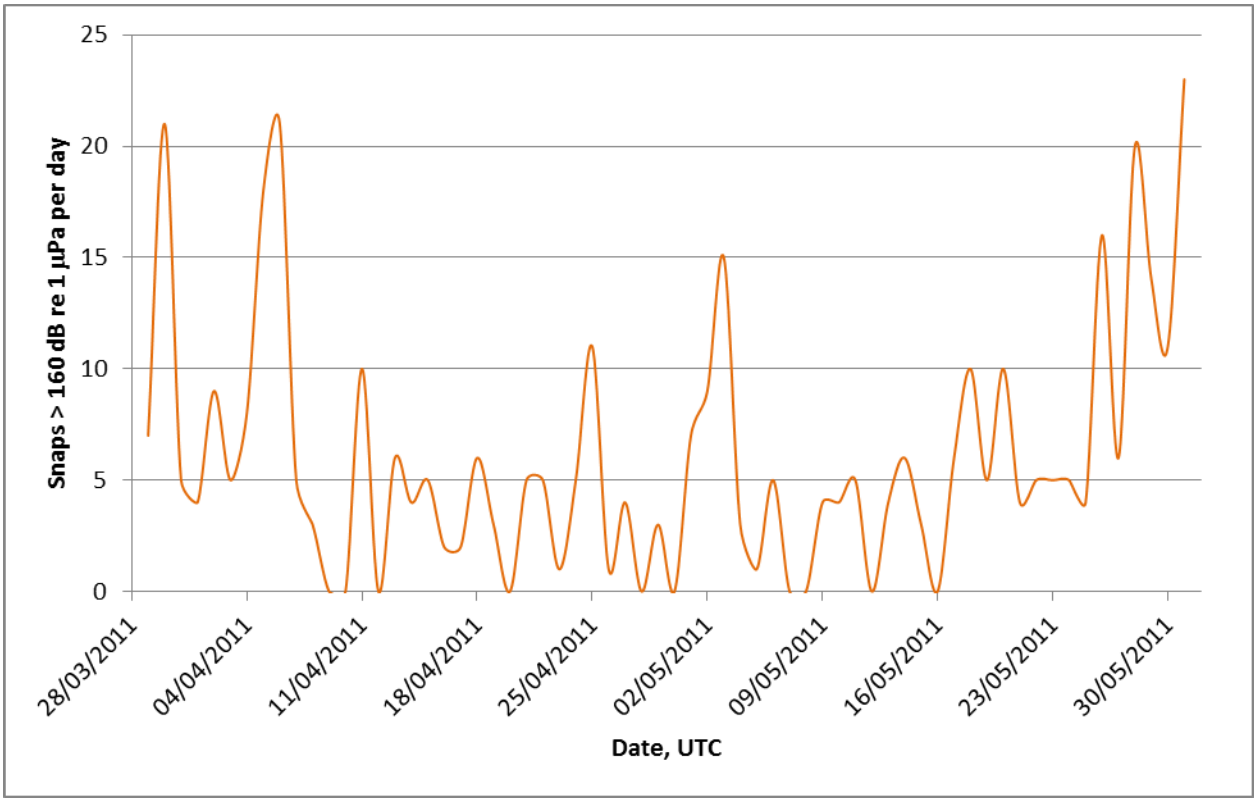

Figure 36: Snaps detected per day with a peak SPL > 160 dB re 1 µPa, HYWIND station, spring deployment.

4. Discussion

4.1. Stability of Sound Levels

The mean spectral densities (50th percentiles from Figure 10, Figure 13, Figure 22 and Figure 25) for both stations and both deployments are shown on one plot in Figure 37. The sound levels show remarkable stability. All four data sets coverage within 1 dB in the range of 40 – 120 Hz, which is the main frequency band of heavy commercial shipping (Andrew 2011). Above 120 Hz, the two spring recorders and the two summer recorders have measured the same sound levels. Below 40 Hz the Control station recorded very similar sound levels for both deployments; however, the HYWIND data varies by up to 7 dB. This appears to be due to differences in strum induced noise. The strum noise is discussed in Section 4.4.1. Differences between the two deployments can be seen in the two-week spectrograms in Appendix A.

The only significant difference between the two stations is in the broad tones present in the HYWIND data. These are believed to be related to the power generation equipment on the HYWIND platform.

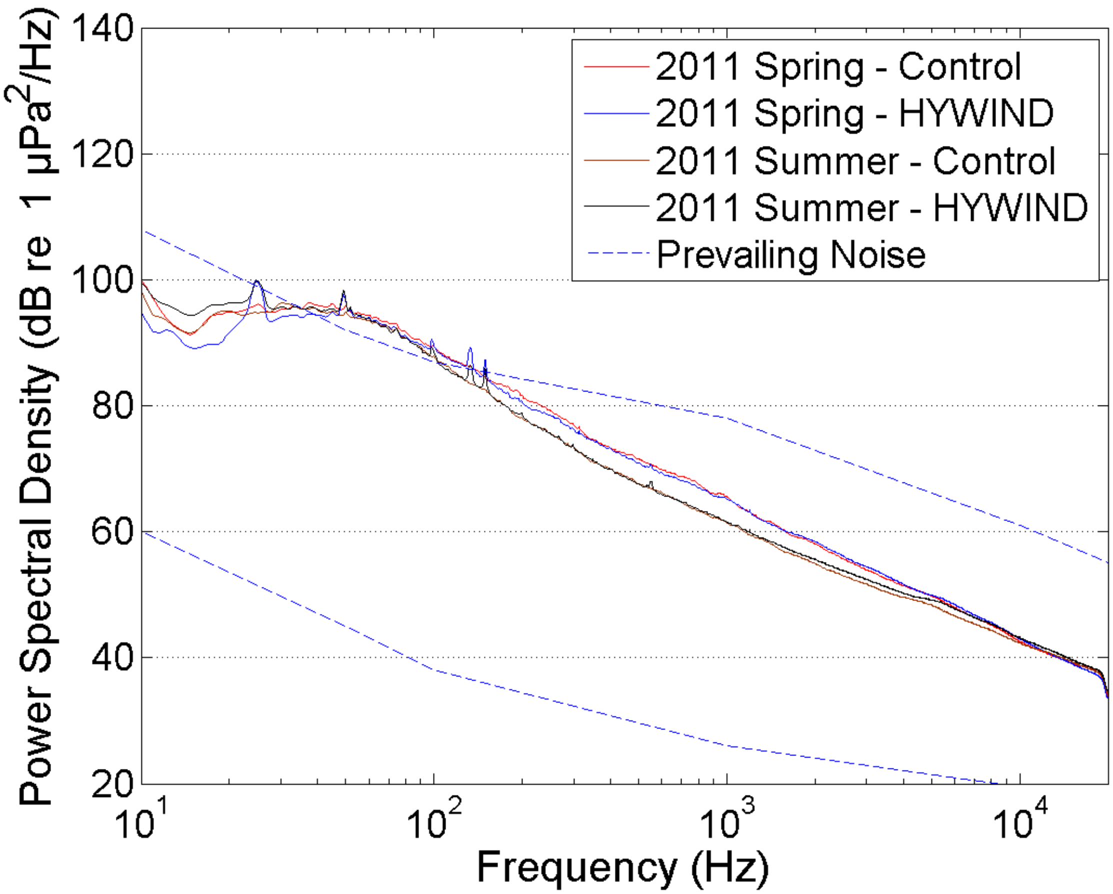

Figure 37: Percentile 1-min power spectral density levels (dB re 1 µPa²/Hz) showing 50th percentiles for the control and HYWIND sites during spring and summer 2011.

4.2. Impact of Flow Noise

Figure 8 and Figure 9 show the hourly energy for the Control site and HYWIND during the first deployment. These suggest that the Control station may have higher noise levels than HYWIND. Figure 20 and Figure 21 show the energy levels for the second deployment, and suggest that the HYWIND station had higher noise levels. However, Figure 37 suggests that the mean sound levels were very similar at both station for each deployment, with the exception of frequencies below ~50 Hz.

JASCO believes that majority of the absolute sound levels that are expressed in the energy figures are due to pseudo-noise caused by water flow around the hydrophones, as well as natural low frequency sound sources (waves, seismic activity … see Figure 3). Figure 38 and Table 1 provide evidence to support this conclusion. Figure 38 plots the third octave band sound pressure levels. The red curve and blue curve show the average levels at both recorders for the entire spring deployment. Like Figure 37, they show very similar sound levels at the recorders, with the exception of the bands below 20 Hz. The green curve traces the one hour average levels for 19:00 on 5 April at the control recorder, which is one of the highest energy events shown in Figure 8. Clearly the majority of the energy is below 50 Hz. As a contrast, the average levels six hours later (01:00 6 April) are shown in purple. In this case the energy levels are much lower at the low frequencies.

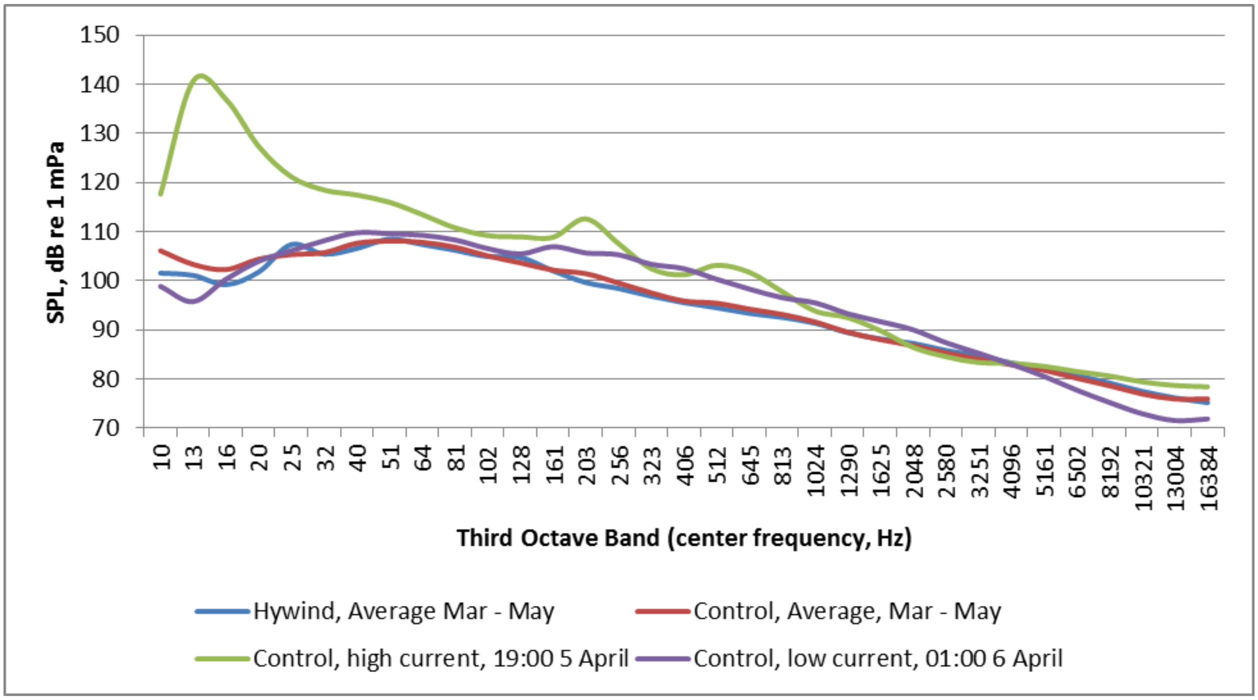

Figure 38: Comparison of 1/3rd octave band levels for spring 2011 deployment. This figures shows very similar average sound levels for the HYWIND and control stations. To demonstrate the effect of current on the noise levels, the one hour average levels from 19:00 on 5 April 2011 and 01:00 6 April 2011 are shown. 19:00 5 April is associated with one of the high energy spikes in Figure 8. 01:00 6 April is the low energy period 6 hours after the high energy spike.

Table 1 contains numeric values for the key results from Figure 38. The Control and HYWIND recorders had on 68% and 60% of their average sound energy contributed by frequencies below 18 Hz. During the hour of 19:00 on 5 April, which is believed to correleate with high current levels due to tides, 98% of the sound energy levels were below 18 Hz. Six hours latter, presumably during a period of low or zero current due to tides, only 21% of the sound energy was contributed by frequencies below 18 Hz.

Table 1: Sound levels comparing average sound levels during the spring deployment to high and low current cases, as shown in Figure 38.

Data Sample	Average RMS sound level, dB re 1 μPa	Average RMS sound level, 0 – 18 Hz, dB re 1 μPa	Percentage of RMS sound levels below 18 Hz.
Hywind, spring deployment	120.4	118.2	60
Control, spring deployment	121.5	119.8	68

Control, 19:00 – 20:00, 5 April 2011	142.8	142.7	98
Control 01:00-02:00 5 April 2011	119.6	112.7	21

4.3. Sound Levels near HYWIND

Figure 37 demonstrates that the average spectral noise densities in the HYWIND area are a several dB above the maximum limit of prevailing noise described by Wenz (Wenz 1962). Andrew (Andrew 2011) showed that the noise levels in the band of 40 – 100 Hz have risen by up to 10 dB due to increased commercial shipping traffic. As a result, we can conclude that the sound levels at HYWIND are at or below the maximum sound levels found anywhere in the oceans. This is not un-expected since the HYWIND area is located within kilometers of a major shipping fairway.

The percentile plots, such as Figure 13, show a significant spread in the energy levels below 100 Hz from the 5th percentile to the 95th. As shown in Figure 17 and Figure 29 seismic surveys were detected in approximately 75% of the data, generally with a higher received SPL at the control station than at HYWIND, indicating that the surveys were north of the study area. Figure 39 shows a sample of the seismic signals detected. Most of the energy is below 100 Hz, which suggests that seismic surveys could be contributing to the increased energy below 100 Hz in the 25th and 95th percentiles.

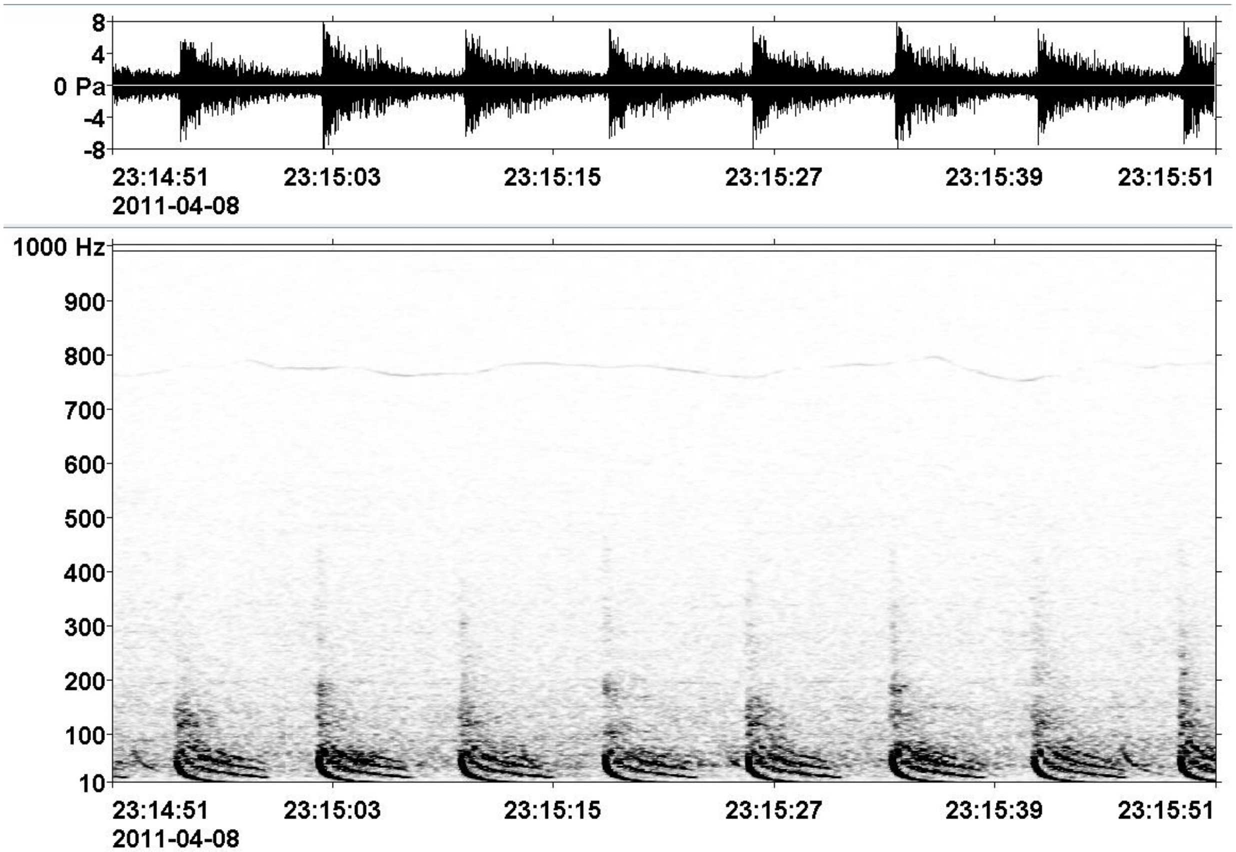

Figure 39: Sample of long range detections of a seismic survey with an 8 second spacing, Control station. Peak levels were 130 dB re 1 μPa sound pressure level. 32768 point FFT, 20000 real points, 18000 point overlap

4.4. Data Issues

JASCO discovered two data quality issues during the data analysis. This subsection discusses the impact of cable strum and a short section of corrupted data on the overall results.

4.4.1. Cable Strum

The project specification required that the monitoring hydrophones be placed at a depth of 91 meters below the surface. Since the water depth as over 200 meters at both locations, JASCO had to design the moorings with a long tether to the bottom and a large sub-surface float to suspend the hydrophone. Further, the float had to be large enough to minimize the deflection of the hydrophone in currents, so that the location of the hydrophone could be accurately modeled later in case that acoustic data is used to extract source levels for HYWIND. JASCO used a faired tether cable to reduce its drag and reduce the possibility of cable strum. The mooring calculations and design are presented in the HYWIND Measurement Phase Report from August 2011.

Despite JASCO's best efforts, it appears that the mooring cable strum occurred on many days during the programme. It is particularly noticeable as the regular maxima in the Peak Sound Energy plots from the spring deployment (Figure 8and Figure 9). Figure 40 shows the effect well. The effects of strum can be seen as the high intensity (red) data below 100 Hz. The strongest peaks occurred every 12 hours (May 9 – 17), however, from May 17-23 lower energy peaks appeared every 6 hours, which is consistent with tidal effects. This data suggests that there are complex currents present in the HYWIND area.

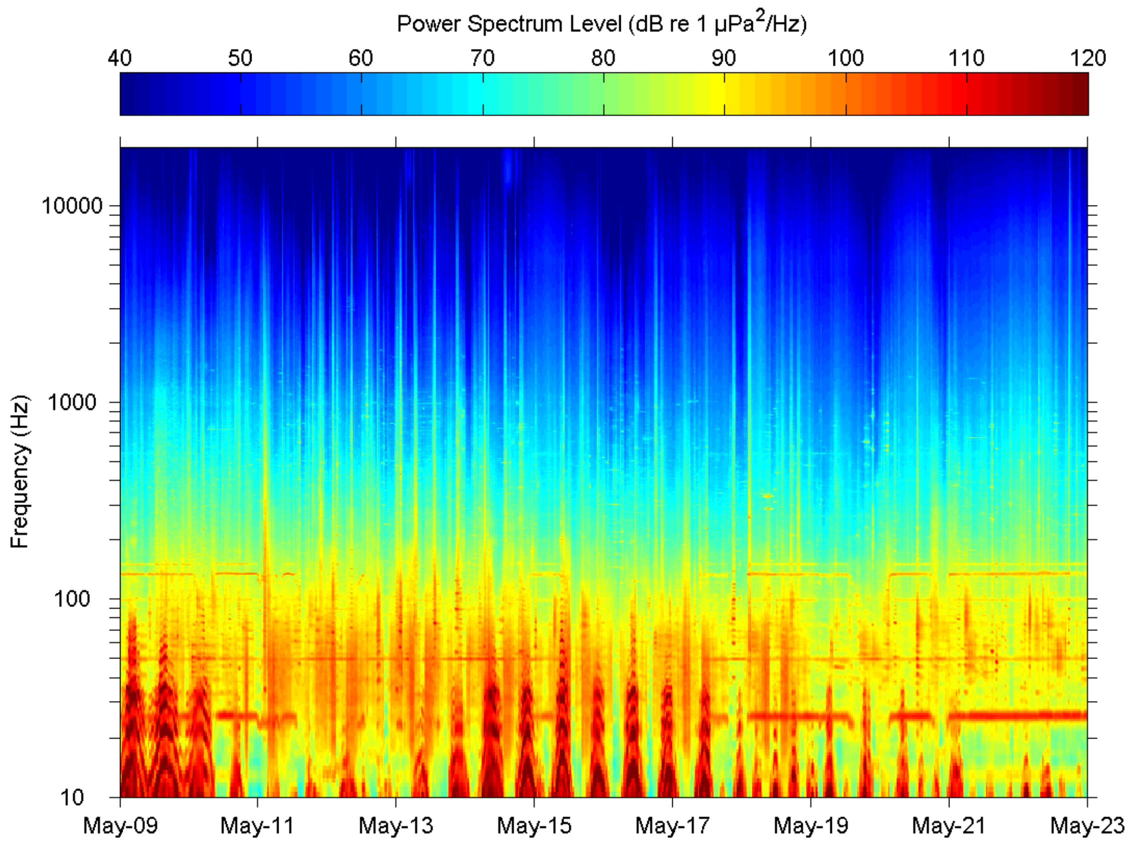

Figure 40: Two week spectrogram from May 9 - May 23, HYWIND Station.

JASCO attempted to correlate measured currents with the acoustic data; however, the current data is not available for periods during the deployments. Figure 41 is a comparison of data availability for the first deployment. It shows the same 12 hour peak structure as the acoustic data.

The cable strum has not significantly affected data analysis or conclusions. The strum effects are limited to the region below 100 Hz and especially below 50 Hz. Further, the strum effect is present for less than 50% of the time, even for the worst case of noise.

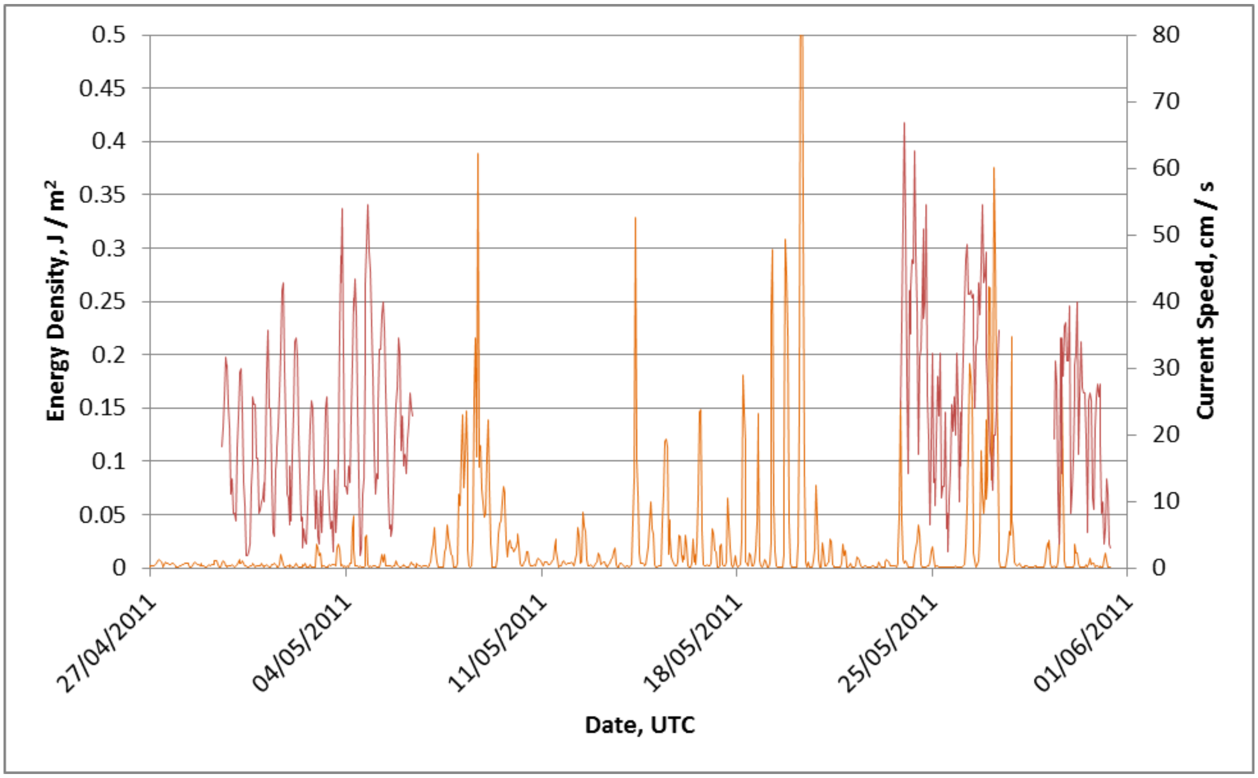

Figure 41: Comparison of peak sound energy (orange) to measured currents (red). Current data was not available when the red curve is absent.

Figure 9 shows that the strum energy is very strong for less than half of the days. Figure 42 shows the one minute energy density during the strongest period of strum noise (17 – 20 May). Even for this case the noise is 20 dB below its peak value at least one half the time. Therefore, the 50th and 25th percentiles are likely unaffected, even below 100 Hz. The 5th percentile is definitely affected below 50 Hz.

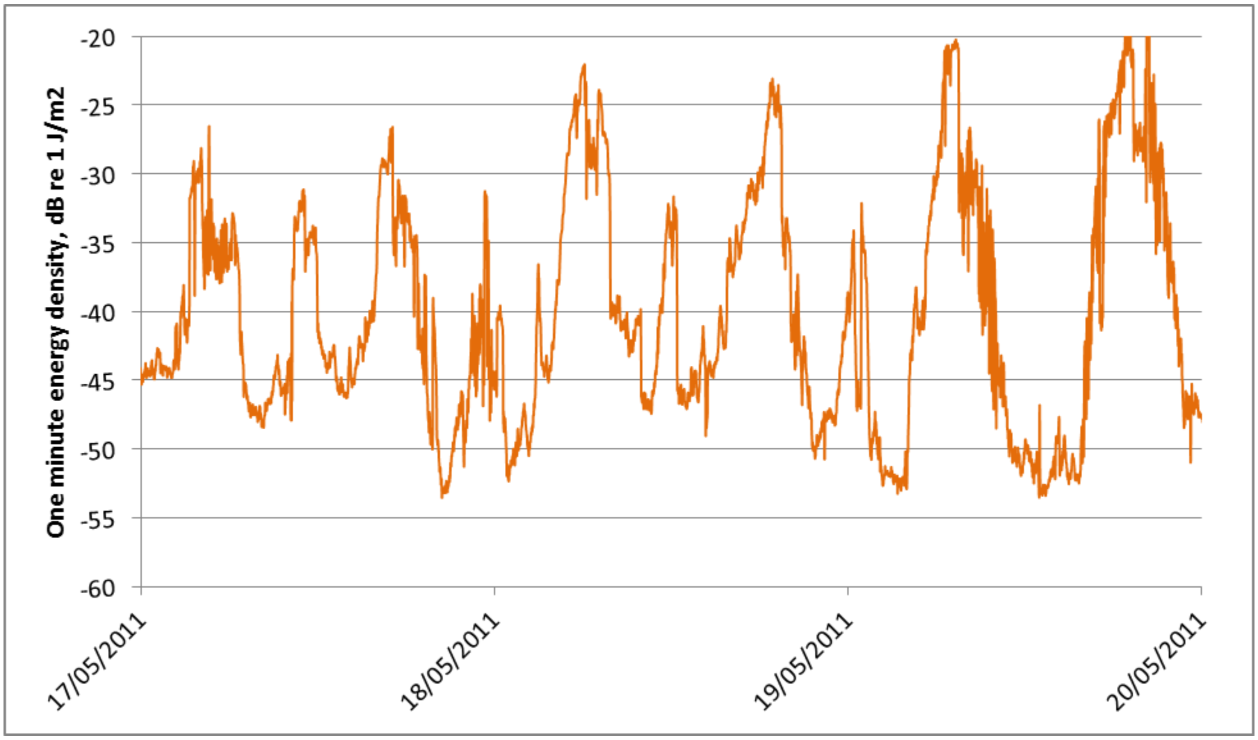

Figure 42: One minute energy density, HYWIND station, 17 - 20 May.

4.4.2. Corrupted Data, 31 May – 13 June

The peak sound level plots from the HYWIND station (Figure 7) shows a large number of very high level events (>165 dB) during the period of 31 May – 13 June. JASCO conducted a detailed review of this data and discovered that 1/16th of the data are occasionally out of place. The sections of data that are incorrect are very short, often only 0.04 seconds in length. A high resolution view of one section of data is shown in Figure 43.

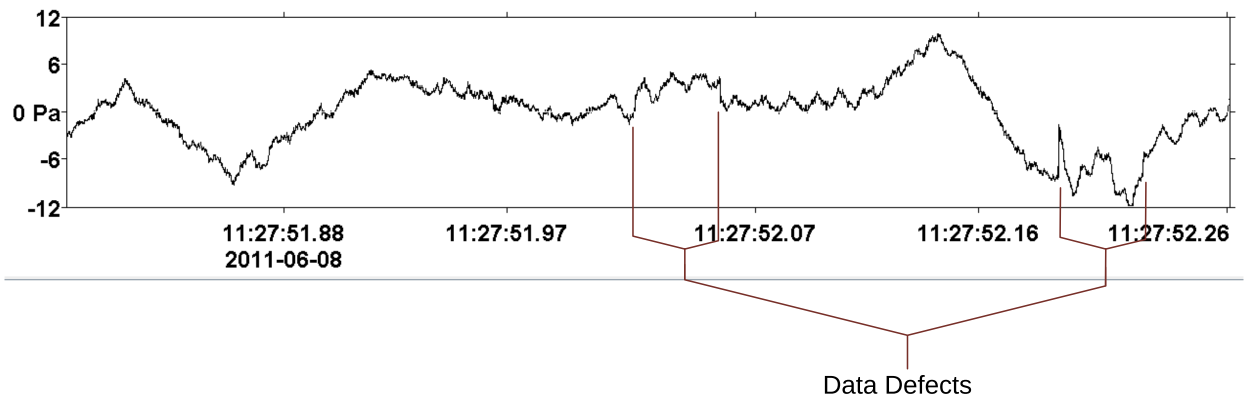

Figure 43: Time series display of data from 8 June 2011, HYWIND Station. Two out-of-place data sequeneces are identified.

One minute of data with the spectrogram is shown in Figure 44. This shows that the misplaced data has a minimal effect on the data interpretation.

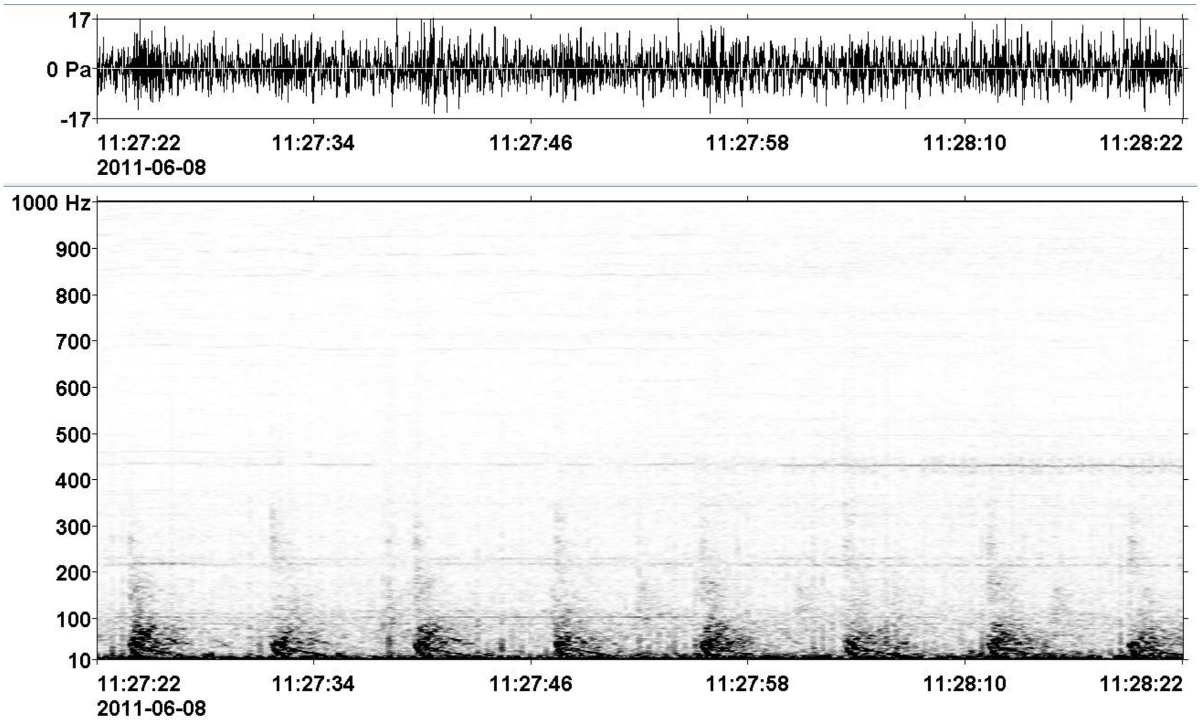

Figure 44: One minute of data from 11:27 8 June, HYWIND station. The misplaced data is not visible in the time series. The spectrogram shows very subtle vertical striations from the occasional discontinuities. The distant seismic events and tonal characteristics of the data are not significantly affected by the discontinuities since the data is only misplaced by several minutes. 32768 point FFT, 20000 real points, 18000 point overlap. Peak levels during this minute of data were 145 dB re 1 μPa. Seismic activity does not appear to be the dominant source for peak levels in this data set.

JASCO's analysis revealed that the AMAR recorder had a single drop of water damage on the address lines of one memory module. This caused the data to be read out-of-order for one of the sixteen memory chips on the module. As a result, data is out of place in the order of minutes, $1/16^{th}$ of the time. Additionally, the error checking codes are affected, resulting in occasional samples of data that are invalid. These samples are the ones that cause the large spikes that affected the peak sound level plot (Figure 7).

These effects are limited to two weeks of the whole deployment, and are limited to $1/16^{th}$ of the data for only a fraction of the time. As shown in Figure 44, the true sounds in the data are clearly detected and characterized even with the discontinuities present. A review of one sound file that had no discontinuities in the first 10 minutes, and regular discontinuities every 0.51 seconds for the next 10 minutes showed that there was less than a 0.25 dB difference in the measured RMS levels. Therefore, these discontinuities do not affect the data analysis results.

5. Conclusions

The initial analysis of the HYWIND acoustic data demonstrated that:

1. Ambient sound levels are at or above the expected levels of prevailing noise described in Wenz 1962. This is due to the high level of commercial shipping in the North Sea and the presence of near continuous seismic surveys to the north of the study area.
2. The HYWIND structure generates a variety of signature components that can be detected above the background noise level. These appear to be related to gear meshing and electrical generation. None of these components exhibited levels that exceeded 115 dB re 1 μPa^2 / Hz.
3. The HYWIND structure produces occasional 'snapping' transients that have received peak levels above 160 dB. The frequency content of the transients extends throughout the recorded frequency range of 0 – 20000 Hz. Between 0 and 23 of these transients occurred per day. These transients are thought to be related to tension releases in the mooring system.

Literature Cited

Andrew, R.K., Howe, B and Mercer, J. Long-time trends in ship traffic noise for four sites off the North American West Coast. *J. Acoust. Soc. Am. 129:642-651*.

Arveson, P.T. and D.J. Vendittis. 2000. Radiated noise characteristics of a modern cargo ship. *J. Acoust. Soc. Am.* 107:118-129.

National Research Council. 2003. *Ocean Noise and Marine Mammals*. National Academy Press, Washington, D.C. by the National Academy of Sciences.

Oppenheim A.V. & R.W. Schafer. 1975. *Digital Signal Processing*. Englewood Cliffs, New Jersey: Prentice-Hall.

Southall, B.L., A.E. Bowles, W.T. Ellison, et al. 2007. Marine mammal noise exposure criteria: Initial scientific recommendations. *Aquatic Mammals* 33(4).

Wenz, G.M. 1962. Acoustic ambient noise in the ocean: Spectra and sources. *J. Acoust. Soc. Am.* 34:1936–1956.

Appendix A. Biweekly Ambient Noise Plots

A.1. 28 March – 11 April 2011

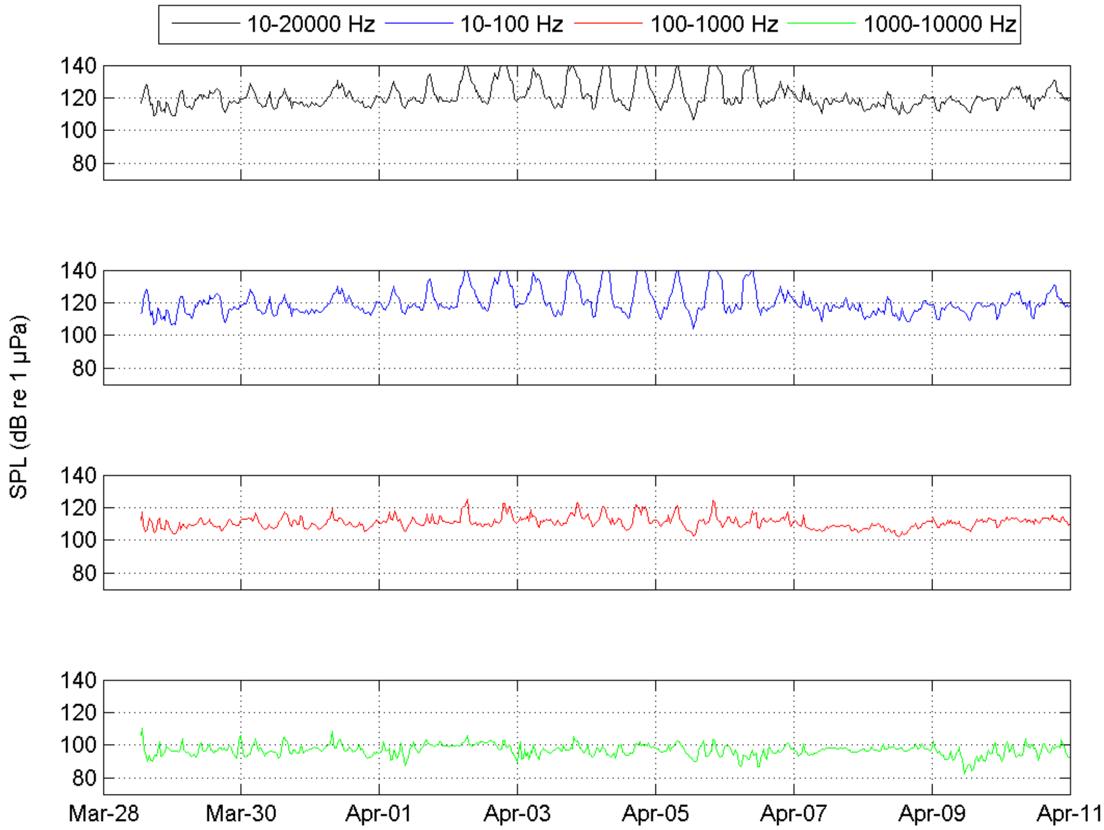

Figure 45: Broadband and decade band sound pressure levels (SPL) for 2-weeks of the 2011 spring deployment at HYWIND Control Station.

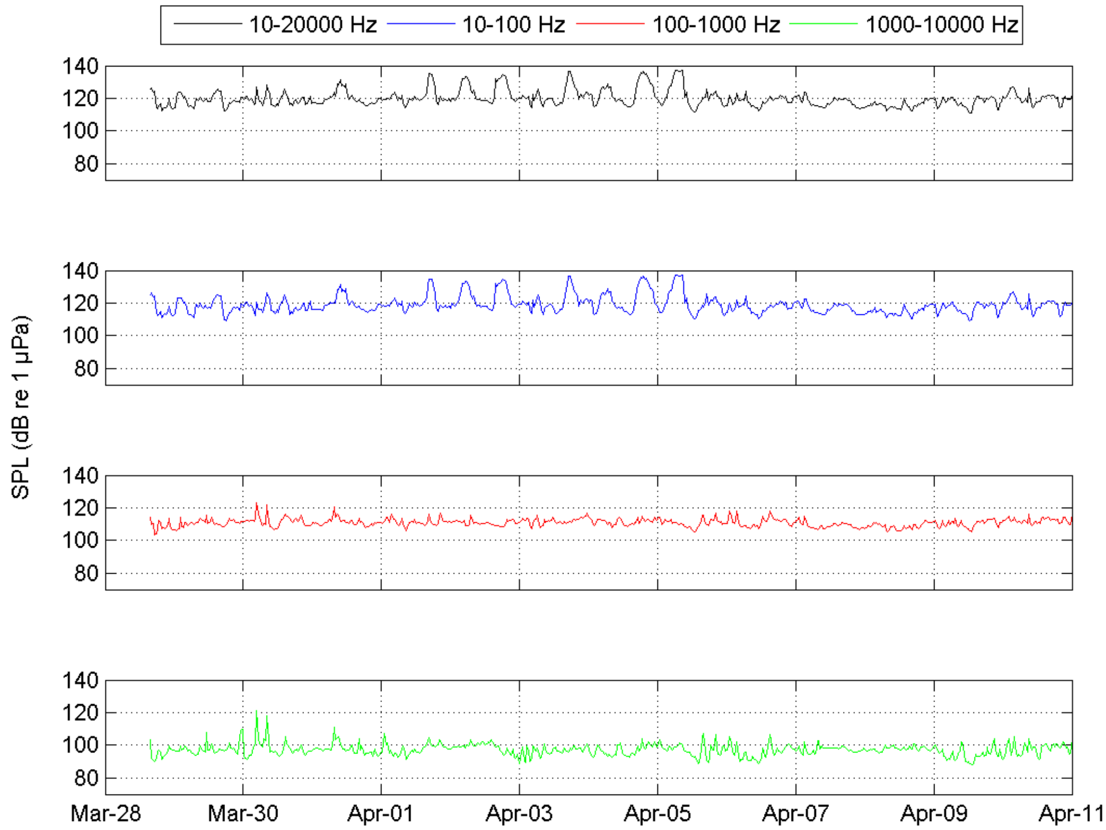

Figure 46: Broadband and decade band sound pressure levels (SPL) for 2-weeks of the 2011 spring deployment at HYWIND Monitoring Station.

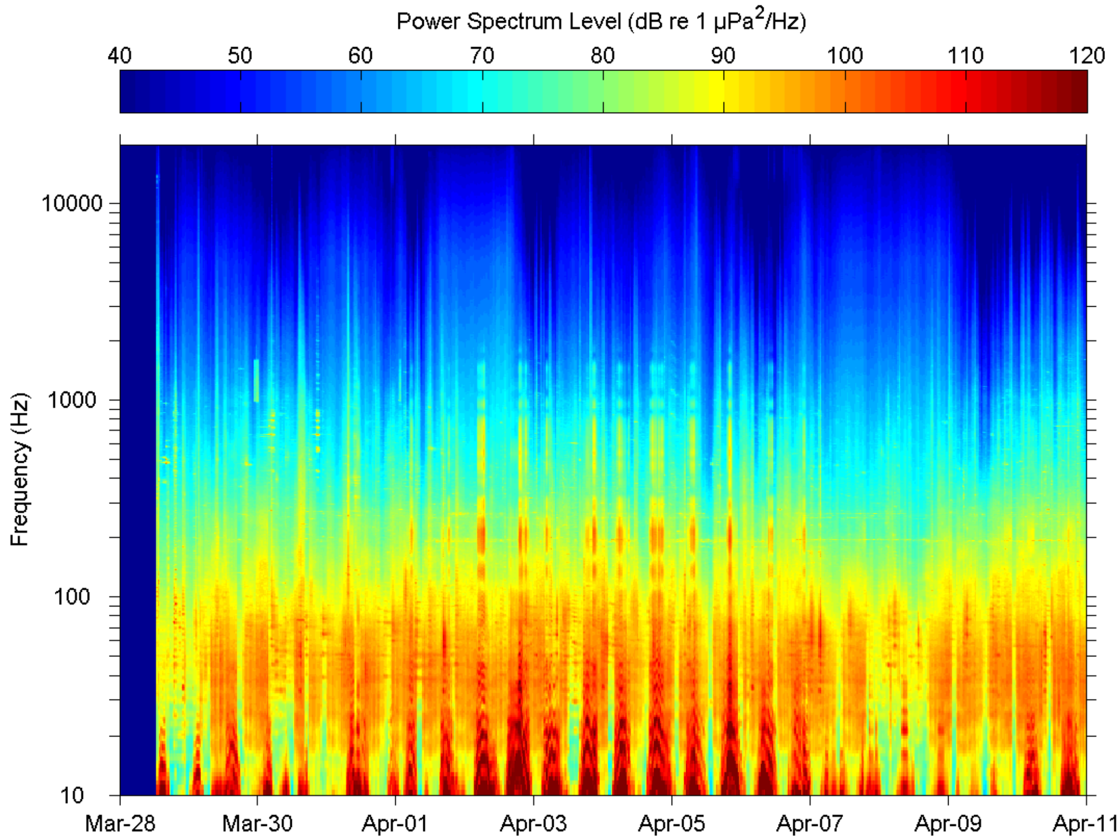

Figure 47: Spectrogram of 2-weeks of underwater sound for the spring 2011 deployment at the HYWIND Control Station.

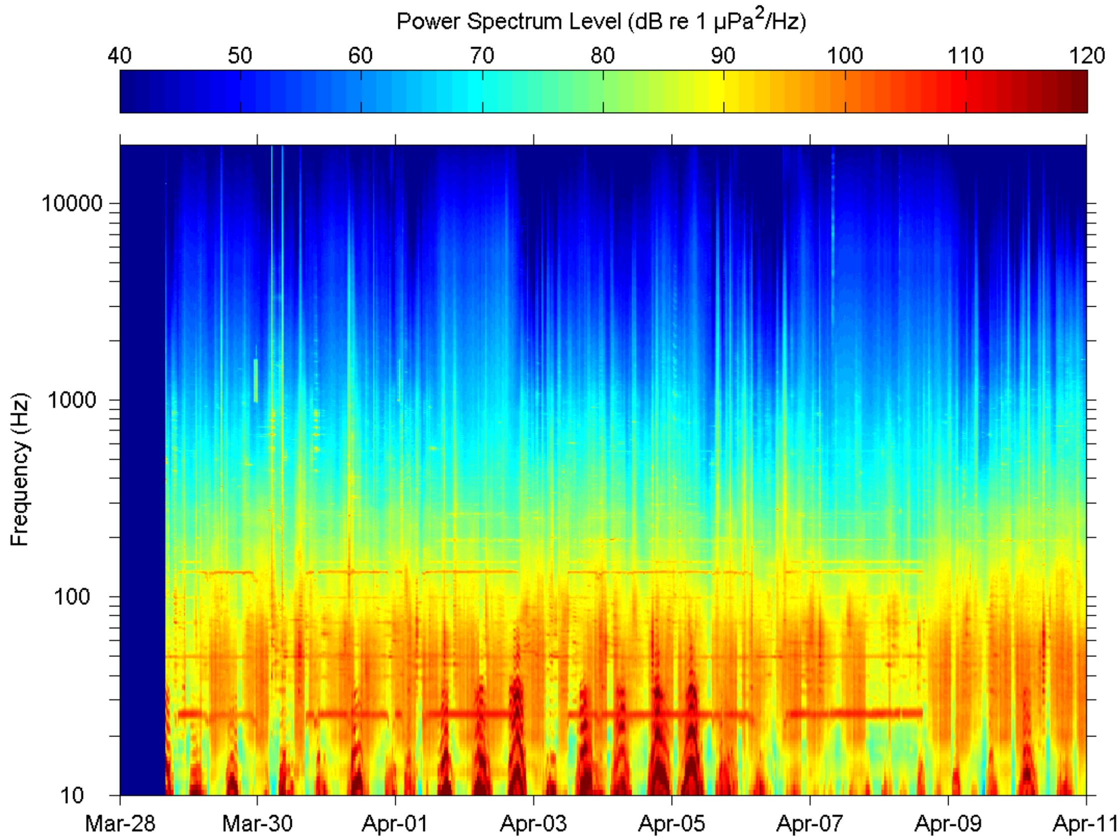

Figure 48: Spectrogram of 2-weeks of underwater sound for the spring 2011 deployment at the HYWIND Monitoring Station.

A.2. 11 April – 25 April 2011

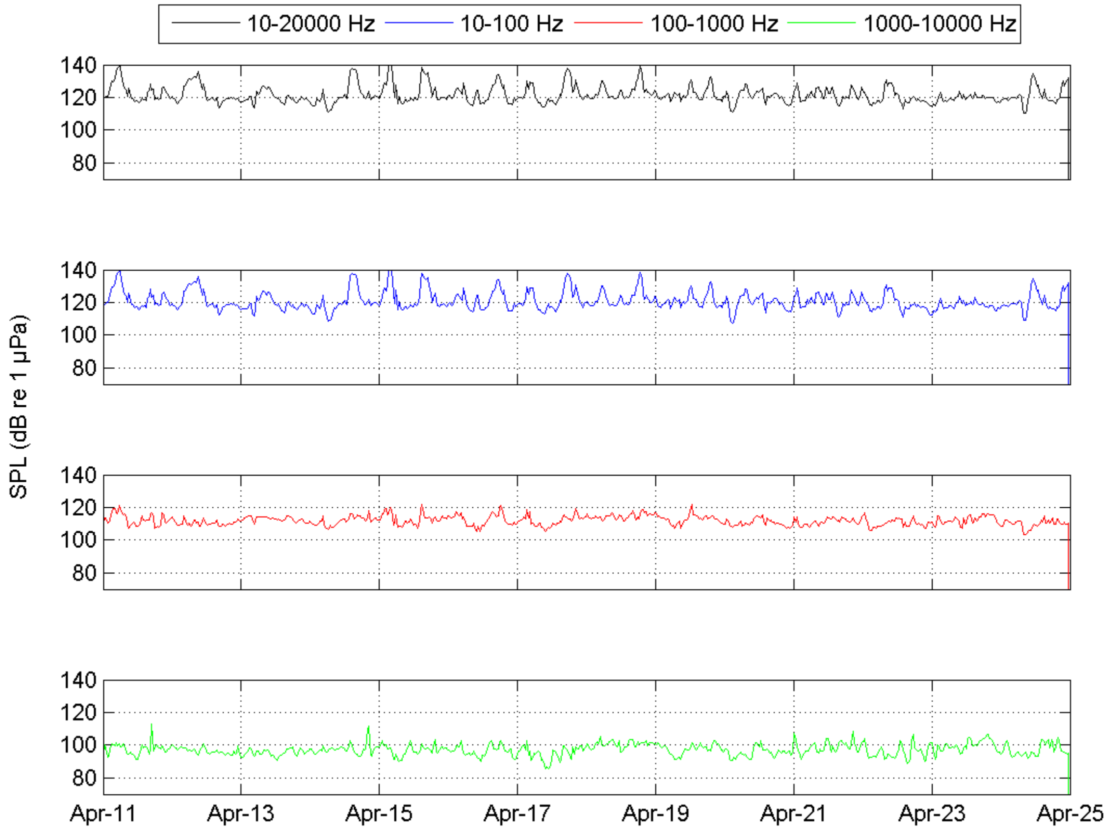

Figure 49: Broadband and decade band sound pressure levels (SPL) for 2-weeks of the 2011 spring deployment at HYWIND Control Station.

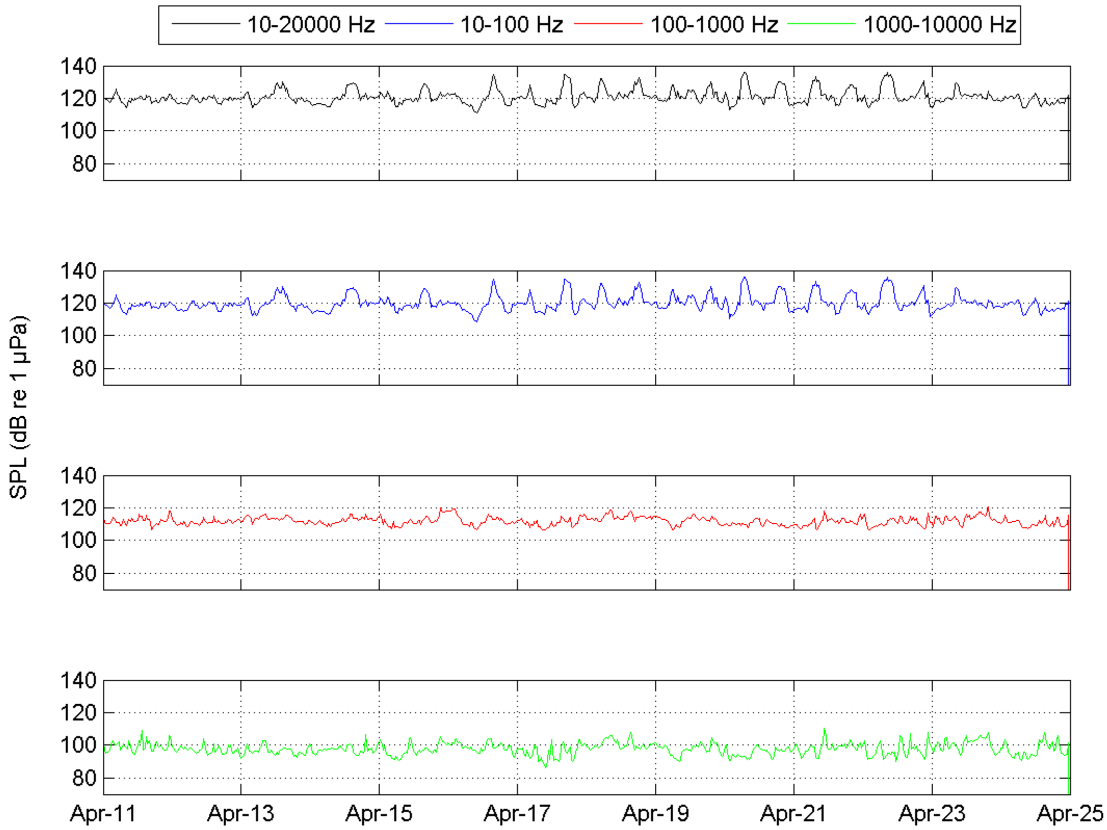

Figure 50: Broadband and decade band sound pressure levels (SPL) for 2-weeks of the 2011 spring deployment at HYWIND Monitoring Station.

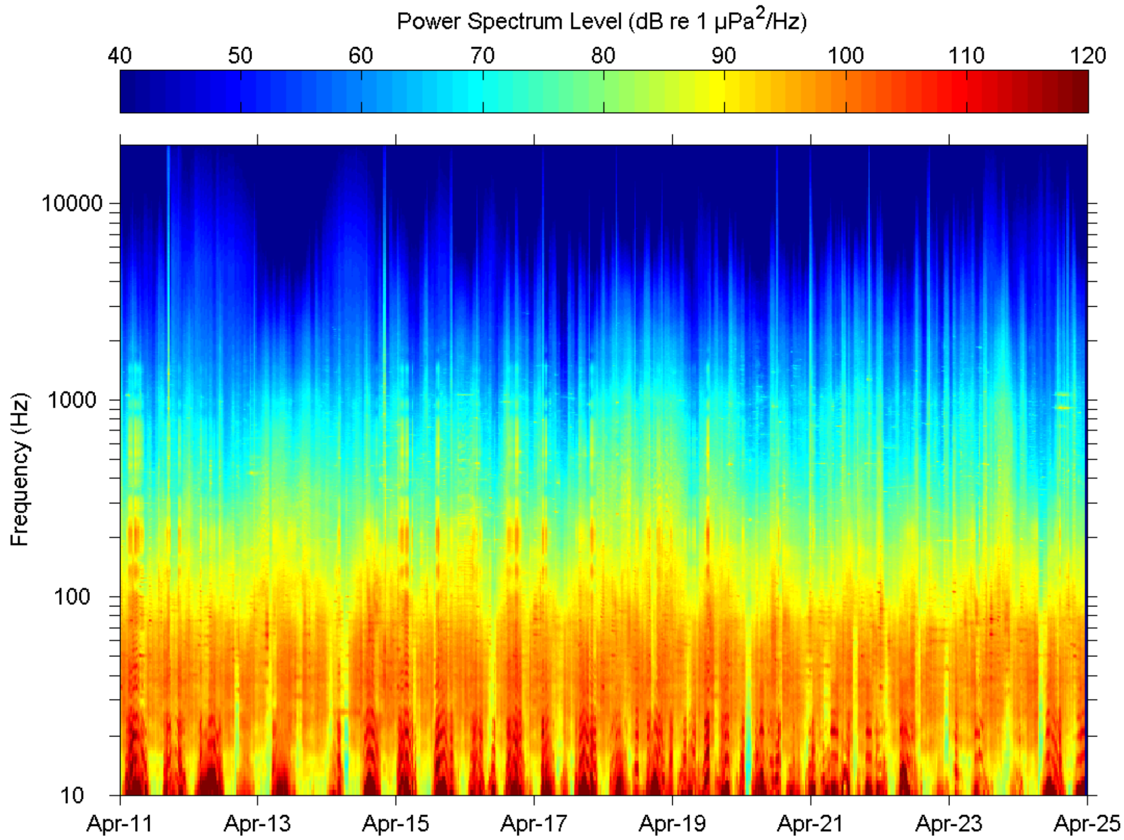

Figure 51: Spectrogram of 2-weeks of underwater sound for the spring 2011 deployment at the HYWIND Control Station.

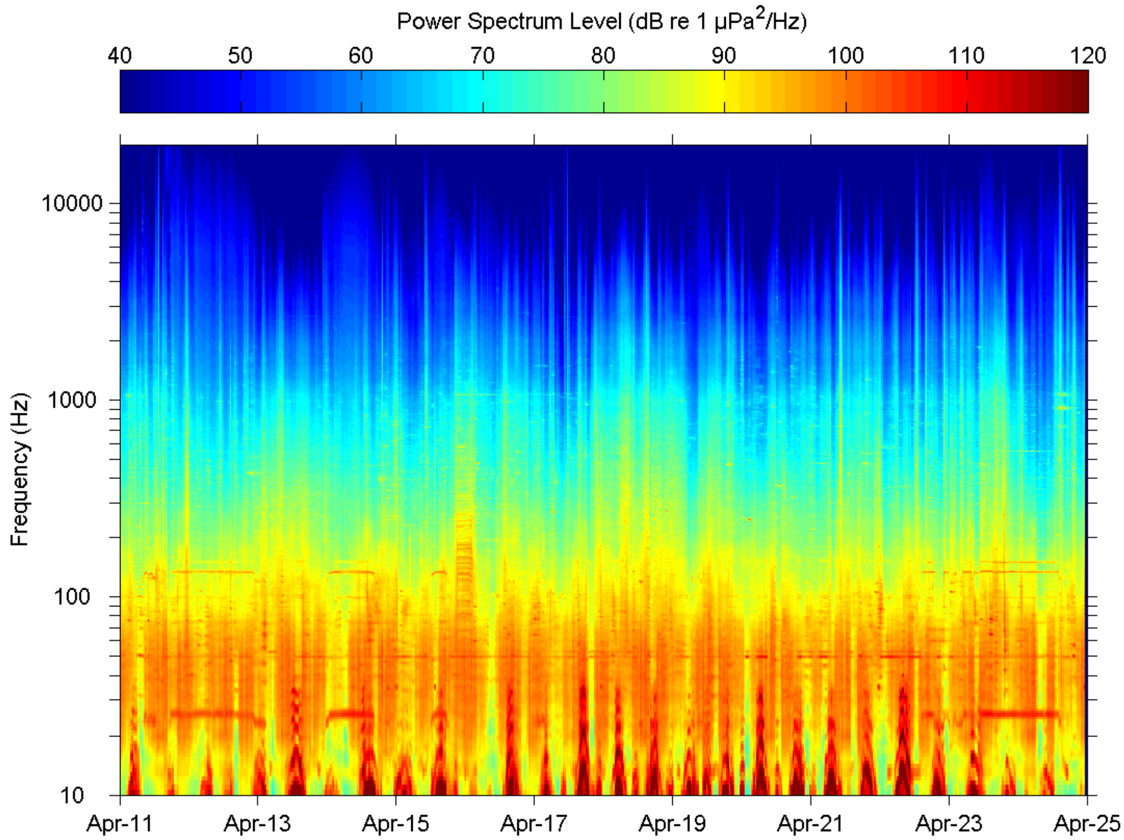

Figure 52: Spectrogram of 2-weeks of underwater sound for the spring 2011 deployment at the HYWIND Monitoring Station.

A.3. 25 April – 9 May 2011

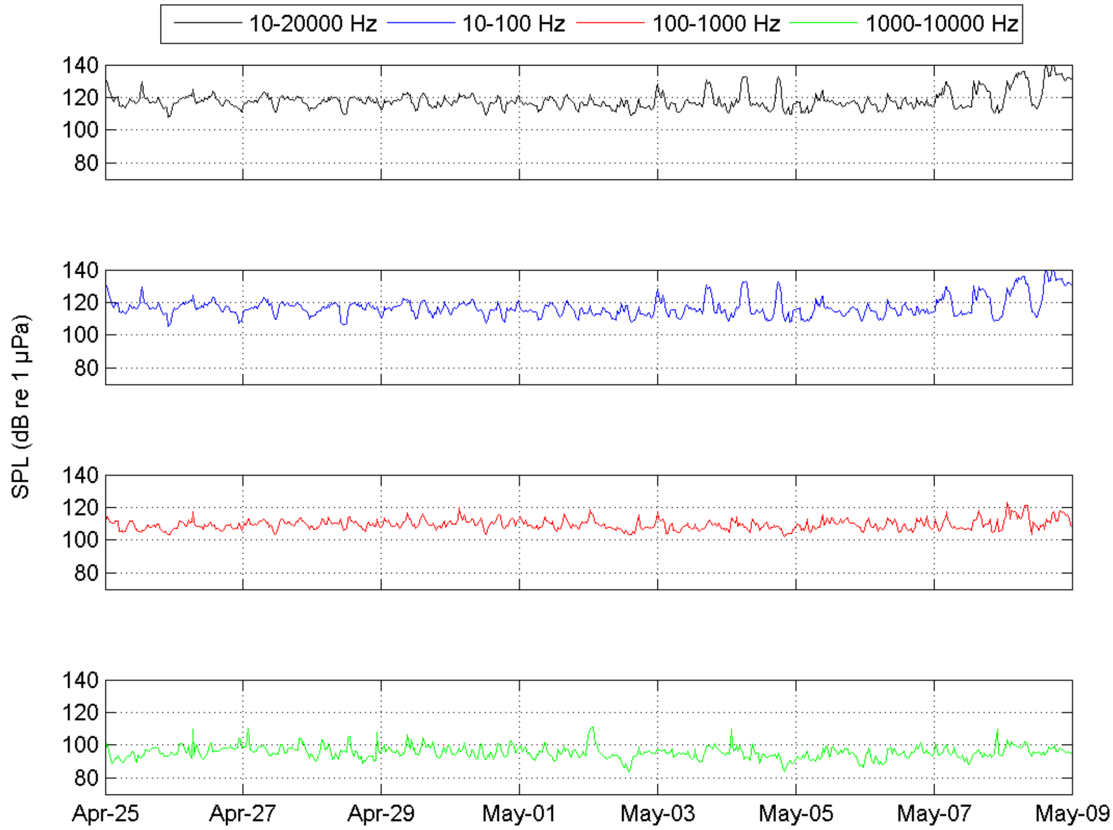

Figure 53: Broadband and decade band sound pressure levels (SPL) for 2-weeks of the 2011 spring deployment at HYWIND Control Station.

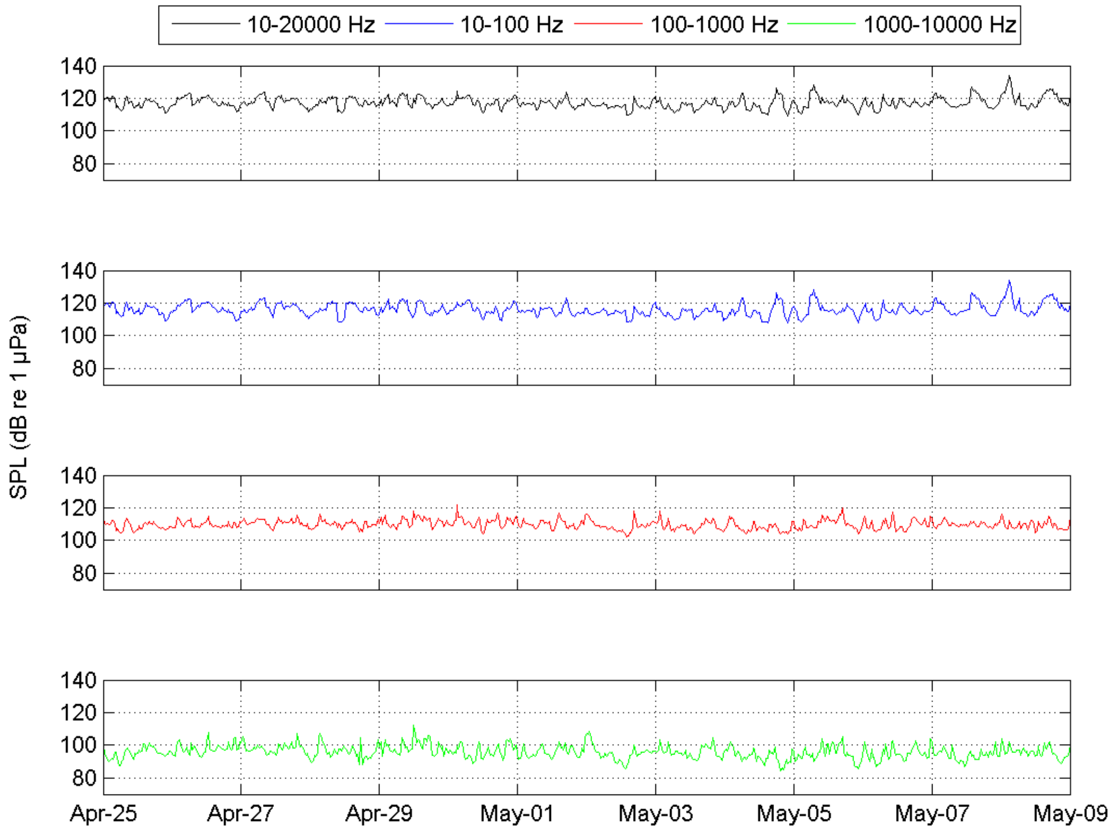

Figure 54: Broadband and decade band sound pressure levels (SPL) for 2-weeks of the 2011 spring deployment at HYWIND Monitoring Station.

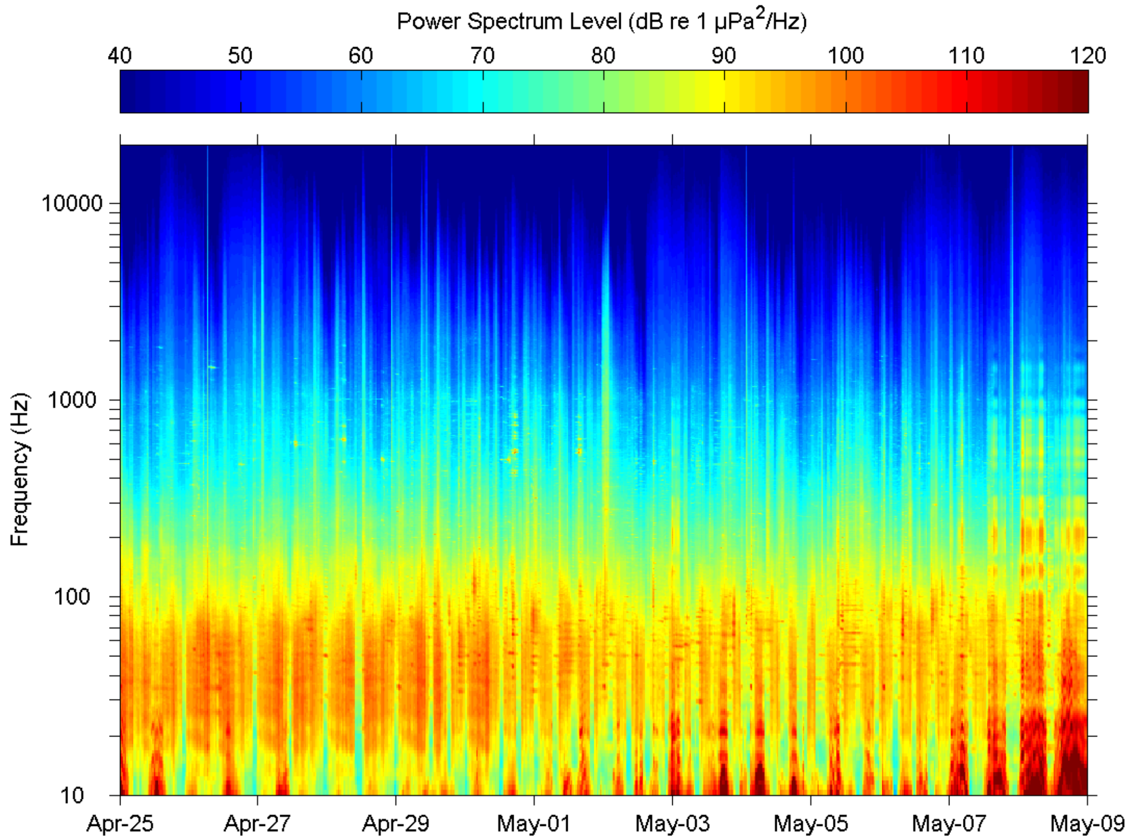

Figure 55: Spectrogram of 2-weeks of underwater sound for the spring 2011 deployment at the HYWIND Control Station.

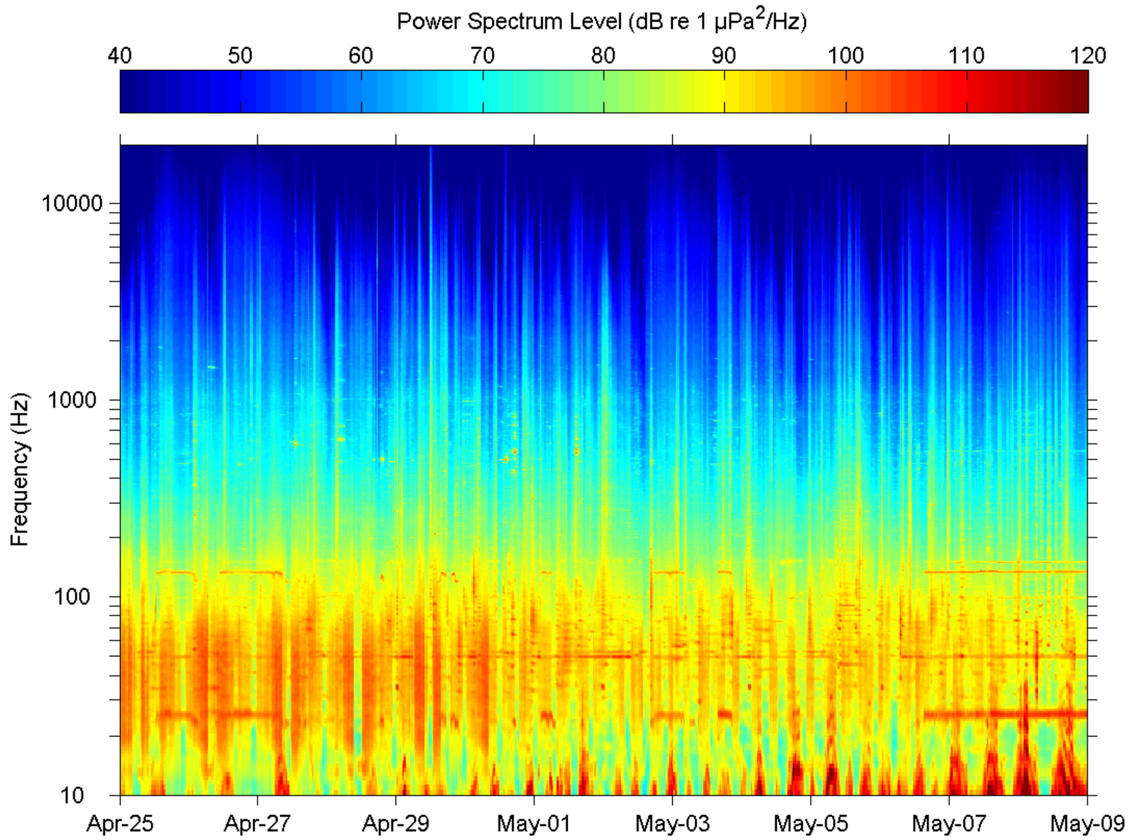

Figure 56: Spectrogram of 2-weeks of underwater sound for the spring 2011 deployment at the HYWIND Monitoring Station.

A.4. 9 May – 23 May 2011

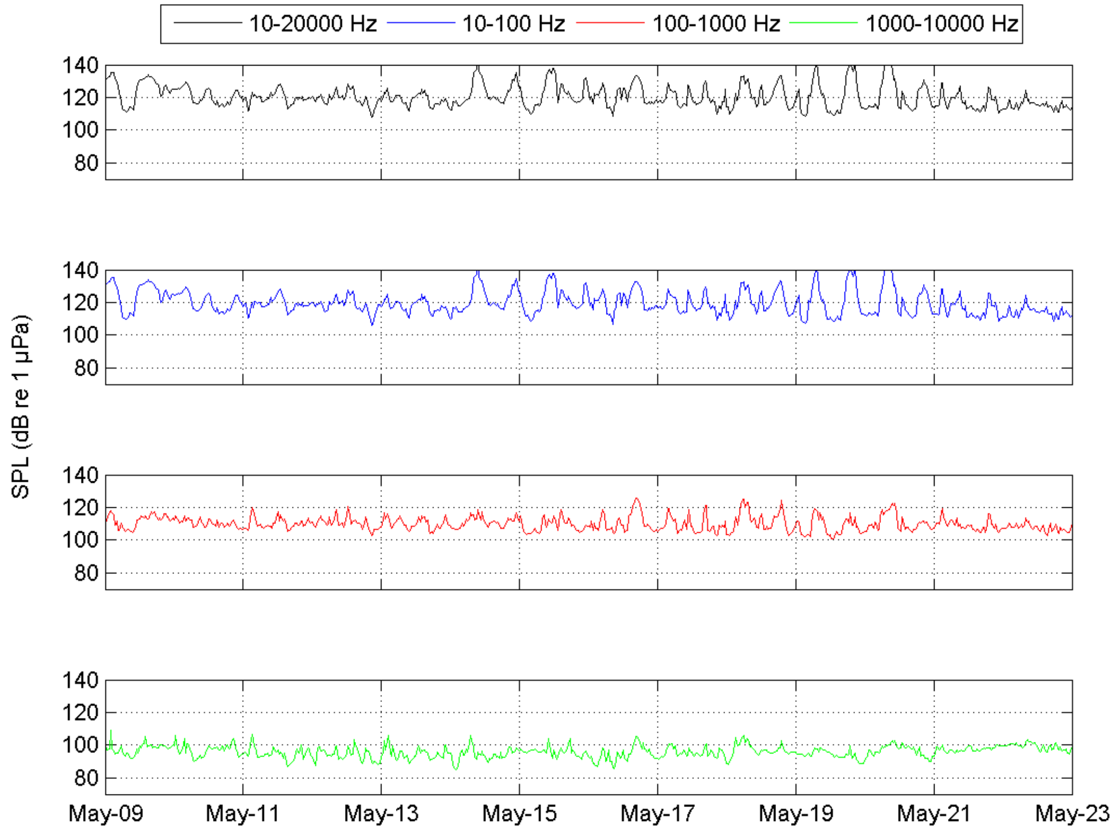

Figure 57: Broadband and decade band sound pressure levels (SPL) for 2-weeks of the 2011 spring deployment at HYWIND Control Station.

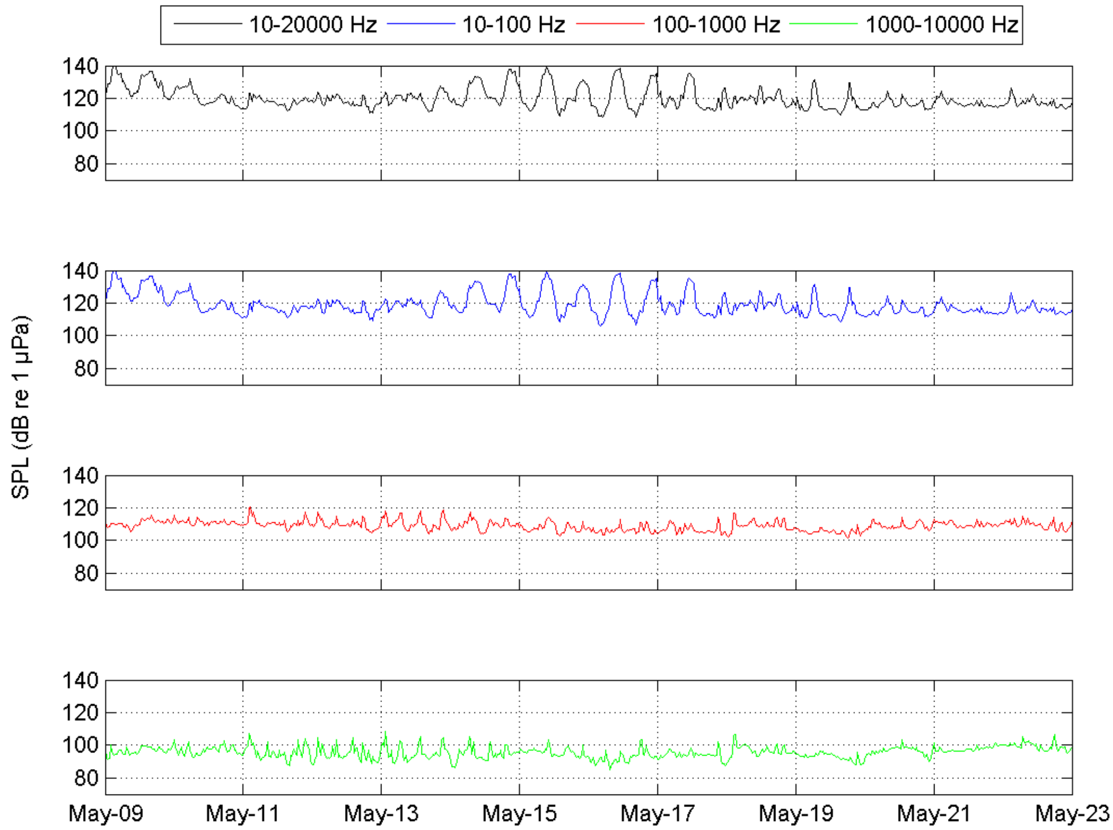

Figure 58: Broadband and decade band sound pressure levels (SPL) for 2-weeks of the 2011 spring deployment at HYWIND Monitoring Station.

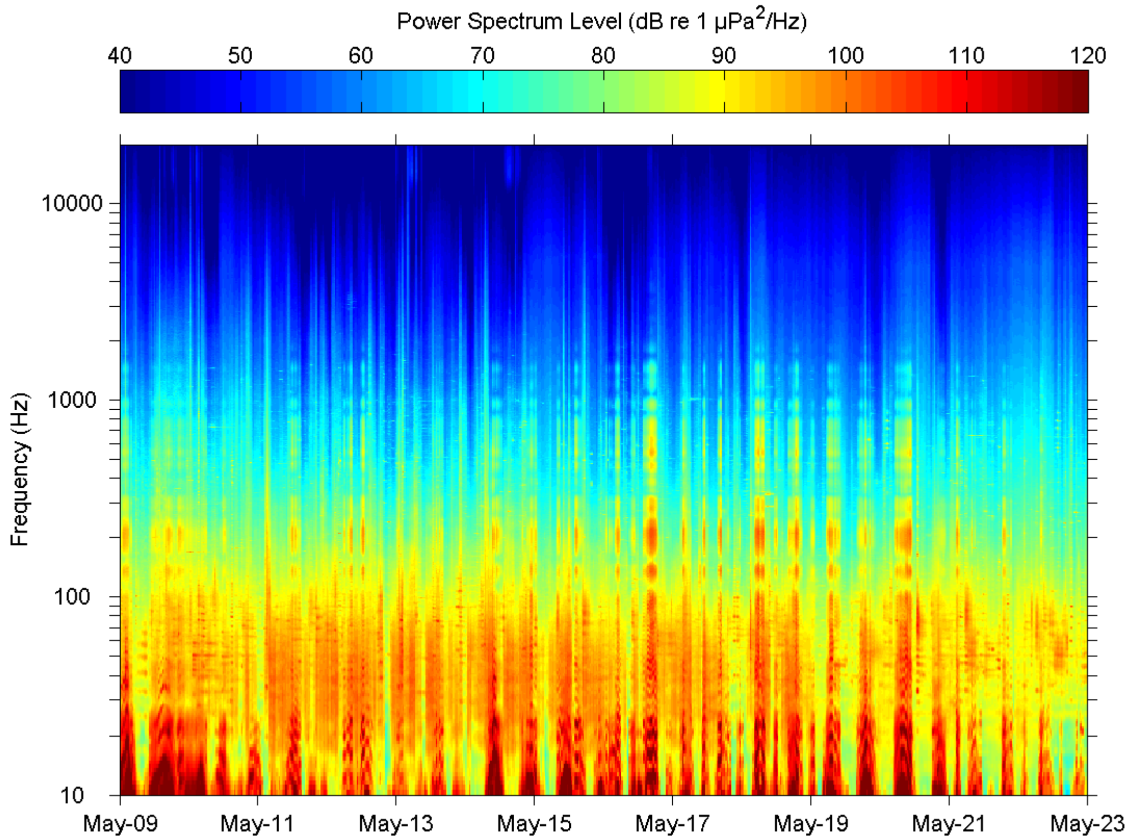

Figure 59: Spectrogram of 2-weeks of underwater sound for the spring 2011 deployment at the HYWIND Control Station.

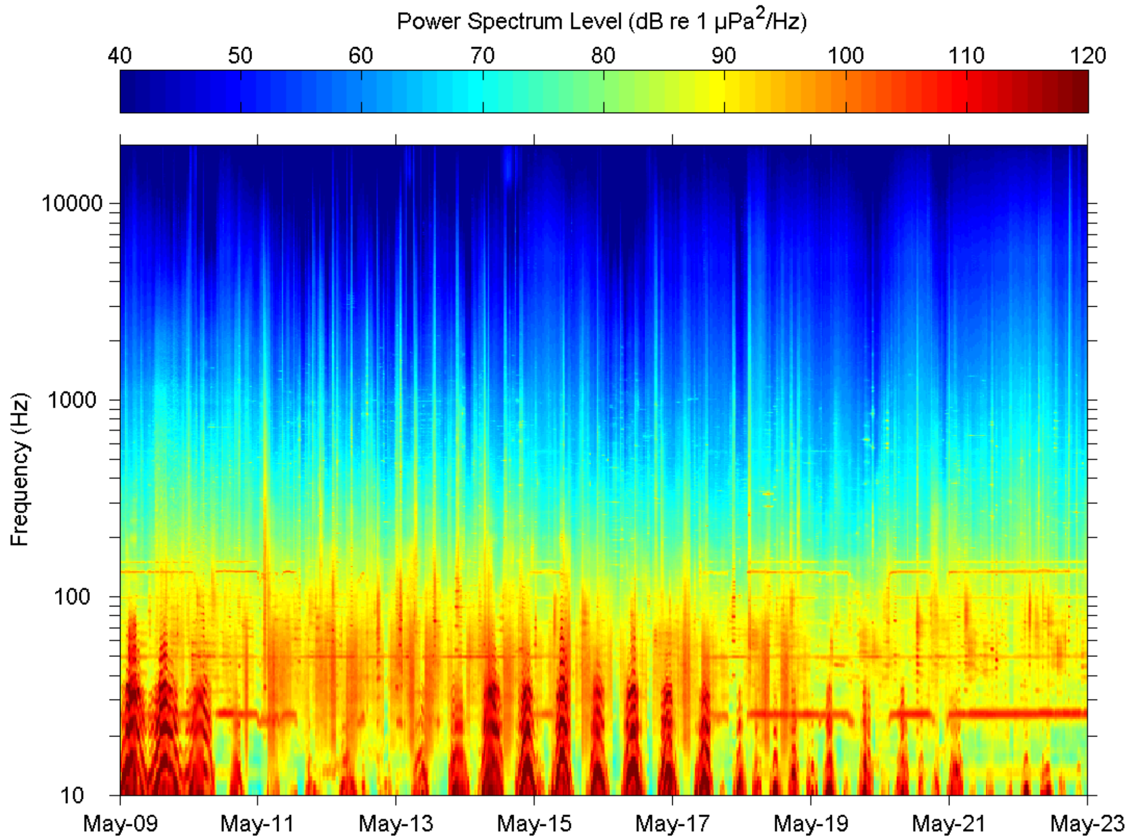

Figure 60: Spectrogram of 2-weeks of underwater sound for the spring 2011 deployment at the HYWIND Monitoring Station.

A.5. 23 May – 6 June 2011

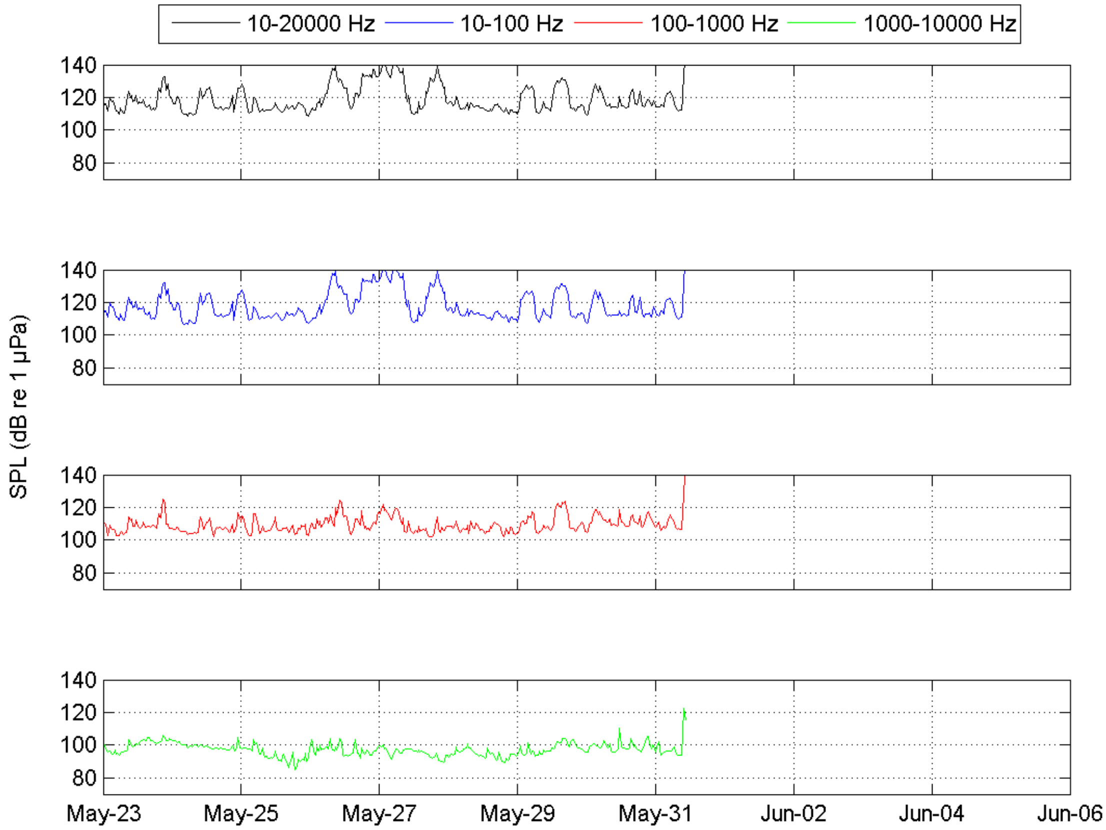

Figure 61: Broadband and decade band sound pressure levels (SPL) for 2-weeks of the 2011 spring deployment at HYWIND Control Station.

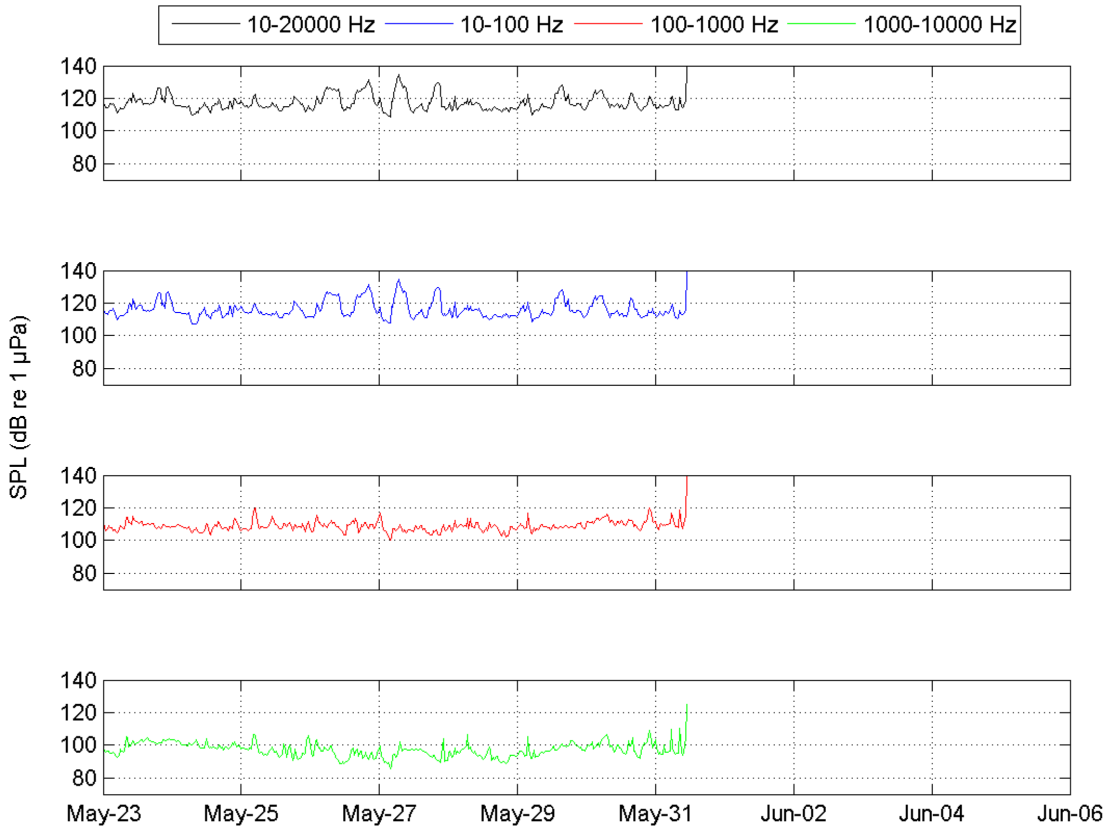

Figure 62: Broadband and decade band sound pressure levels (SPL) for 2-weeks of the 2011 spring deployment at HYWIND Monitoring Station.

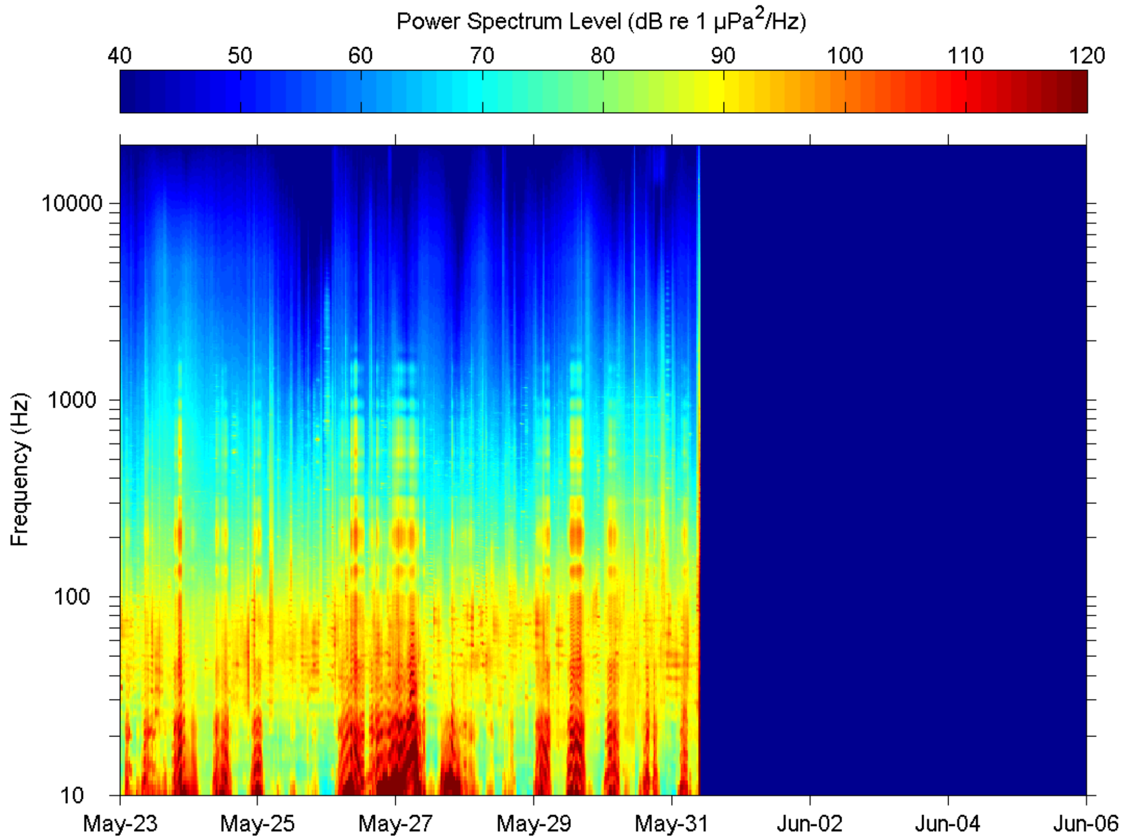

Figure 63: Spectrogram of 2-weeks of underwater sound for the spring 2011 deployment at the HYWIND Control Station.

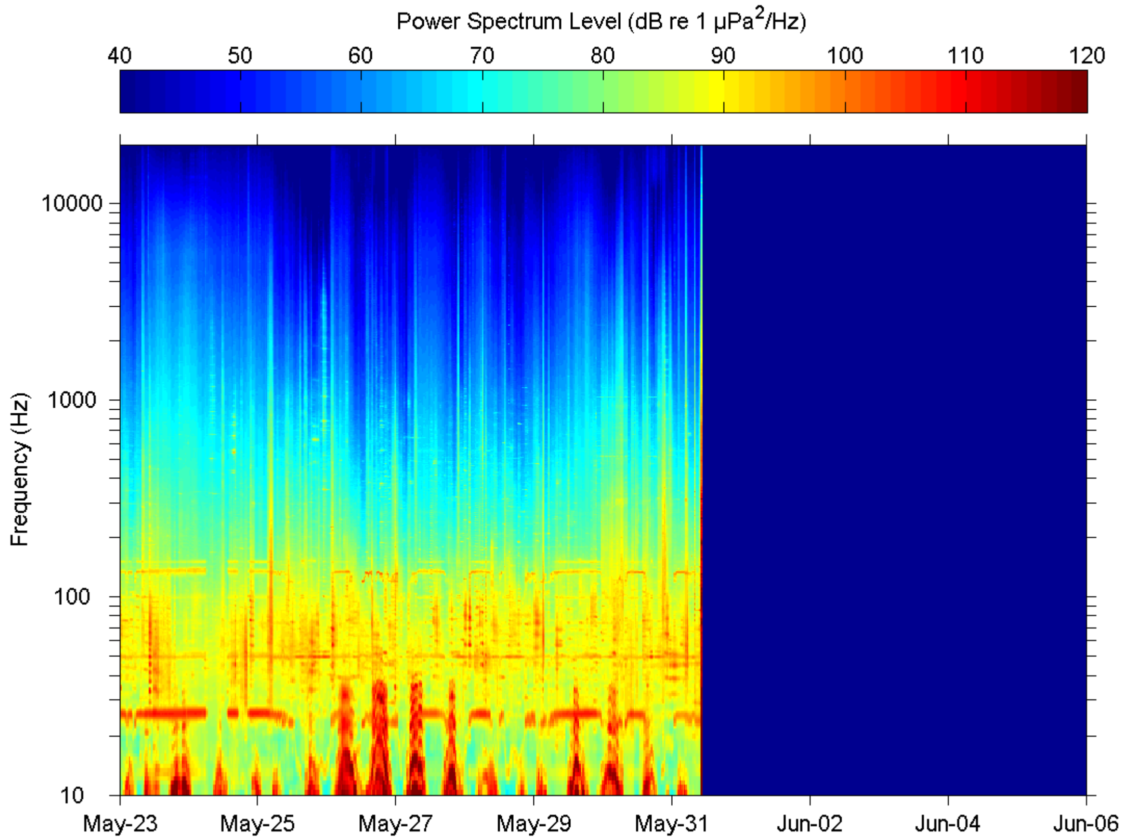

Figure 64: Spectrogram of 2-weeks of underwater sound for the spring 2011 deployment at the HYWIND Monitoring Station.

A.6. 31 May – 14 June 2011

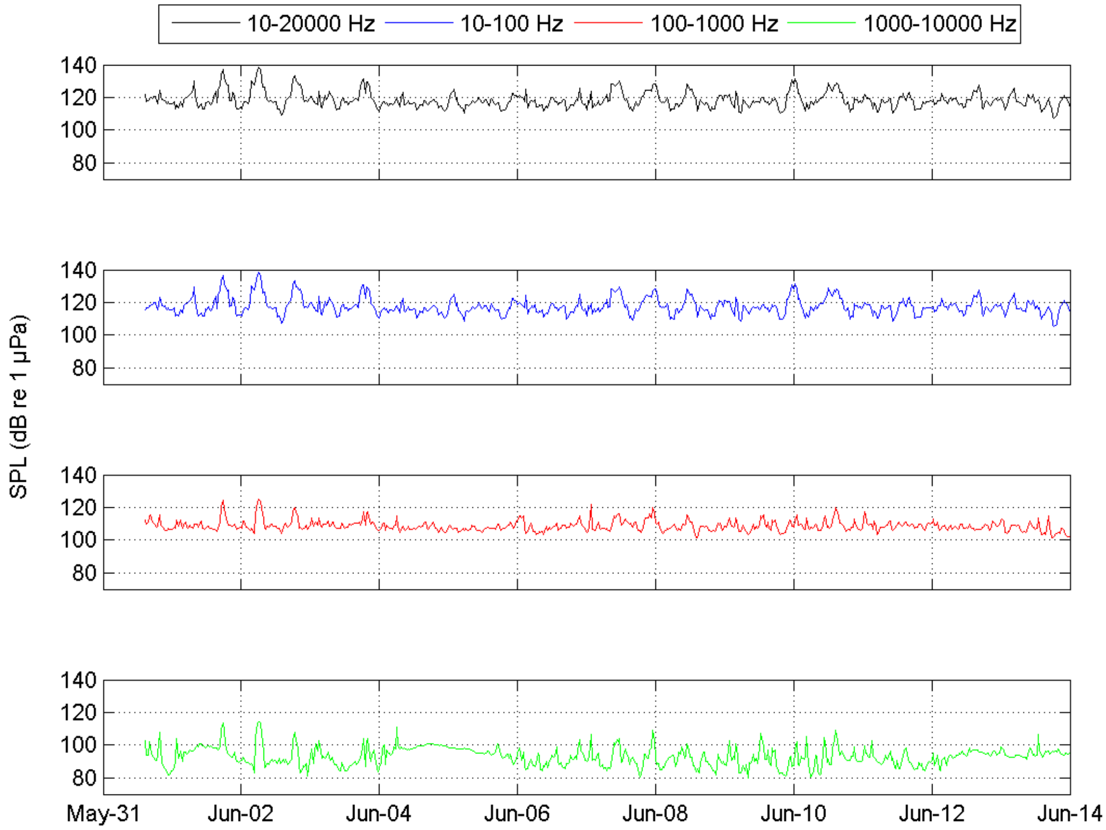

Figure 65: Broadband and decade band sound pressure levels (SPL) for 2-weeks of the 2011 summer deployment at HYWIND Control Station.

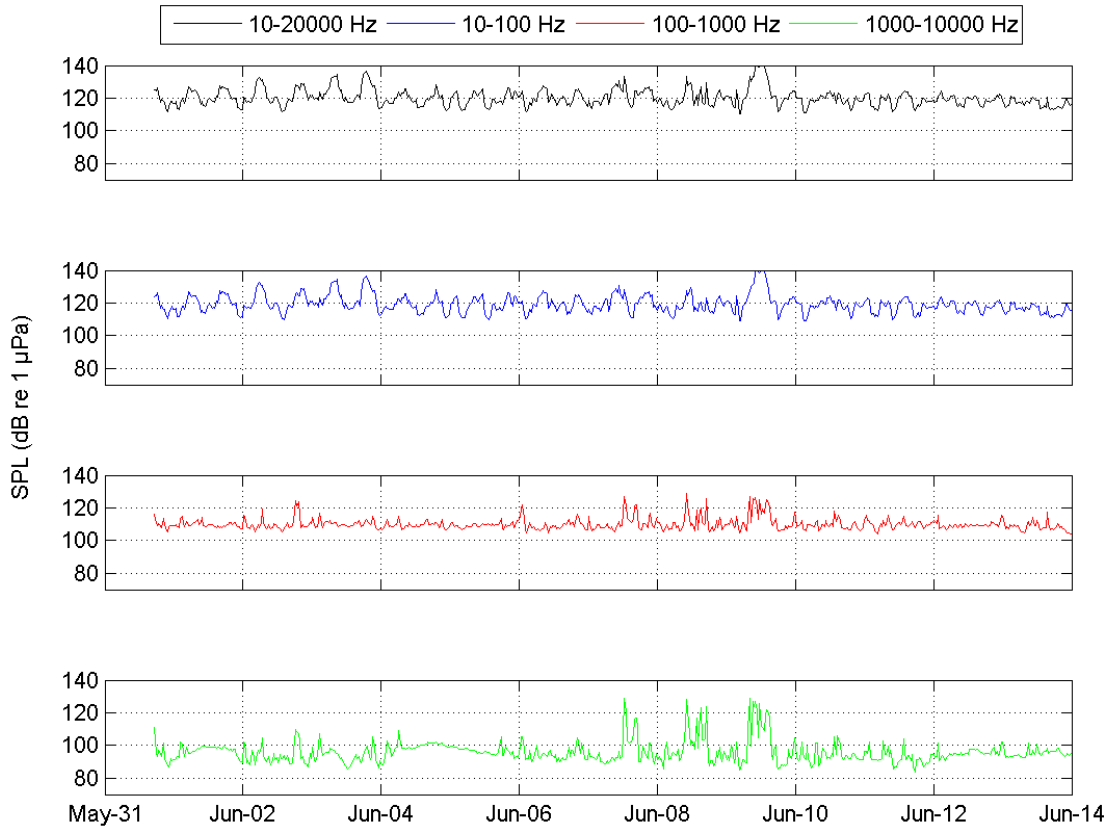

Figure 66: Broadband and decade band sound pressure levels (SPL) for 2-weeks of the 2011 summer deployment at HYWIND Monitoring Station.

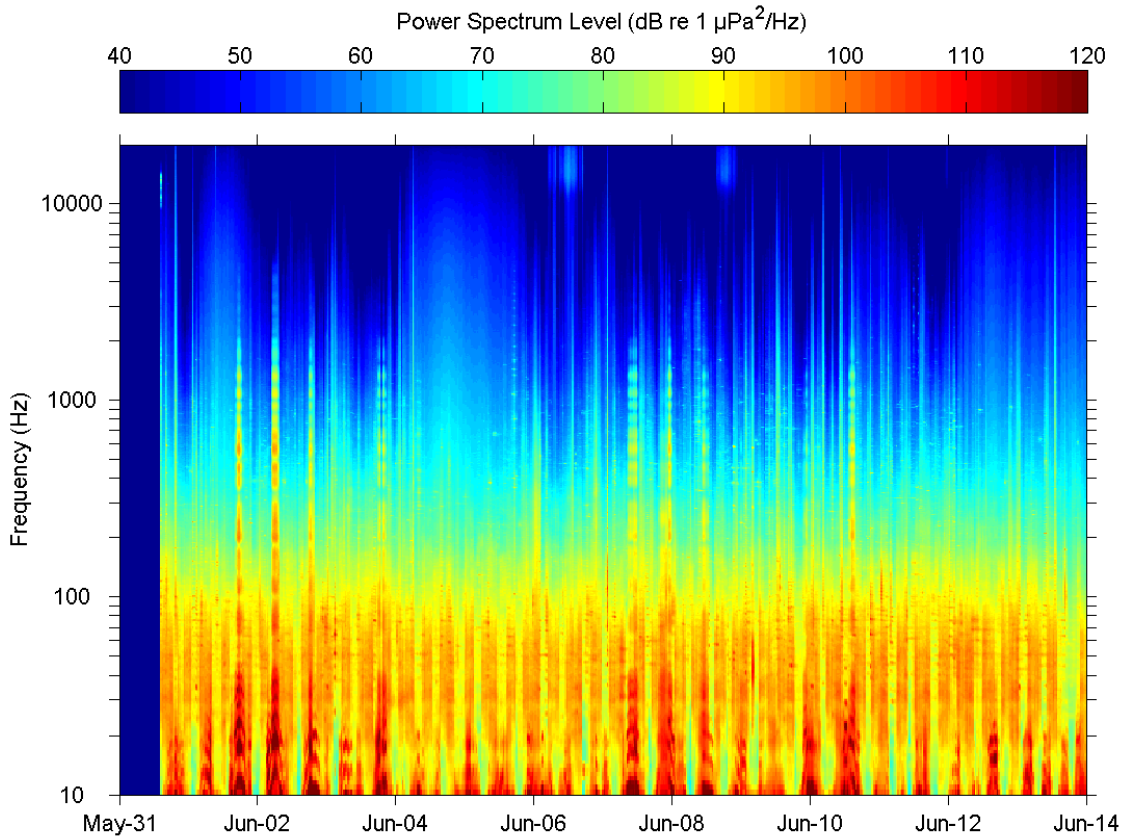

Figure 67: Spectrogram of 2-weeks of underwater sound for the summer 2011 deployment at the HYWIND Control Station.

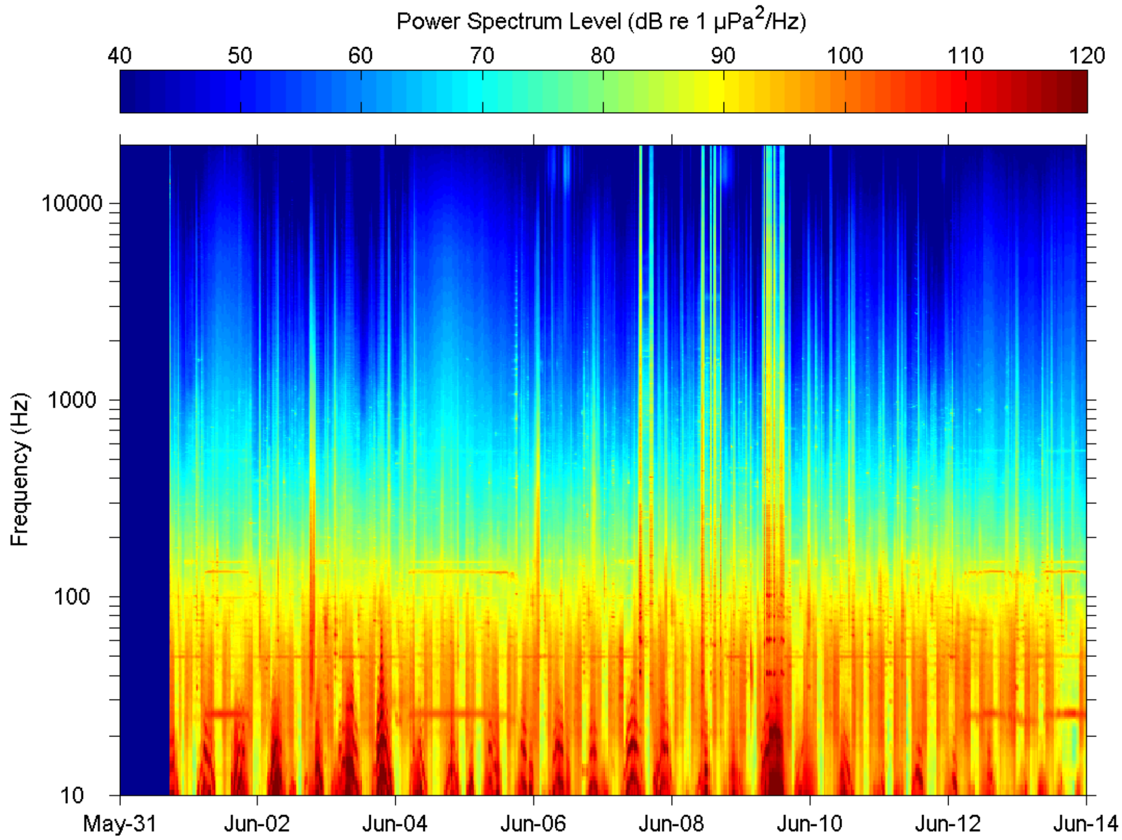

Figure 68: Spectrogram of 2-weeks of underwater sound for the summer 2011 deployment at the HYWIND Monitoring Station.

A.7. 14 June – 28 June 2011

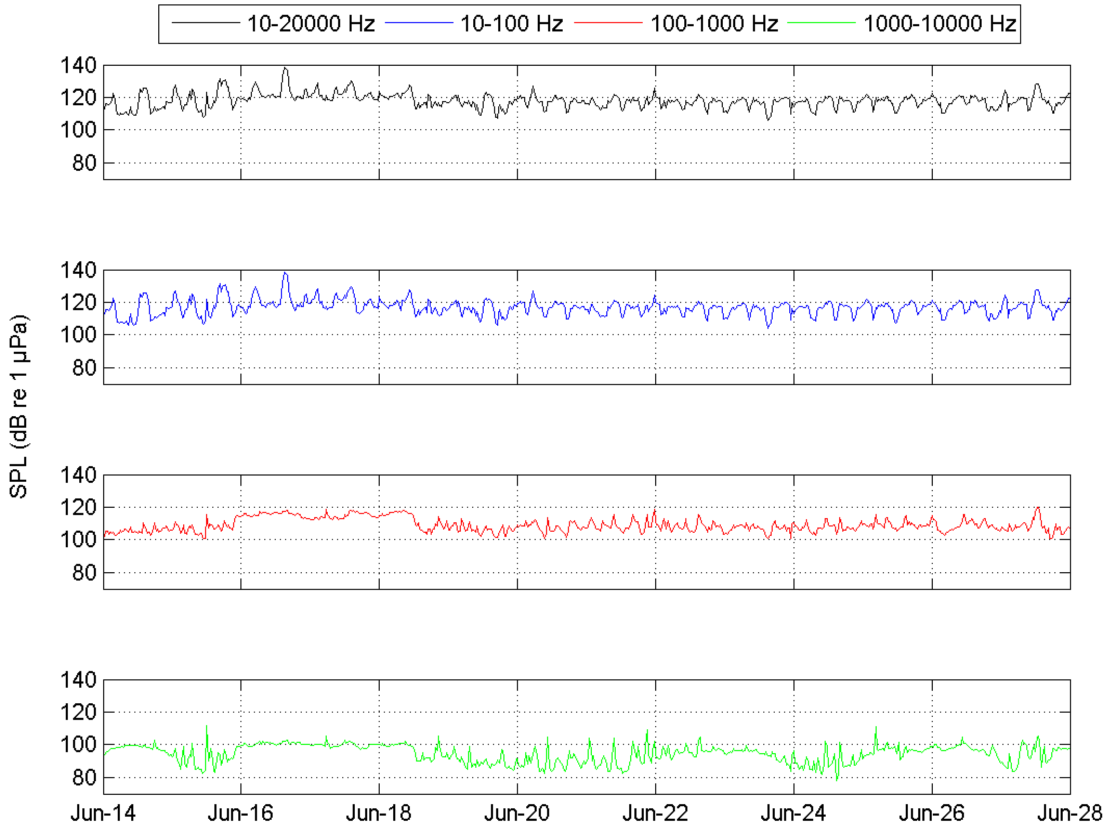

Figure 69: Broadband and decade band sound pressure levels (SPL) for 2-weeks of the 2011 summer deployment at HYWIND Control Station.

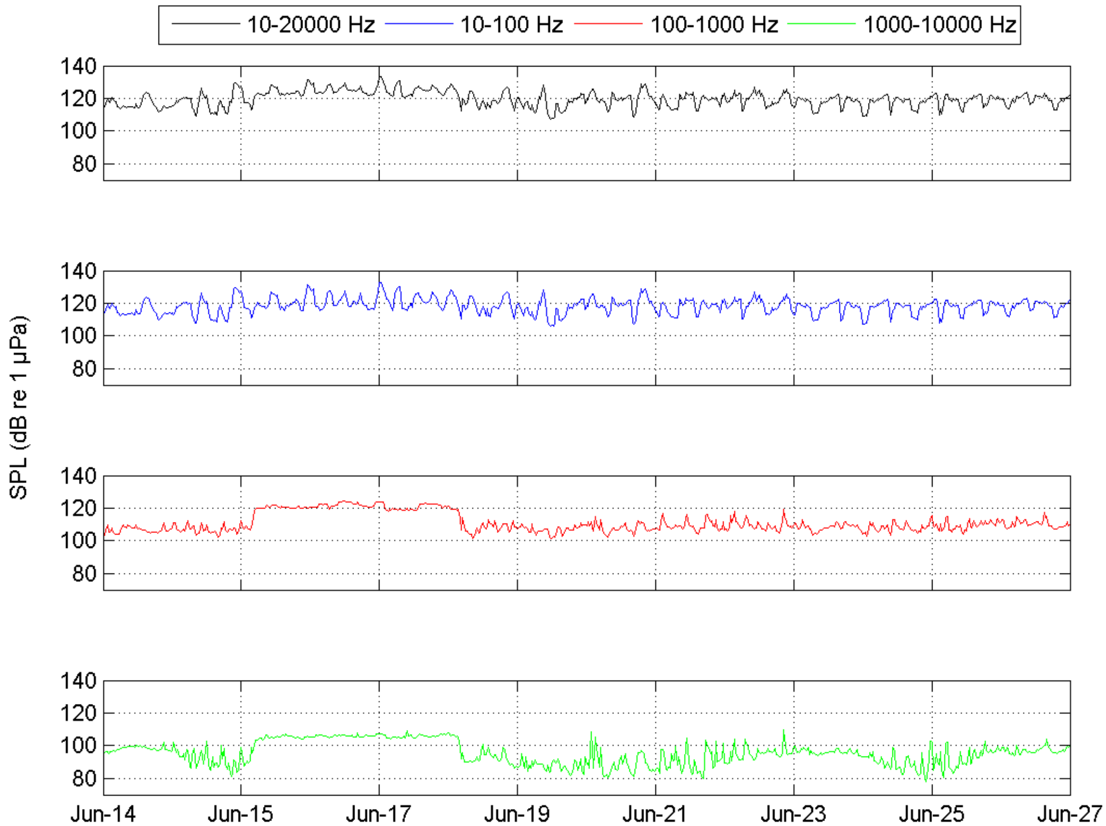

Figure 70: Broadband and decade band sound pressure levels (SPL) for 2-weeks of the 2011 summer deployment at HYWIND Monitoring Station.

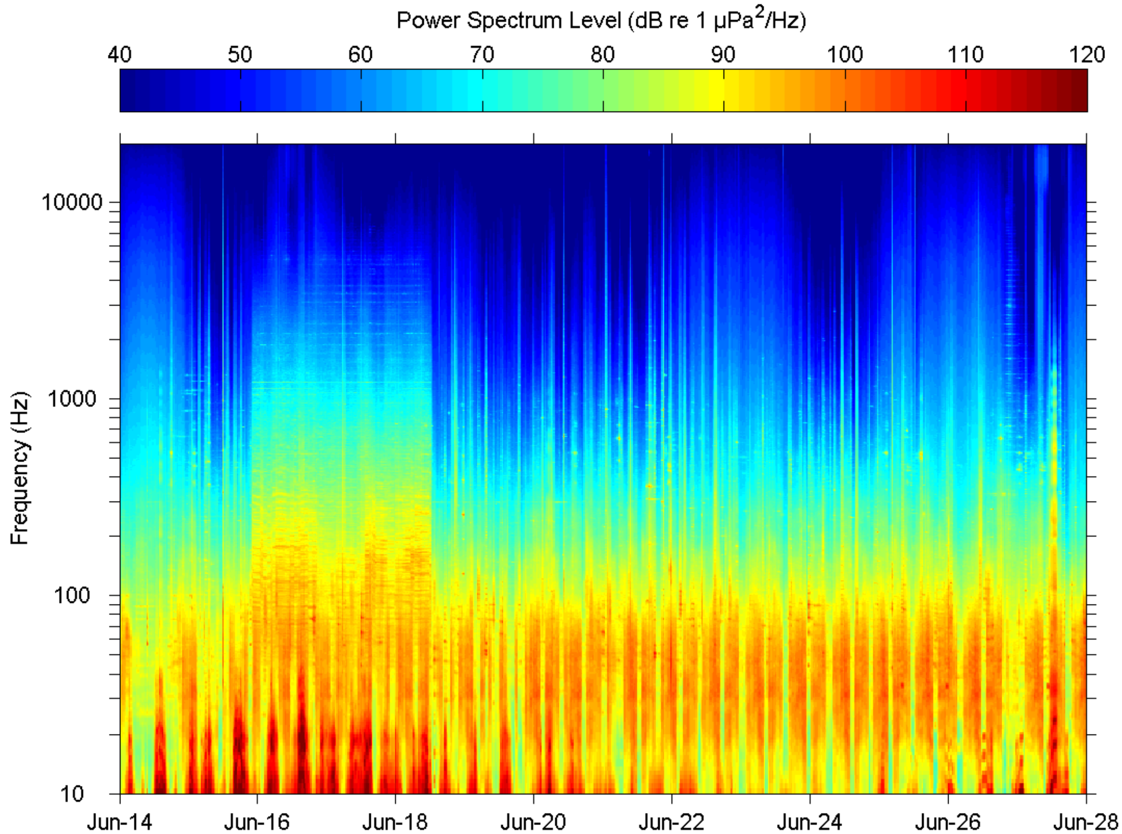

Figure 71: Spectrogram of 2-weeks of underwater sound for the summer 2011 deployment at the HYWIND Control Station.

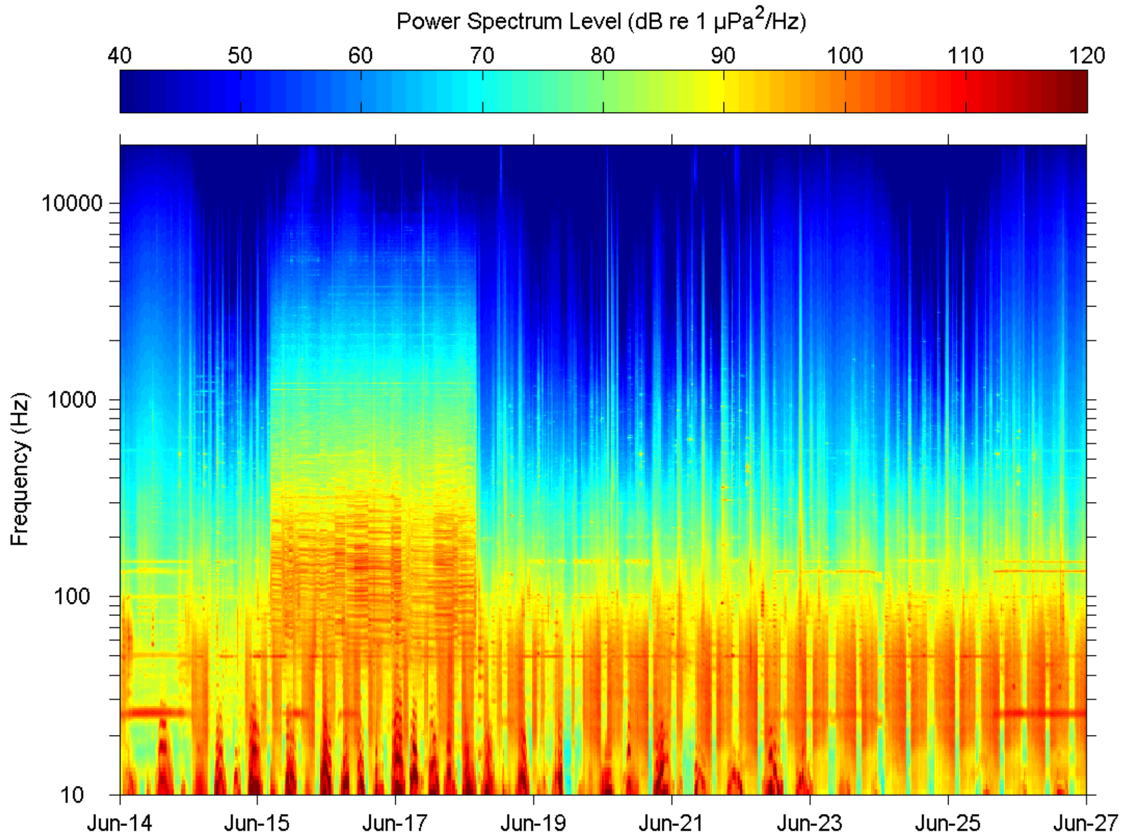

Figure 72: Spectrogram of 2-weeks of underwater sound for the summer 2011 deployment at the HYWIND Monitoring Station.

A.8. 28 June – 12 July 2011

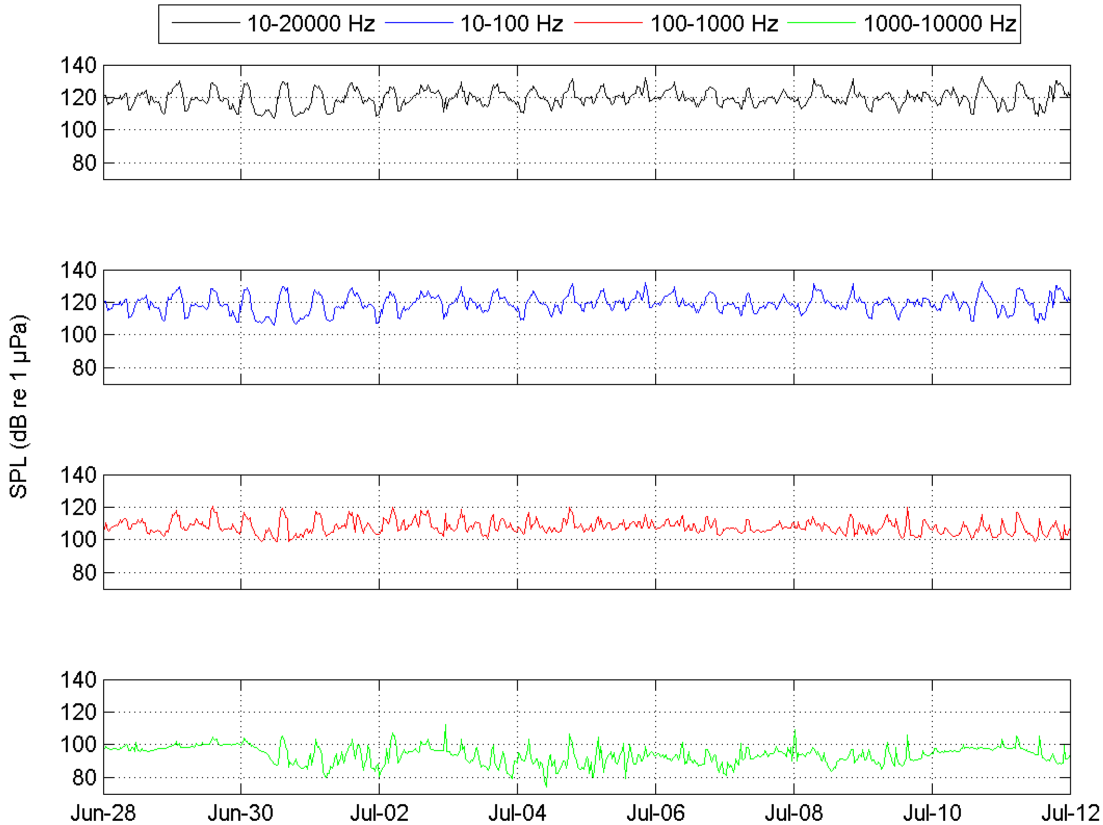

Figure 73: Broadband and decade band sound pressure levels (SPL) for 2-weeks of the 2011 summer deployment at HYWIND Control Station.

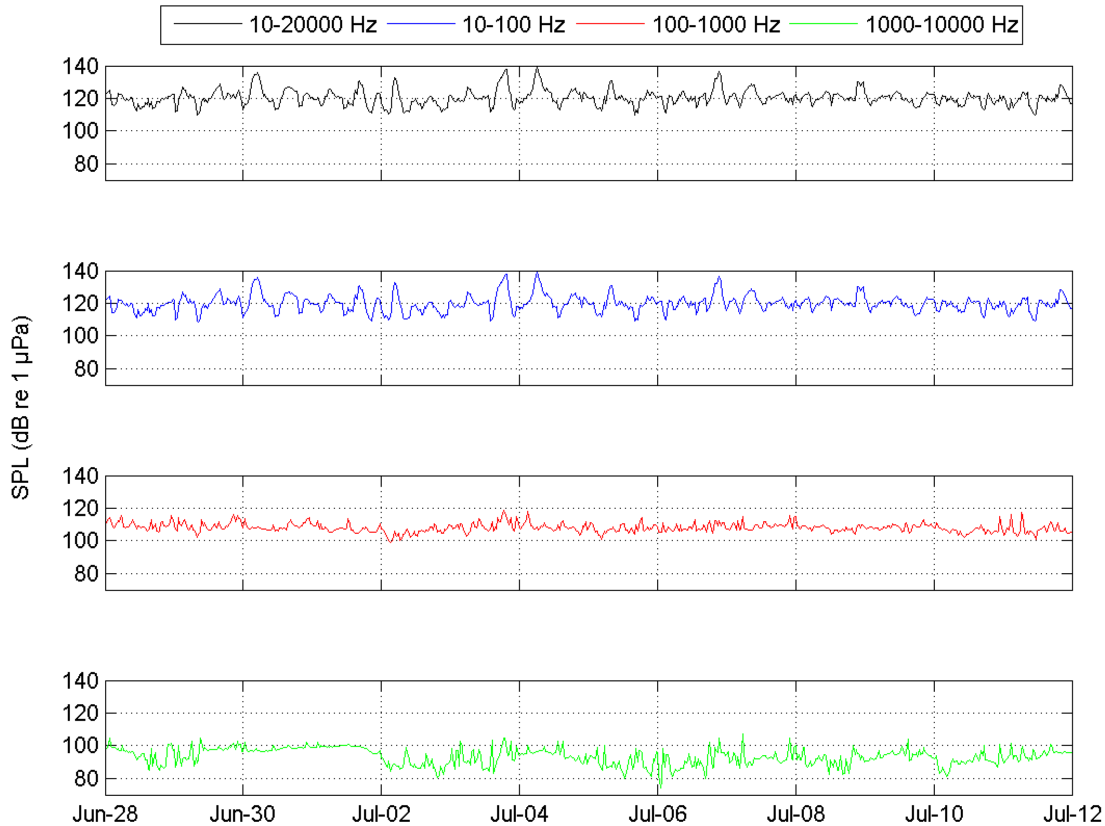

Figure 74: Broadband and decade band sound pressure levels (SPL) for 2-weeks of the 2011 summer deployment at HYWIND Monitoring Station.

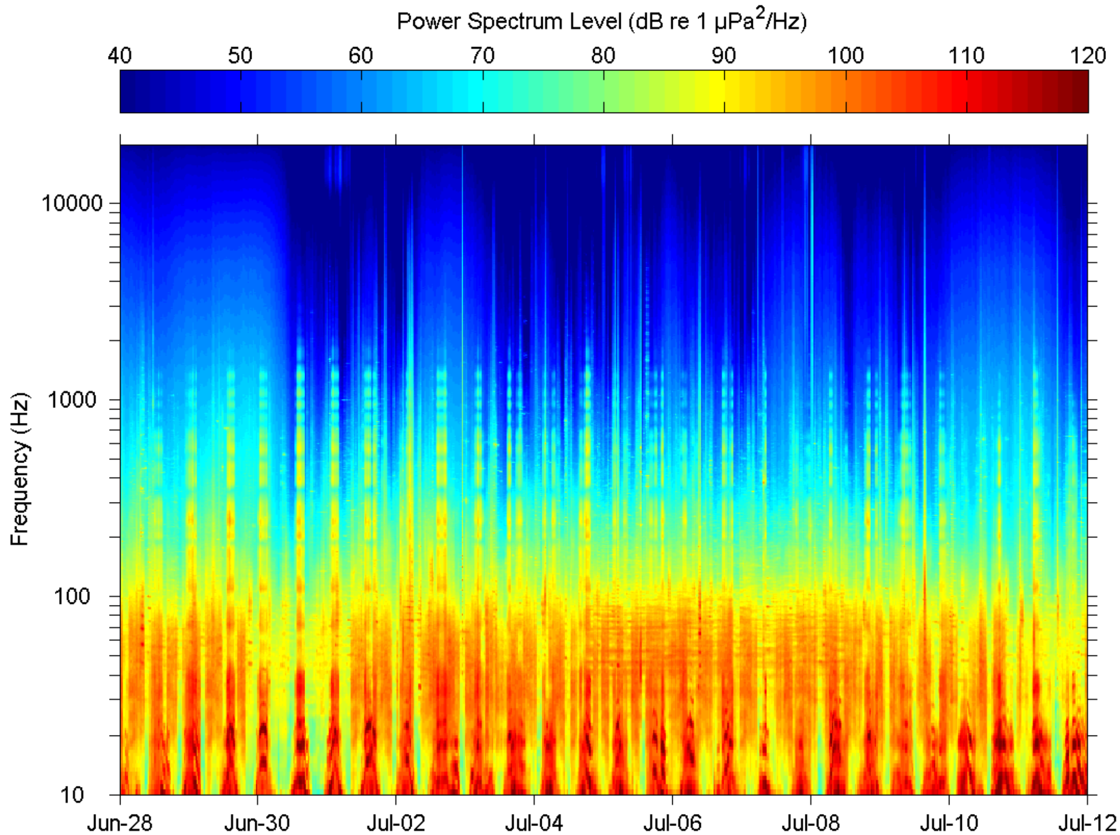

Figure 75: Spectrogram of 2-weeks of underwater sound for the summer 2011 deployment at the HYWIND Control Station.

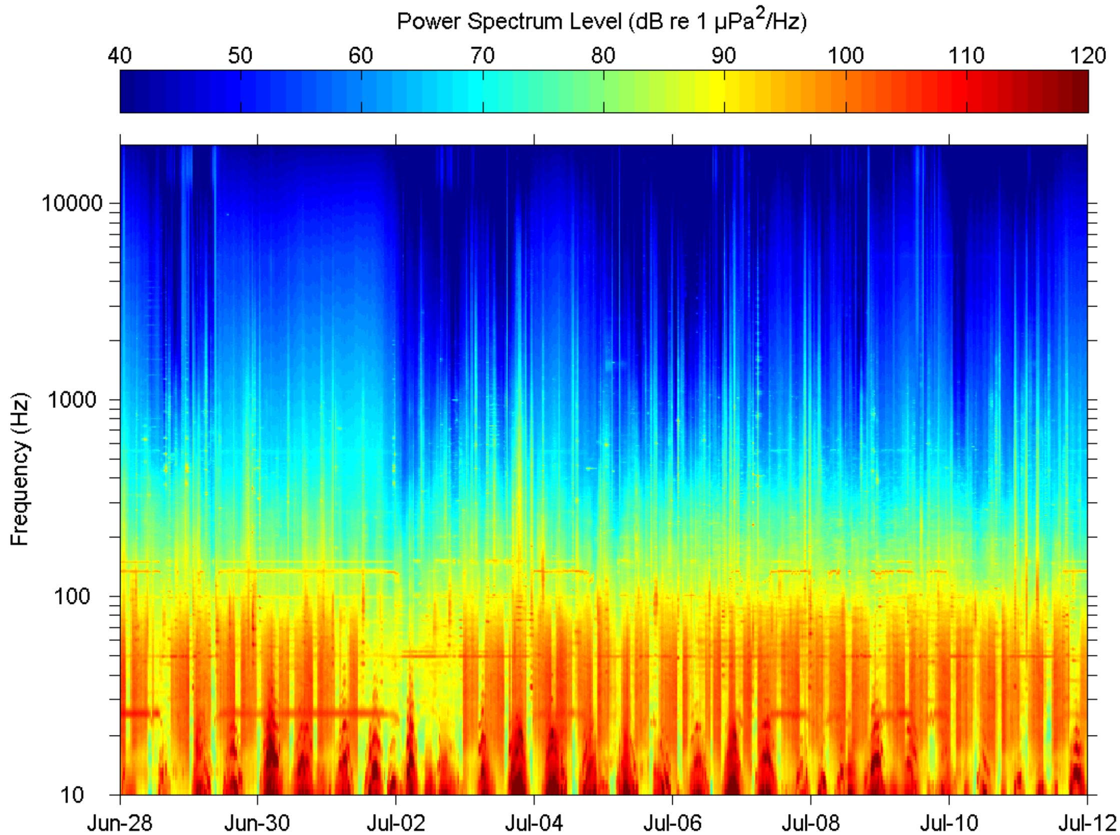

Figure 76: Spectrogram of 2-weeks of underwater sound for the summer 2011 deployment at the HYWIND Monitoring Station.

A.9. 12 July – 26 July 2011

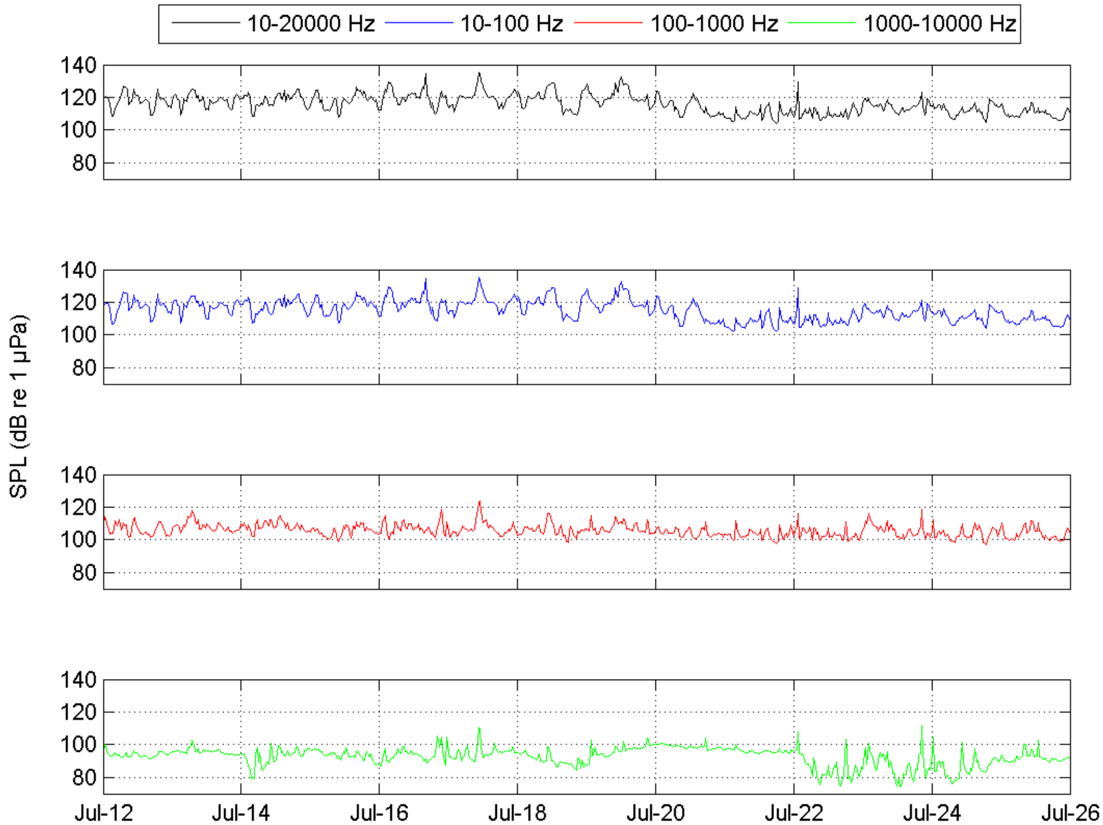

Figure 77: Broadband and decade band sound pressure levels (SPL) for 2-weeks of the 2011 summer deployment at HYWIND Control Station.

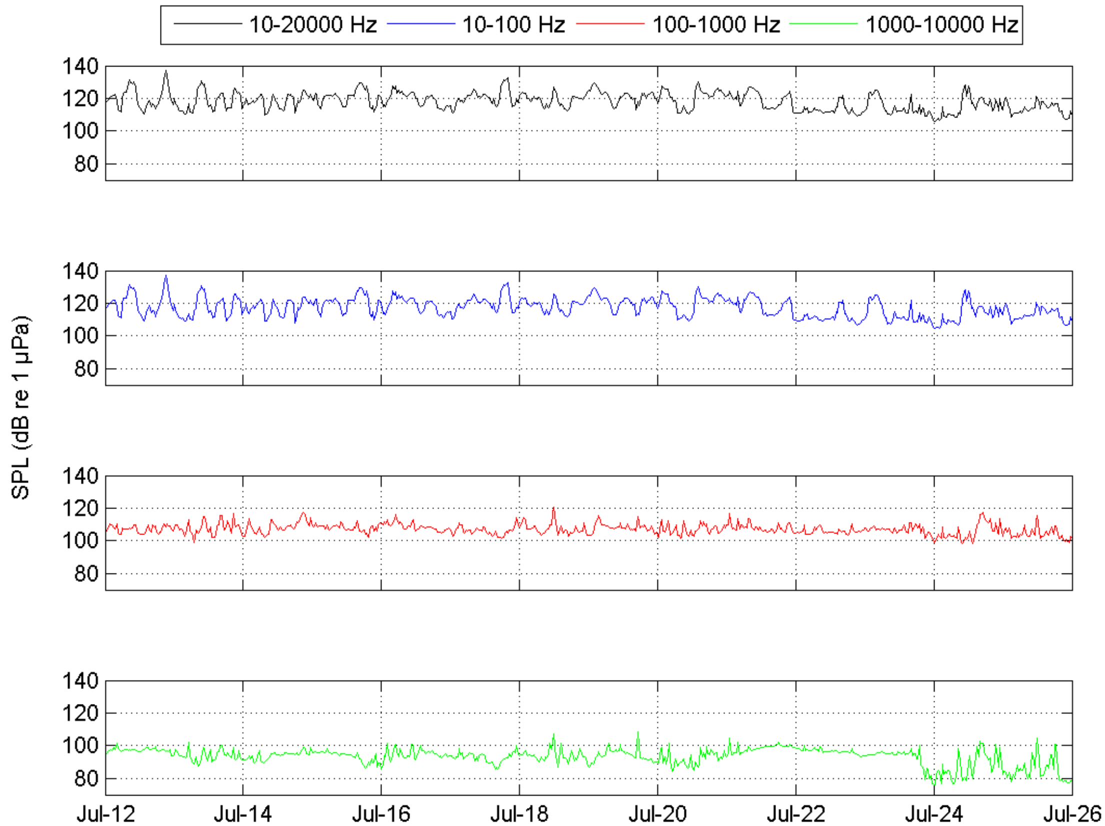

Figure 78: Broadband and decade band sound pressure levels (SPL) for 2-weeks of the 2011 summer deployment at HYWIND Monitoring Station.

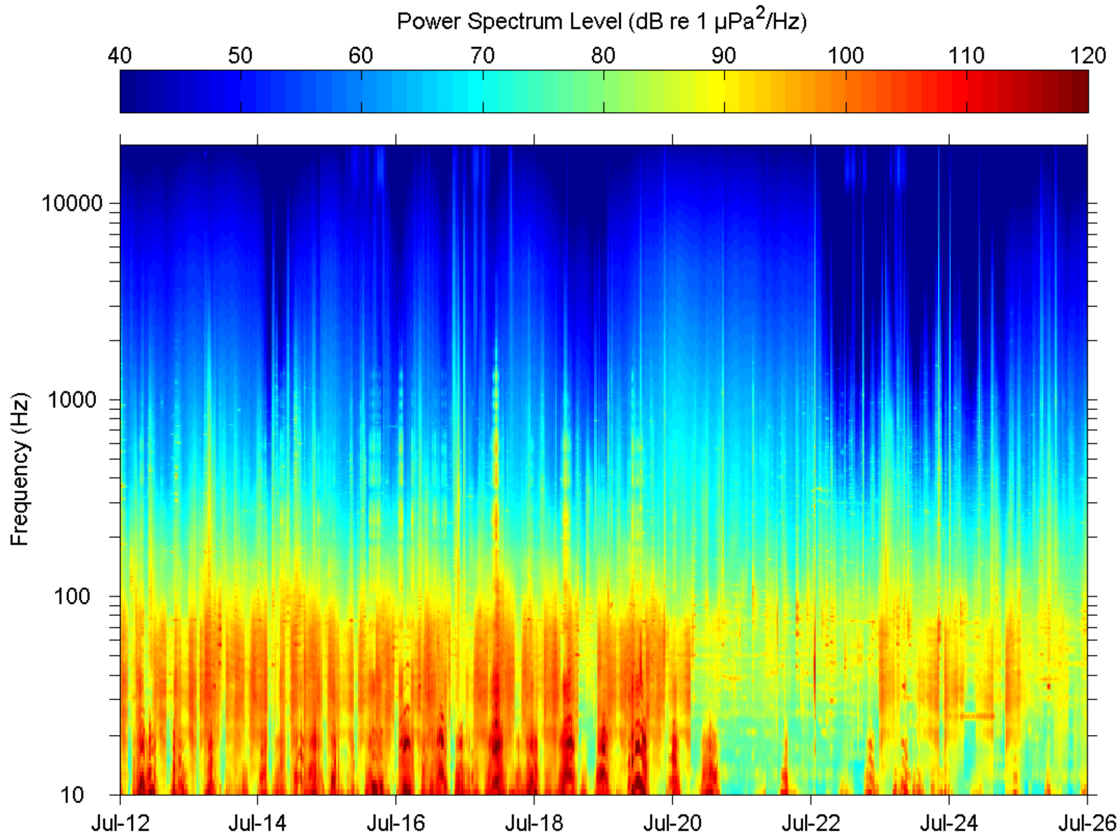

Figure 79: Spectrogram of 2-weeks of underwater sound for the summer 2011 deployment at the HYWIND Control Station.

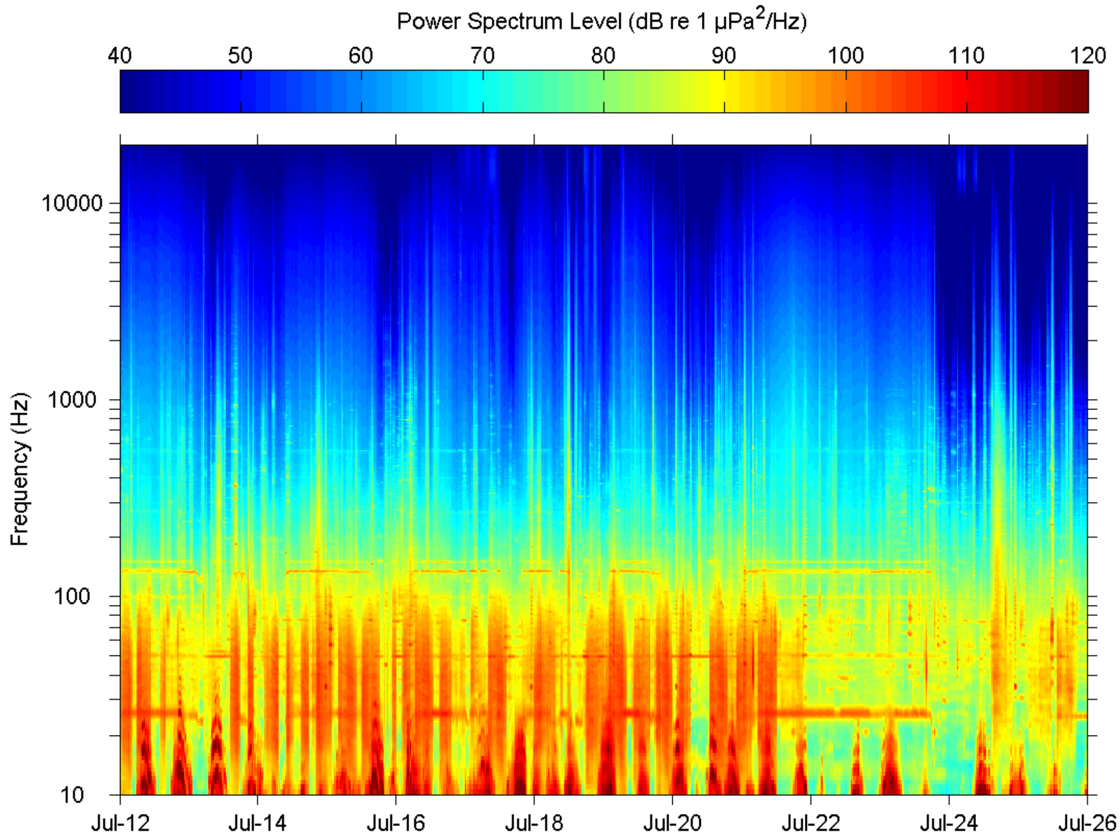

Figure 80: Spectrogram of 2-weeks of underwater sound for the summer 2011 deployment at the HYWIND Monitoring Station.

A.10. 26 July – 9 August

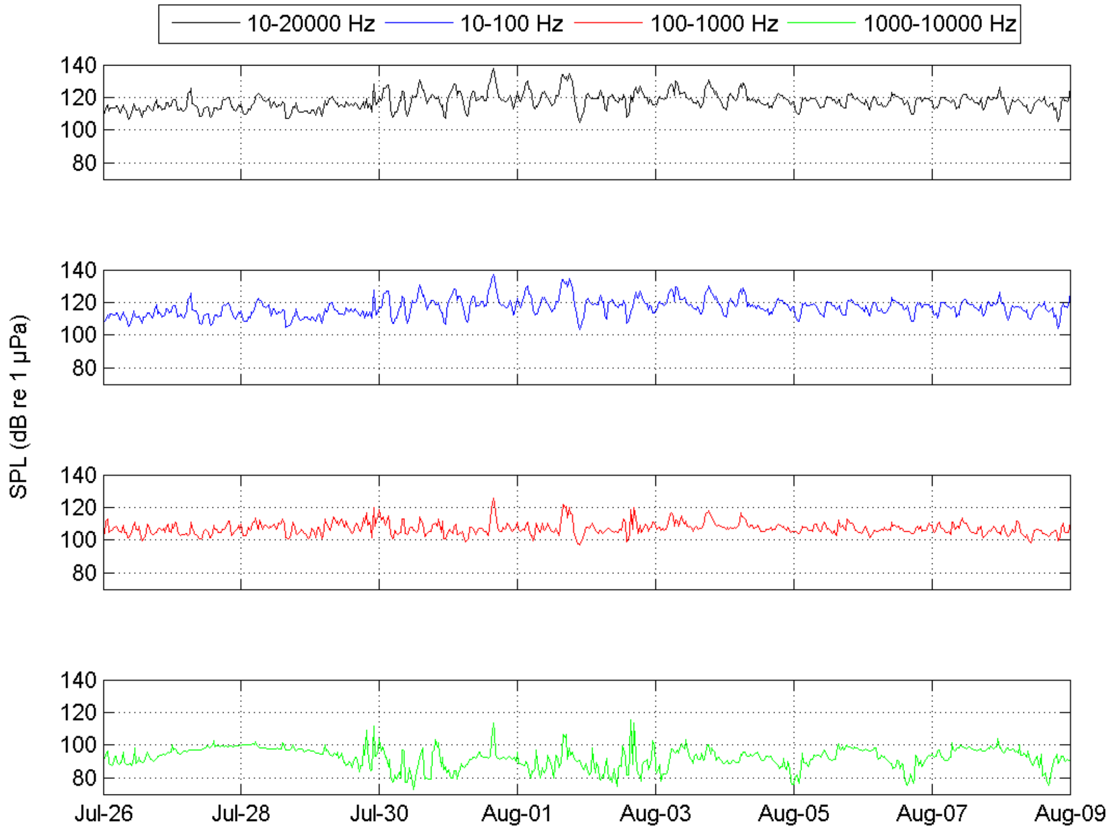

Figure 81: Broadband and decade band sound pressure levels (SPL) for 2-weeks of the 2011 summer deployment at HYWIND Control Station.

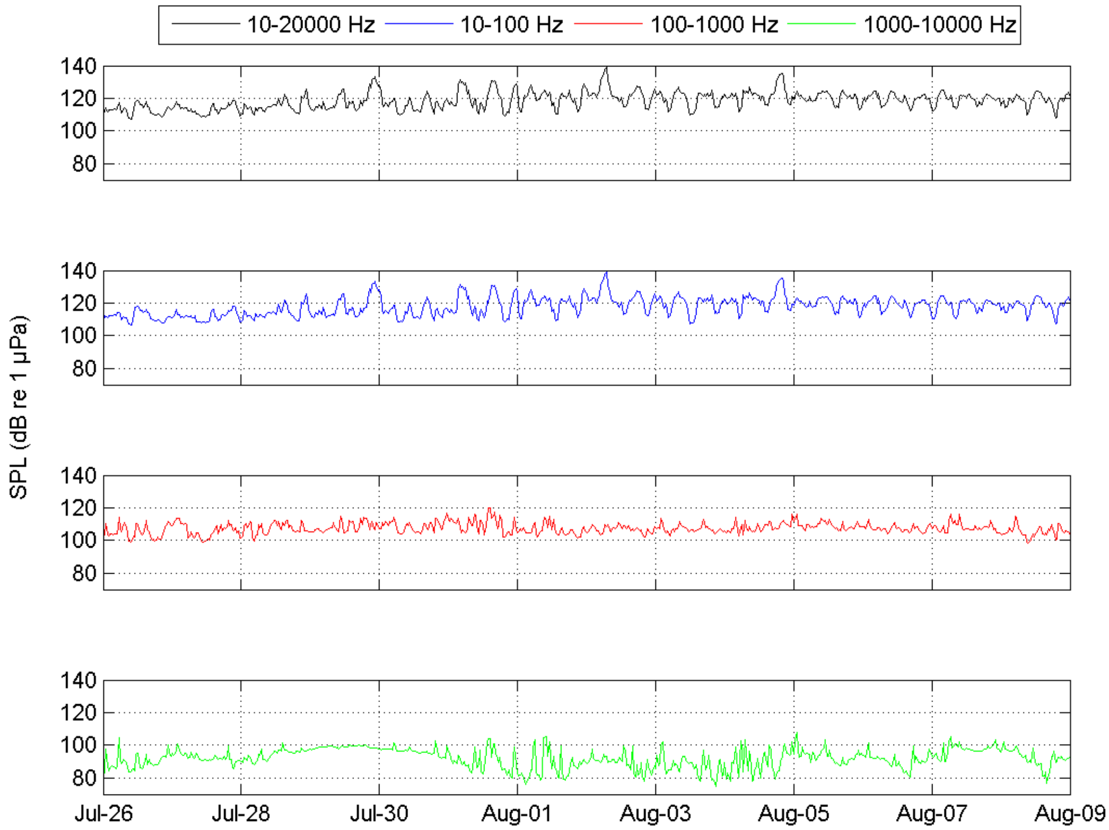

Figure 82: Broadband and decade band sound pressure levels (SPL) for 2-weeks of the 2011 summer deployment at HYWIND Monitoring Station.

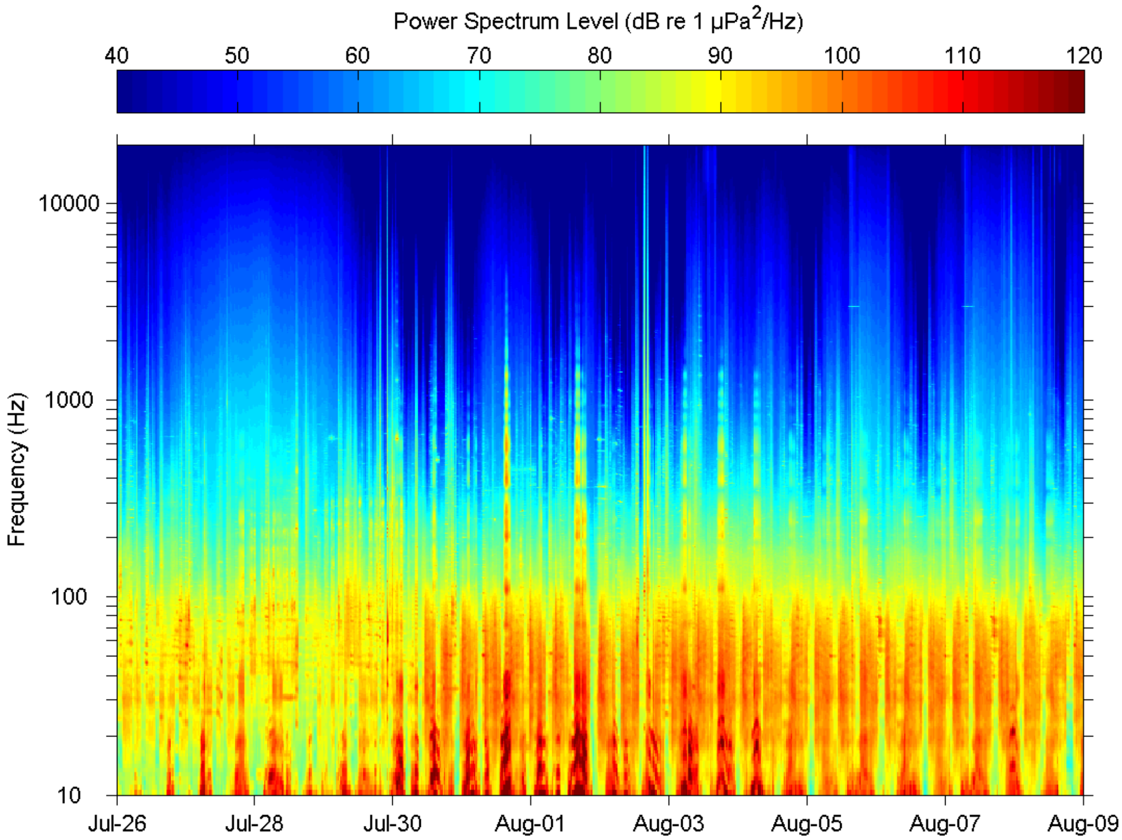

Figure 83: Spectrogram of 2-weeks of underwater sound for the summer 2011 deployment at the HYWIND Control Station.

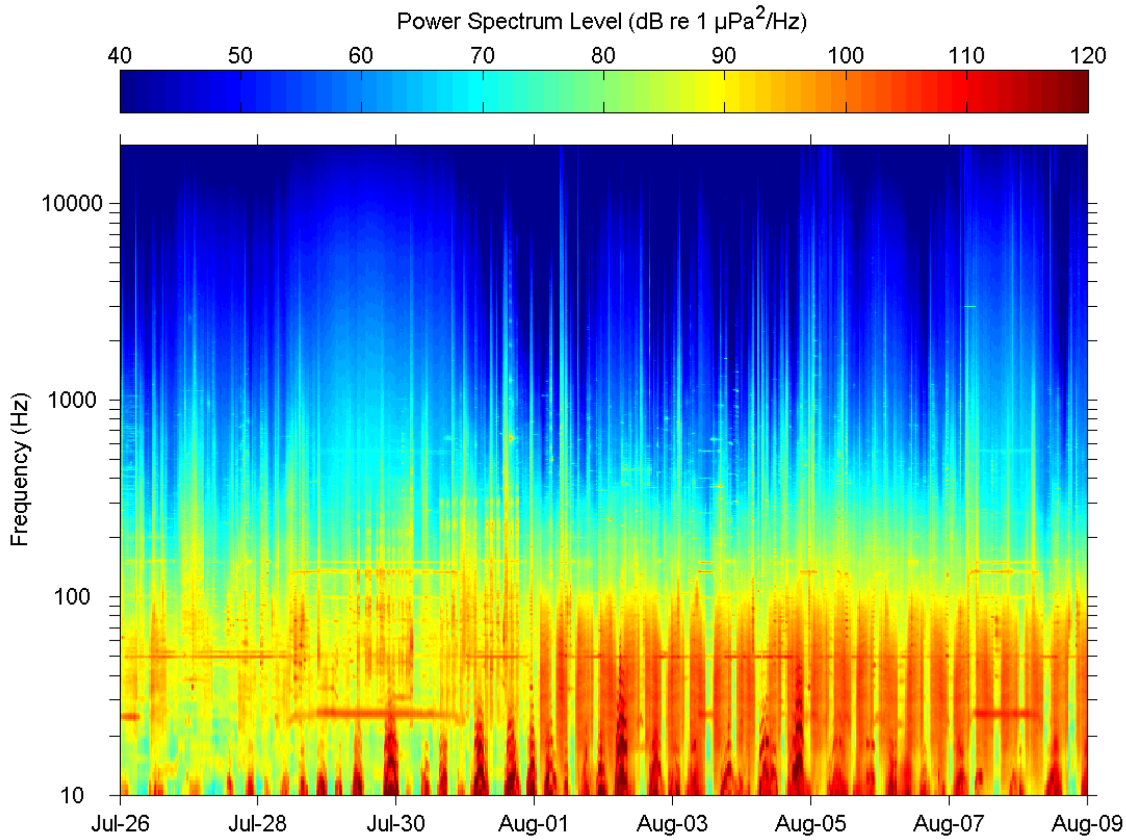

Figure 84: Spectrogram of 2-weeks of underwater sound for the summer 2011 deployment at the HYWIND Monitoring Station.

A.11. 9 August – 23 August 2011

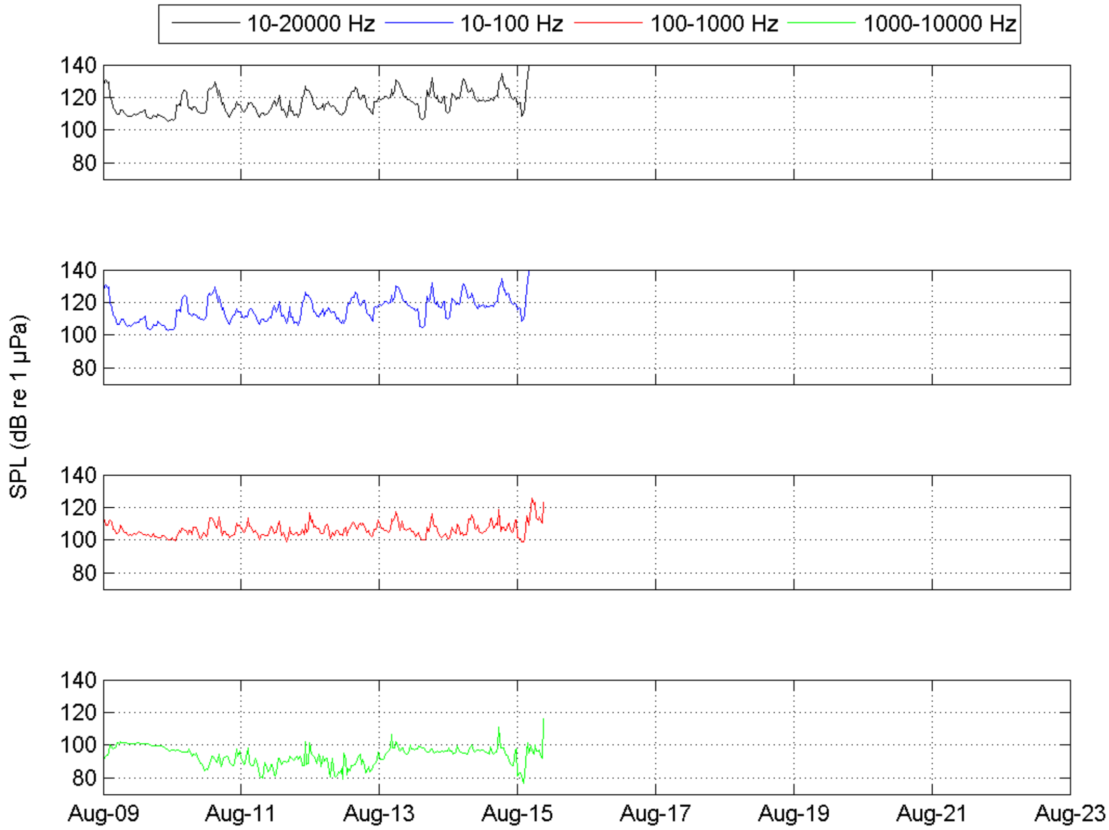

Figure 85: Broadband and decade band sound pressure levels (SPL) for 2-weeks of the 2011 summer deployment at HYWIND Control Station.

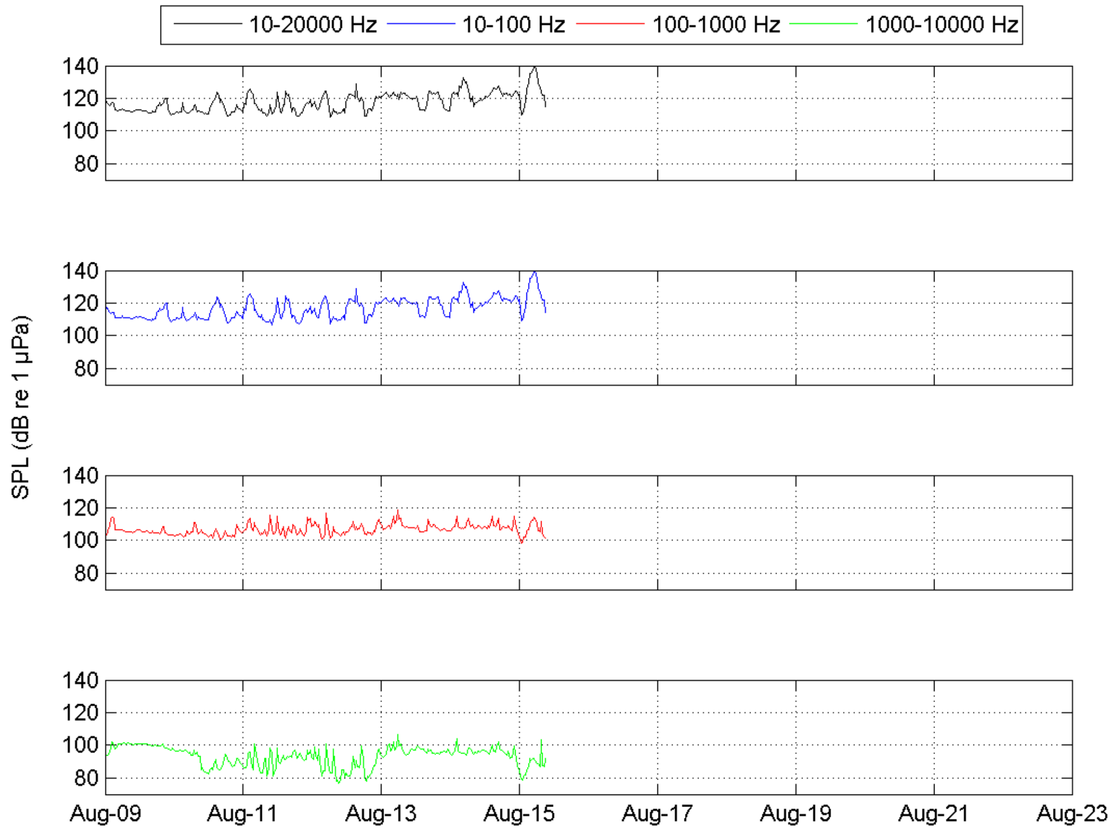

Figure 86: Broadband and decade band sound pressure levels (SPL) for 2-weeks of the 2011 summer deployment at HYWIND Monitoring Station.

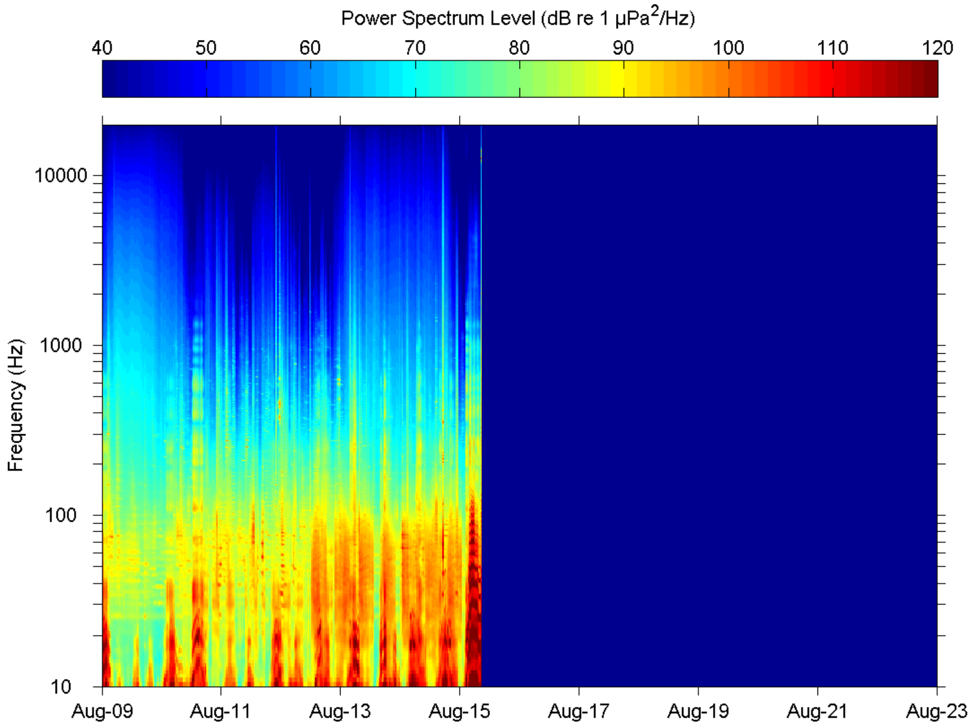

Figure 87: Spectrogram of 2-weeks of underwater sound for the summer 2011 deployment at the HYWIND Control Station.

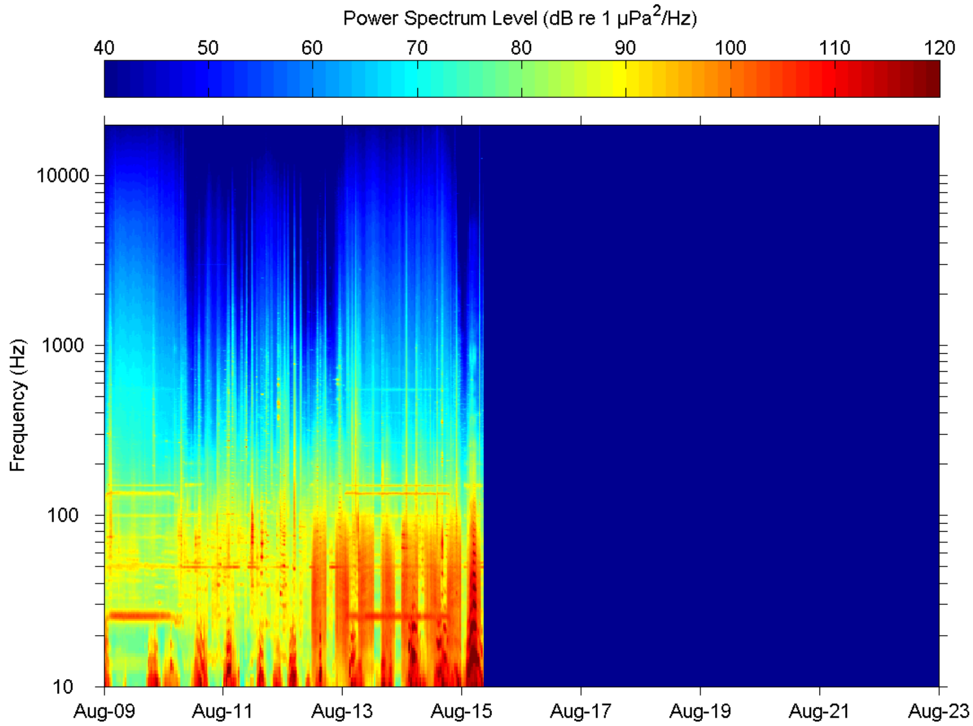

Figure 88: Spectrogram of 2-weeks of underwater sound for the summer 2011 deployment at the HYWIND Monitoring Station.

Appendix B. Data Format Descriptions

B.1. Minute-by-Minute Results Files

JASCO has provided a comma-separated-value file (CSV) for each deployment and each recorder. These are human readable text files where the values for each column of data are separated by commas. Each row of data are results for one minute of the acoustic wave files. The top row contains the column headers. The column descriptions are contained in Table 2.

Table 2: Minute-by-minute column descriptions.

Column Name	Column ID (if opened with Microsoft Excel)	Description and Units
Time	A	UTC time of the data, rounded to the starting minute, format is DD/MM/YYYY HH:mm
0.0-20000	B	Total broadband sound pressure level, computed by summing all FFT bins and averaging 120 FFT's with one second of data each, overlapped by 50%. dB re 1 Pa.
10.0(8.9-11.22) to 16384.0(14596.48-18390.41)	C to AI	Third octave sound pressure levels. The first value is the nominal center frequency, along with the actual edge frequencies used to compute the levels. Computed summing data in the band and averaging 120 FFT's with one second of data each, overlapped by 50%. dB re 1 Pa.
50.0(8.9-100.0) to 5000.0(1000.0-10000.0)	AJ to AL	Decade sound pressure levels. The first value is the nominal center frequency, along with the actual edge frequencies used to compute the levels. Computed summing data in the band and averaging 120 FFT's with one second of data each, overlapped by 50%. dB re 1 Pa
pk(db re 1microPa)	AM	Peak sound level measured during that minute. dB re 1 Pa.
pkpk(db re 1microPa)	AN	Peak-to-peak sound levels measured during that minute. dB re 1 Pa.
rms(db re 1microPa)	AO	Root-mean-square sound levels measured during that minute. dB re 1 Pa.

shipping tonals	AP	Number of stable tonals detected in the current minute, and 2-out-of-3 of the following minutes
seismic pulses	AQ	Number of seismic pulses detected in the current minute of data
max seismic spl	AR	Maximum sound pressure level measured for seismic pulses in the current minute of data, dB re 1 mPa.
Unknown	AS	Number of transient events detected in the current minute of data with at least 200 Hz bandwidth and longer than 0.4 seconds.

B.2. Hourly Peak Amplitude and Peak Sound Energy Files

JASCO has provided a comma-separated-value file (CSV) for each deployment and each recorder. These are human readable text files where the values for each column of data are separated by commas. Each row of data are results for one hour of the acoustic wave files. The top row contains the column headers. The column descriptions are contained in Table 2.

Table 3: Minute-by-minute column descriptions.

Column Name	Column ID (if opened with Microsoft Excel)	Description and Units
Time	A	UTC time of the data, rounded to the starting minute, format is DD/MM/YYYY HH:mm
Peak SPL	B	Peak sound pressure level for that hour of data, in dB re 1 μPa
Hourly Energy Density	C	Total energy density for that hour, in J/m^2